MODEL-BASED RADIOSTEREOMETRIC ANALYSIS OF AN UNCEMENTED MOBILE-BEARING TOTAL ANKLE ARTHROPLASTY SYSTEM

by

Jason W. Fong

Submitted in partial fulfilment of the requirements
for the degree of Master of Applied Science

at

Dalhousie University
Halifax, Nova Scotia
August 2010

DALHOUSIE UNIVERSITY

SCHOOL OF BIOMEDICAL ENGINEERING

The undersigned hereby certify that they have read and recommend to the Faculty of Graduate Studies for acceptance a thesis entitled "Model-based Radiostereomentric Analysis of an Uncemented Mobile-Bearing Total Ankle Arthroplasty System" by Jason W. Fong in partial fulfillment of the requirements for the degree of Master of Applied Science.

Dated: August 24, 2010

Supervisor: _____

Co-supervisor: _____

Readers: _____

_____

DALHOUSIE UNIVERSITY

DATE: August 24, 2010

AUTHOR: Jason W. Fong

TITLE: Model-based Radiostereometric Analysis of an Uncemented Mobile Bearing Total Ankle Arthroplasty System

DEPARTMENT OR SCHOOL: School of Biomedical Engineering

DEGREE: MASc CONVOCATION: October YEAR: 2010

Dedication

This thesis is dedicated to my mother, Lisa Yit-Hoo Kan, whom has always been a source of light in my life. Despite all the burdens that she carries, she has always done her best to care for her six children during hard times. She has given selflessly for her family and has ensured that we all had the opportunities that she never had.

Table of Contents

List of Tables

Page

List of Figures

Page

Abstract

Model-based radiostereometric analysis (MBRSA) of a total ankle arthroplasty (TAA) prosthesis was studied for the first time.

The TAA MBRSA system precision was determined from the double exams of 20 patients implanted with the Mobility™. The MTE for any direction was 0.07mm for the tibial component. The MTE was 0.09mm and the MRE was 0.51° for the talar component. The MTPM detection limits were 0.22mm and 0.85mm for the tibial and talar components.

Both components followed the typical subsidence-stabilization pattern. There was little detectable continuous migration at one to two years. The median(range) MTPM at two years was 0.96mm(0.17–2.28mm) and 1.23mm(0.39–1.9 mm) for the tibial and talar components.

There was no detectable inducible displacement observed for any components at two years, except one talar component. The median(range) MTPM induced by the loading at two years was 0.08mm(0.03–0.18mm) and 0.39mm(0.27–1.06mm) for the tibial and talar components.

Glossary

3D	Three-dimensional space; typically defined by orthogonal Cartesian coordinates (x, y, z).
Ankle Arthrodesis (AA)	Surgical fusion of the ankle joint.
Ankle Joint	The talocrural joint that allows for primarily dorsiflexion and plantarflexion of the foot at the interface between the tibia and talus.
Aseptic Loosening	The process by which an implant becomes loose with respect to the bone in which it is embedded without the presence of infection often as the result of an immune response associated with polyethylene wear.
Bone Markers	Tantalum RSA markers implanted into a bone, used to represent a bone rigid body and act as a reference coordinate frame.
CAD Model	Computer-aided design model; 3D model used in the manufacture of an implant.
Centroid	The center of mass for a CAD or reverse-engineered model, and the mean position of the markers in a marker model.
Condition Number (CN)	Is numerically determined number from the RSA software that provides a measure of the distribution of RSA markers and its related rotational accuracy.
Confidence Interval (CI)	Of the sample; 95%CI = $\pm 1.96 \times SD$.
Continuous Migration	Migration of an implant beyond a set threshold from 1 to 2 year followup; typically MTPM $\geq$ 0.2mm is the threshold based on studies of total knee and total hip replacements.
Contour Difference (DIFF)	The difference between an implant's radiographic contour and virtually projected CAD/RE model contour.
Crossing-Line Distance (CLD)	The shortest distance between the back projection lines of the same marker from each of its radiographic positions back to their respective Xray sources.

Detection Limit (DL) — For (x, y, z, R_x, R_y, R_z) the DL = $\pm 1.96 \times$SD from the DBX. For MTPM the DL = maximum from the DBX.

Double Exams (DBX) — The migration between two RSA exams that are taken at the same follow-up time. As this migration should be theoretically zero, double exams give a measure of RSA system error.

Elementary Geometric Shapes (EGS) — The simplification of a CAD/RE model into one or more implant features that are basic 3D geometric shapes, such as a sphere or a cone. The shape's parameters and position are determined by minimizing the contour difference.

End-stage Ankle Arthritis (ESAA) — A disease of the ankle joint resulting in severe pain and disability.

Implant Markers — Tantalum RSA Markers attached to the implant, used to represent an implant rigid body and act as a moving coordinate frame.

Inducible Displacement (ID) — The instantaneous 3D motion of an implant as a result of loading; determined by comparing a loaded condition (standing) RSA exam with an unloaded condition (supine) RSA exam.

Longitudinal Migration — The 3D motion of an implant over time with respect to the postoperative RSA exam.

Marker Model (MM) — The mathematical representation of x, y, and z coordinates for several points defined by a rigid body's marker positions.

Maximum Rotational Error (MRE) — The worst of the three rotational (R_x, R_y, R_z) errors determined from the double exams, expressed as a standard deviation.

Maximum Translational Error (MTE) — The worst of the three translational (x, y, z) errors determined from the double exams, expressed as a standard deviation.

Maximum Total Point Motion (MTPM)
: The maximum movement of any marker or any point on the surface of CAD/RE model from one RSA exam to another.

Model-based RSA 3.2
: Software package by Medis specials (Leiden, the Netherlands) that performs model-based radiostereometric analysis of RSA exams.

Mean Error (ME)
: Also known as Mean Error of Rigid Body Fitting, is numerically determined number from the RSA software that provides a measure of rigid body marker stability.

Model-based Radiostereometric Analysis (MBRSA)
: RSA in which the implant position is determined by minimizing the contour difference of a virtual implant (CAD/RE model) without the need for implant markers.

Osteoarthritis (OA)
: Degenerative arthritis or joint disease; mechanical abnormalities in the articular cartilage and/or subchondral bone.

Osteoporosis
: Abnormal loss of bony tissue resulting in fragile porous bones.

Radiostereometric Analysis (RSA)
: Also known as Roentgen Stereophotogrammetric Analysis. The process of determining an implant's movement with respect to a reference bone in which the implant is embedded through the analysis of RSA exams.

Reverse Engineered (RE) Model
: A 3D model or mesh generated from the laser scanning of an implant.

Rheumatoid Arthritis (RA)
: Chronic, systemic inflammatory disorder that principally attacks the synovial joints.

Rigid Body
: A solid body that is assumed to be un-deformable and can be represented in 3D space by three or more points on or within the body.

RSA Exam
: Two simultaneous radiographs that are taken during followup to a procedure that allow for the determination of the implant position and bone positions in 3D space.

Subsidence	A gradual sinking to a lower level.
Standard Deviation (SD)	Sample standard deviation.
Total Ankle Arthroplasty (TAA)	The surgical repair of an ankle joint by inserting an artificial joint that replaces both articulating surfaces.
Total Ankle Replacement (TAR)	Synonymous with total ankle arthroplasty.

Acknowledgements

I gratefully acknowledge the numerous individuals and organizations that have contributed to this thesis.

I am deeply indebted to my supervisors, Dr. Mark Glazebrook and Dr. Michael Dunbar, whom were vital to the success of this project. I am thankful for their show of trust in me, having let me in on their research and allowed me access to their numerous fields of expertise.

David Wilson has been an excellent resource, tutor and mentor in RSA research at Dalhousie. I would have been lost without his guidance.

The members of the Cabal Group and Dalhousie's Dynamics of Human Motion (DOHM) Laboratory are duly appreciated for their tough love and great feedback on my research in ankles and RSA. They knew how to ask all the right questions and truly set the bar high.

I am obliged to thank Sandy Mansfield for her forceful deadline reminders, her endless kindness and having continuously kept my spirits high.

I recognize the students, faculty and staff of Dalhousie's School of Biomedical Engineering and Dalhousie's Orthopaedic Research group for having made Halifax a world-class research centre in biomedical engineering. They have always kept things from getting boring.

DePuy, Inc. had generously provided funding for this research.

CHAPTER 1 : INTRODUCTION

1.1 Overview

Approximately 15% of the world's adult population suffers from joint pain and disability caused by osteoarthritis (OA).[74] Up to thirteen percent of this afflicted population has ankle osteoarthritis.[19]

End-stage ankle arthritis is a debilitating disease of the talocrural joint or ankle joint resulting in severe pain and loss of function. It is a growing problem and has dramatically negative effects on a patient's health-related quality of life.[19] In a recent study, Glazebrook et al (2008) had shown that a patient's health related quality of life is negatively affected in an equal manner by either end-stage ankle or hip arthrosis.[20]

Ankle arthrodesis (AA) or joint fusion is the current 'gold standard' of surgical treatment for end-stage ankle arthritis.[13, 23, 40] There is approximately 90% patient satisfaction post-fusion.[8] Studies have shown that ankle arthrodesis has had questionable long term outcomes[8] and leads to ipsilateral periarticular degenerative joint disease.[8, 48] There is a lack of knowledge amongst clinicians about this treatment's long-term effects.[8] Some clinicians are dissatisfied with this treatment technique and see a growing potential to improve treatment by means of total ankle arthroplasty (TAA).[11, 13, 15, 40]

The first total ankle replacements took place in 1972.[16] Very high initial failure rates led to this treatment being abandoned in favor of arthrodesis. Recently there has been renewed interest in total ankle arthroplasty (TAA) due to design innovations in recent

generations of total ankle prostheses.[9, 23, 48] TAA has been reported to be a viable alternative to arthrodesis or joint fusion in many recent studies for selected patients.[11, 15, 23] These new generations of TAA have been shown to improve gait biomechanics over arthrodesis,[13, 56] and to have improved survivability in vivo over previous generations.[3, 6, 7, 23, 24, 49] TAA has shown dramatic improvements over earlier stages of development.[3] Current designs have a failure rate of 10-12% at around 5 years.[23] There are approximately 20 different TAA prostheses currently available worldwide or are in the final design stages.[9, 11, 15, 23] Lewis (2004),[40] has indicated that there is the need for focused research to address controversies and gaps in the literature on TAA that examine these designs.

Patient outcomes, component design, reproducible surgical techniques, and adequate measurement of migration are crucial in the development and advancement of total ankle arthroplasty (TAA). The very high compressive forces at the ankle create substantial problems with implant fixation and bearing wear.[18] Therefore, it is prudent to utilize the lessons learned from the research and development of hip and knee arthroplasty in order to accelerate the TAA development. The carefully monitored introduction of new implant designs, surgical techniques and cement formulations through radiostereometric analysis (RSA) trials is quickly gaining international support.[2, 14, 17, 32, 34, 35, 47] RSA research can improve TAA product development and minimize patient risk.[19]

Radiostereometric analysis (RSA) is a highly accurate yet minimally-invasive technique for evaluating micromotion in three-dimensional space.[51, 52, 55, 58, 60, 63] RSA has been

used extensively since its development in 1974,[66] with joint replacement assessment being the main focus. Valstar et al (2005) indicated, "It is a highly accurate three-dimensional method of quantifying the motion between an implant and the host bone, for assessing motion between bony structures that have been fixed, and for measuring wear."[78] Long-term implant survival is strongly related to implant migration. A few pioneering studies have shown in hip[32] and knee[59] arthroplasty that RSA measurements over a two year period is predictive of aseptic loosening. The established value of RSA in studying knee and hip replacements makes it a viable candidate in assessing the biomechanical stability of TAA.[7, 49]

1.2 The Ankle Joint

The ankle joint is also known as the talocrural joint. It acts primarily as a hinge allowing for dorsiflexion or plantar flexion of the foot.[84] The ankle is a synovial joint which connects the distal tibia and fibula of the shin with the proximal talus of the foot. Like all synovial joints, the interfaces of the bones are lined with articular cartilage that reduces shock forces and distributes load over the range of motion. The ankle joint couples with the subtalar, or talocalcaneal, joint to form the ankle joint complex that allows for three directions of foot rotations.[84]

1.3 End-Stage Ankle Arthritis

The incidence of symptomatic ankle arthritis is approximately one-ninth that of hip or knee arthritis.[10] End-stage ankle arthritis is a debilitating disease of the talocrural joint in

which the cartilage and subchondral bone of the contact surfaces of the tibia and talus are degraded, Figure 1.1. The thickness of the cartilage at the ankle is 1-1.7 mm, much less than the 1-6mm at the knee, but the ankle has five times the contact forces of the knee.[10, 67, 74, 80] This disease results in pain and loss of function of the joint and adversely affects a patient's health related quality of life.

Figure 1.1: End-stage ankle arthritis. *Left:* Anterior-posterior (AP) radiograph of shank and foot. *Right:* Arthroscopic image showing degradation of tibia and talus.

End-stage ankle arthritis is differs from arthritis of the other lower extremity joints in its mechanism of onset. The ankle is the most commonly injured joint of the body.[10] It has been shown that over 70% of the incidences of ankle arthritis are related to traumatic injury.[25, 74, 75, 80] The remainder is composed of non-posttraumatic osteoarthritis,

rheumatoid arthritis, or is related to other health issues such as osteoporosis.[75] As traumatic injury can often occur early in life, the mean age of surgical treatment for end-stage ankle arthritis is younger than that seen in total knees or hips at 41 years of age.[8]

1.4 Ankle Arthrodesis

Ankle arthrodesis (AA) is a surgical intervention for end-stage ankle arthritis in which the talus and tibia are fused by mechanical fixation. In this procedure, diseased cartilage and cortical bone tissue are removed from the contacting surfaces of the talus and tibia. The void between the two resurfacings is filled with bone graft or bone graft substitute. After the two bones are positioned in the appropriate position, the bones are rigidly fixed by internal (i.e.- with orthopaedic compression screws) or less likely, external (i.e.- Charnley compression technique) methods. Postoperative immobilization ranges from six weeks to 11 months.[8]

There have been over 30 techniques of ankle arthrodesis described since its first documented description in 1879.[8, 72] A more recently developed technique is shown in Figure 1.2, the fibular-sparing Z-osteotomy (FSZO). This technique retains the anatomy of distal fibula allowing for a later revision to implant a total ankle replacement.[22]

Despite having a high fusion success rate of 80-100% based on pain relief and function, there are high complication rates associated with ankle arthrodesis.[72] There are reported complications of a 10-30% non-union rate, a 9% revision rate and a 5% below-knee amputation rate.[8, 13, 23]

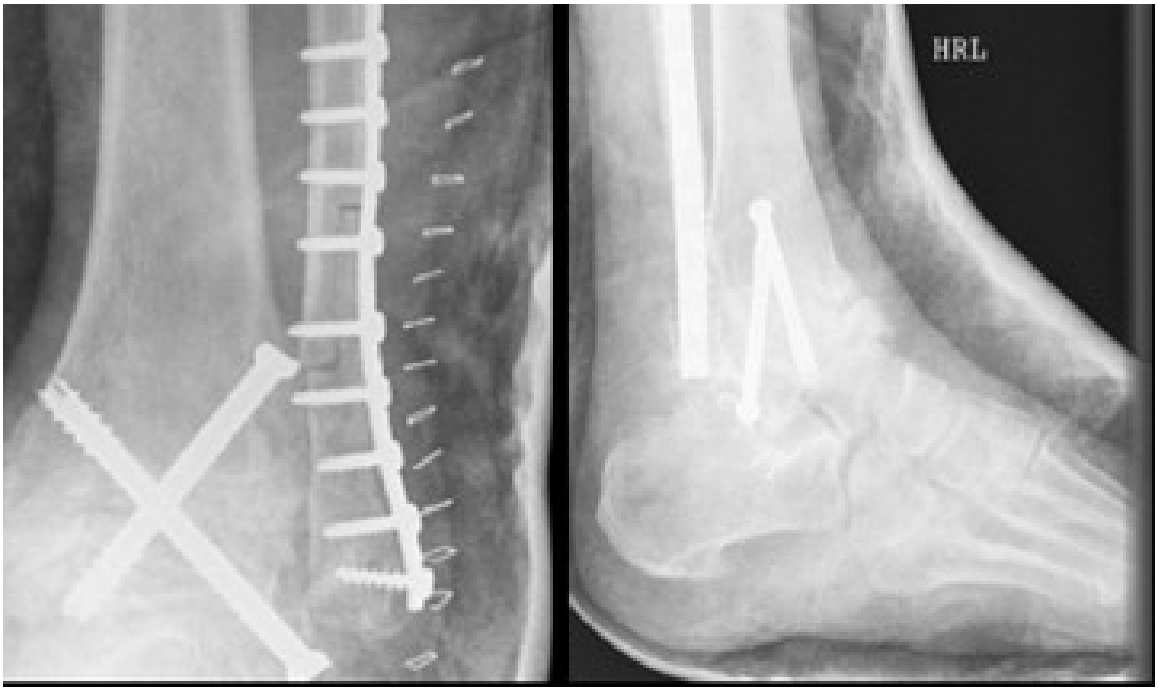

Figure 1.2: Example of an ankle arthrodesis. AP and lateral radiographs of fibular sparing z-osteotomy (FSZO) technique. The Z-shaped cut through the fibula allows reduction while retaining the function of distal fibular soft tissues to allow for future total ankle replacement.[22]

Even if the fusion is successful, there are issues with long immobilization times,[13] altered gait mechanics,[13, 56, 72, 82] and ipsilateral periarticular degeneration of the contiguous foot joints.[8, 23, 56, 72] There are reports of a decrease in the range of motion in the subtalar joint,[8, 82] mild to moderate limping,[8] gait asymmetry,[56] and an increase in the ground reaction force shock or transient during heel-strike.[56]

Studies have shown that 67% of patients are completely satisfied with their ankle fusion, while 88% would do it again, and 92% would recommend the treatment to others in the

same circumstances.[8] Some patients eventually become limited by pain and degenerative changes elsewhere in the foot.[8]

1.5 Total Ankle Arthroplasty

Initial attempts at total ankle arthroplasty (TAA) were largely abandoned in the early 1990's due to very high failure rates.[36] These failures were associated with highly constrained cemented designs.[9, 40] However, the limitations of ankle arthrodesis and the success of knee and hip arthroplasty has lead to continued development and improvements in ankle prosthesis designs and surgical techniques.[13, 18, 40, 56] Improvements to implant survivorship in newer generations of TAAs has led to a resurgence of interest in TAA as a viable treatment.[56, 64] Current studies report 5 year survivorship at 88-90%.[21, 23]

The primary design improvements in newer generations of TAA design include a mobile bearing, a cementless fixation, and the minimization of bone resection.[9, 23, 40] An uncemented mobile-bearing TAA implant design is the Mobility™ Total Ankle System (Depuy, Inc., Warsaw, IN), Figure 1.3. It is a three-component design with talar and tibial components constructed of Co-Cr with porous coated surfaces and a mobile bearing made of ultra-high molecular weight polyethylene (UHMWPE).

An UHMWPE mobile bearing is not fixed to either component so as to disrupt the transfer of shear forces between the talar and tibial components. These shear forces are thought to lead to failure at the bone-implant interface.[9] Instead of cement, newer TAA

prostheses have their bone interfaces coated with sintered metal beads (porous coated), hydroxyapatite (HA) and/or titanium nitride (TiN).[40]

Figure 1.3: The Mobility™ Total Ankle System is an uncemented mobile-bearing TAA design. The bone-implant interface surfaces are porous coated to support osteointegration.

The main benefit of TAA over ankle arthrodesis (AA) is the preservation of motion and function.[23, 56, 72] This results in reduced limp and offers protection for the other articulations of the foot.[23, 56] Gait mechanics are maintained at near normal for TAA, but the walking velocity is still reduced, as is also the case with AA or untreated osteoarthritis (OA).[56, 75]

Major complications associated with TAA failure are infections and loosening of components.[23] One study defined loosening based on radiographs alone as the subsidence of the talar component into the talus of greater than 5 mm or a change in

angular position of great than 3°; and greater than 2° with respect to the tibial long-axis for the tibial component.[3] The support for the decisions of these criteria is clearly limited by the metrics used. Assessment of component loosening in vivo is best determined by a precision metric such as radiostereometric analysis.

Innovations in component design, reproducible surgical techniques, and adequate measurement of migration will be key to the development of viable ankle prostheses that provides good clinical outcomes.

1.6 Radiostereometric Analysis

1.6.1 Applications for Radiostereometric Analysis

Radiostereometric analysis (RSA) (a.k.a.- Roentgen Stereophotogrammetric Analysis) permits highly precise characterization of relative motion of marked rigid bodies in all 3 spatial dimensions.[63] Typically RSA is used to assess implant migration from one time instance or condition to a reference time instance or condition.

RSA can be used to study joint kinematics, implant migration, implant wear and implant inducible displacement.[31, 33] There are numerous total joint arthroplasty RSA studies that examine longitudinal migration,[7, 32, 49, 59-61] inducible displacement,[14, 60, 61, 81] and wear.[33] There is a push amongst clinicians and researchers to use RSA to monitor the introduction of new implant designs, surgical techniques and cement formulations.[2, 17, 34,

[35, 47] Lessons from the past RSA studies of total knee and total hip arthroplasty can help accelerate the development of total ankle arthroplasty.

1.6.2 How Radiostereometric Analysis Works

RSA involves the implantation of small 0.5, 0.8, or 1 mm spherical diameter radio-opaque Tantalum (Ta) markers.[78] These markers are inserted during surgery to mark bone and implant rigid bodies. RSA exams are taken postoperatively and at set follow-up times. For each RSA exam, two simultaneous low dose radiographs are taken at different projection angles. The back-projection lines for each marker from film to foci determine 3D marker positions to a spatial resolution of 0.05 mm.[31, 54] The locations of the implants are determined with respect to the reference bone in which the implants are implanted. Multiple RSA exams are used to assess the micromotion of implants with respect to the reference bone from one instance or condition to another.

There are generally two types of studies that determine the motion of an orthopaedic implant with respect to a reference bone in which it is implanted. These are longitudinal migration and inducible displacement studies. For longitudinal studies, the RSA exams are typically in unloaded or supine conditions and each sequential exam compares the implant position with respect to the postoperative implant position. This gives the motion of the implant over a span of time. For inducible displacement studies, the change in position is determined between a loaded condition (i.e.- standing) at a specific time instance to an unloaded condition (i.e.- supine) at the same time instance. This gives the motion of the implant in response to an instantaneous loading.

There are two major methods of determining implant position using RSA; the classical marker-based method developed by Selvik (1989),[66] or the newer model-based method developed in Leiden, The Netherlands.[26-30, 65, 76] Classical marker-based RSA prostheses must have markers attached to the implant. In this case, the implant marker positions are determined by the same back projection method as the bone marker positions. The back projection method is where the lines (projections) from center of the markers are drawn back to radiographic foci for each radiograph in the RSA exams. The marker positions are determined intersections of two back projection lines. The precision of marker-based RSA has been thoroughly demonstrated and is the current 'gold standard' of RSA studies. Model-based RSA (MBRSA) is gaining in popularity as a novel RSA method that avoids the need to attach markers to the implant and instead positions an implant by its radiographic contour.[26, 27, 33, 65, 76]

The accuracy and precision of RSA depends on a large number of factors including radiographic equipment, RSA set-up, number of markers, size of markers, distance between markers and marker configurations.[46, 54, 63, 83] These are all important factors to consider when determining appropriate marker placement as they have an important effect on the accuracy and precision of the study results.

RSA studies can use either a uniplanar or biplanar set-up.[31] The uniplanar set-up is such that both radiographs are co-planar with one another, with the radiographic foci being offset 40° from each other. The uniplanar set-up makes it easier for the patient to enter and exit the calibration region. The tradeoff is a slightly increased out-of-plane error.[83]

For a biplanar set-up the two radiographs are perpendicular to each other with the foci projecting perpendicular to the radiographs.

Marker 3D positions in each RSA exam are determined by the intersection of the back projection lines from each radiograph marker center back to their respective sources. These lines are determined to intersect if the crossing line distance (CLD) is sufficiently small. A typical software default is 0.5 mm.

In order to mark a rigid body (i.e. reference bone or migrating implant), at least three markers should be used and these markers should be placed in a manner such that they are non-collinear.[78] It has been advised that due to an increase in precision with a redundancy of markers, up to six to nine well-scattered bone markers should be used for each bone in the study.[31, 63] Each rigid body acts a local coordinate system where the bone rigid body acts a the reference coordinate system, and the implant rigid body acts as the moving coordinate system.

It is also important that when inserting the markers that they are placed in an arrangement which is not obscured by the components on the various radiographic views. In addition, the markers should be placed relatively close to the component, as increased distance between the rigid body and the component being measured may influence precision due to the increased effects of bone deformation and remodeling. To support these statements, Valstar et al,[78] indicated that the accuracy of the micromotion calculation is influenced by the stability and distribution of marker markers within a rigid body.

The stability of markers is typically assessed by the mean error (ME) of rigid body fitting.[78] This parameter compares the marker positions from one instance to another (i.e.- between two RSA exams).

The ME is defined as minimizing the sum of:

$$ME = \sqrt{\sum \frac{d^2}{n}} \quad (1)$$

where:
d is the length of the residual distance for each of the n markers after the rotation matrix has been optimized by using a least-squares method and the rigid-body displacement has been subtracted.[53, 61]

In short, the ME provides a measure of independent marker movement or rigid body deformation. As a result, ME contributes to the precision of the RSA migration calculation. A guideline proposes that the ME should be less than 0.35 mm.[78] The ME provides a measure of independent marker movement or rigid body deformation. The ME should be near zero in double or inducible displacement exams and grows with time in longitudinal migration. One study noted that stability can be improved by the use of bone wax.[31]

The absolute condition number (CN) is defined as:

$$CN = \sqrt{\frac{1}{d_1^2+d_2^2+\ldots+d_n^2}} \quad (2)$$

where:
d is the distance between each marker and a numerically determined line passing through the cluster of markers that minimizes the CN, and
n is equal to the total number of markers representing the rigid body.[63]

The CN gives a measure of the worst error in the rotation matrix,[69] and inherently represents the mean value for the SD of all three Cartesian directions of rotations[63]. Ryd et al,[63] showed that through analysis of their data from their simulation that the correlation between the CN and the mean rotational accuracy of the measurement system was $r^2 = 0.93$ ($p<0.0001$).[63] It is important to note that the rotational accuracy of a reference bone contributes to translational and rotational accuracies of an implant located with respect to that bone. Hence, an appropriate CN is vital to precise determination of the migration of an implant. The CN is optimally minimized when isotropically distributed, as in an equilateral tetrahedron, a cube, etc.[69] In summary, a high CN indicates poor marker distribution and a low CN indicates satisfactory marker distribution. The goal of any marker placement protocol should take this into thoughtful consideration. A CN below 110 has been deemed reliable and adequate for determination of component migration.[78] However, a CN below 50 was determined to be ideal for assessing implant micromotion based on experience with hip and knee replacements from this institution.

Micromotion is assessed in one RSA exam, such as two year followup, with respect to a reference RSA exam, such as postoperatively. The x, y, z translations are determined in orthogonal Cartesian coordinates. The x, y, z rotations follow a Euler rotation sequence and use the right-hand rule for each axis. The axes are typically oriented with respect to the anatomy or implant of the patient to provide meaningful data.[37, 78] The axes are often aligned to correspond with anterior-posterior, medial-lateral, and superior-inferior, or alternatively distal-proximal directions.

Maximum total point motion (MPTM) is the magnitude of the greatest translation vector of any marker or point on a rigid body with respect to its initial reference position. The reference position is either of the RSA exams in a double exam, the postoperative exam in longitudinal migration, or the unloaded (supine) condition in inducible displacement. The MTPM differs from the x, y, z translations that refer to the change in position of the rigid body's centroid.

1.6.3 Classical Marker-based Radiostereometric Analysis

With classical marker-based RSA, markers must be attached to the implant. The precision of marker-based RSA has been thoroughly demonstrated and is the current 'gold standard' of RSA studies.[7, 32, 34, 49, 58, 59, 63, 77, 78] There are issues with this method including over-projecting of the markers with the implant, the cost of attaching the markers accurately, and modification to the implant requiring separate national health and safety board (e.g.-FDA) approval. Classical marker-based RSA has been used in several of the existing studies of ankle joint biomechanics and orthopaedic treatments.[1, 5, 42-45]

1.6.4 Model-based Radiostereometric Analysis

Model-based radiostereometric analysis (MBRSA) is a method by which implant migration can be determined without markers being attached to the implants.[27, 30, 76] This is a novel approach that avoids the difficulties of accurately attaching markers to implants, that can be expensive, be over-projected by the implant itself and be detrimental to the implant integrity.[27, 30, 31, 33] Determination of the implant's precise 3D

spatial location is obtained through a pose estimation algorithm detailed by Valstar et al (2001) and Kaptein et al (2003, 2004) that minimizes the contour difference between the projected virtual implant outline and the implant outline from the radiograph.[27, 30, 76] These outlines are often termed contours. The virtual implant is a 3D model that is derived from a manufacturer developed CAD model or is reverse engineered (RE) from a laser scan of the physical implant.

The contour difference is defined as:

$$DIFF = \sum_{i=1}^{n_A} \frac{| A_i - A_i^P |}{n_A} \tag{3}$$

where:
A is the actual contour node position (the implant silhouette from the radiograph),
A^P is the nearest (to A) virtual contour node position (the implant model projection onto Radiograph),
i is the node number, and
n_A is the node number.

The total contour difference is the sum of the contour differences from the right and left radiographs; $DIFF = DIFF_{right} + DIFF_{left}$. The DIFF is numerically minimized resulting in the final pose estimation at that minimum. The minimization process is conducted by the MBRSA software program, which iteratively rotates and translates the virtual implant until convergence is achieved.[27, 29, 30, 65, 76] The DIFF is further reduced by having the virtual model closely match the physical implant dimensions, this also results in a reduction in measurement system error.[27] The starting pose can strongly affect the convergence and needs to be controlled by standardized procedures in some cases. The accuracy of the fitted model is very important to the pose estimation accuracy.[27] Figure 1.4 depicts MBRSA pose estimation by minimizing the contour difference.

A variation of MBRSA is Elementary Geometric Shapes (EGS),[29] where by a basic shape such as a sphere can be fitted to the selected contours of an implant (i.e. a spherical tip). The algorithm is similar to MBRSA in which the DIFF is minimized, but the dimensions (i.e. radius) of the shape are also determined in addition to its position. In the example of the EGS sphere, the accuracy of the center and the radius are greatly improved when compared to the pose estimation of the entire implant.

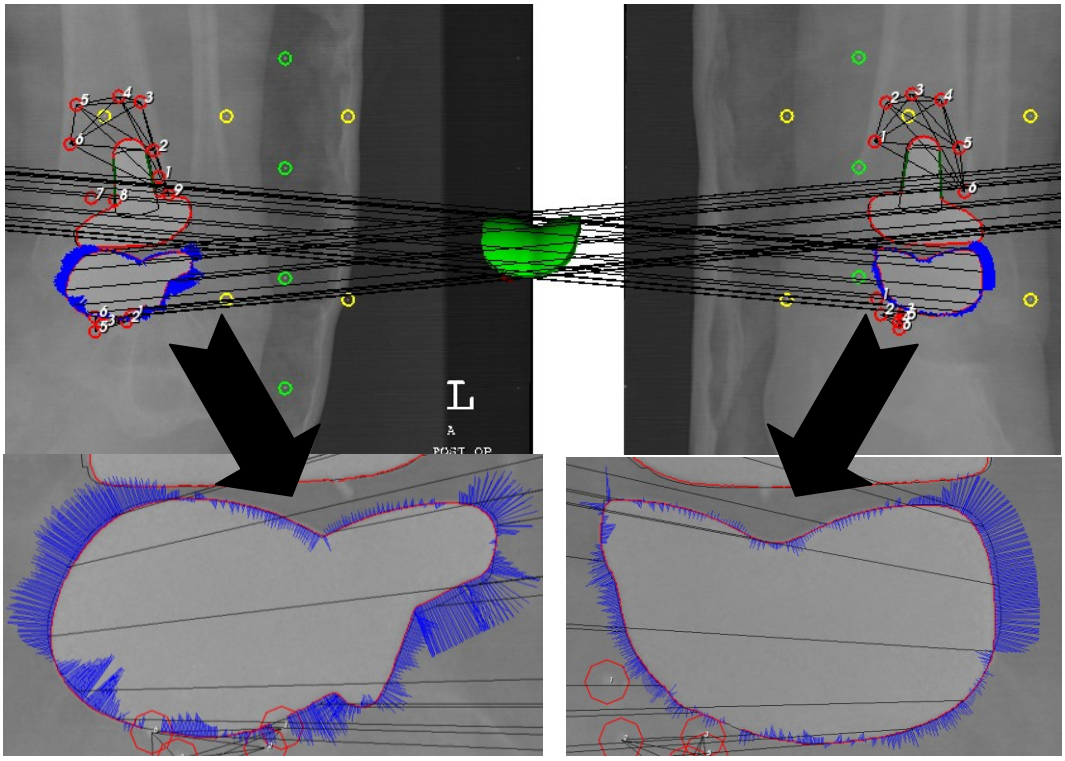

Figure 1.4: Model-based RSA 3.2 software (Medis specials, Leiden, The Netherlands) final pose estimation by minimizing the contour difference. *Red:* actual contour. *Black:* projected contour. *Blue:* 10x amplification of the contour difference.

Additionally, rigid body marker models (MM) use the MBRSA pose estimation, and can be employed when there are issues with sufficient marker visibility and/or independent

marker migration.[28] A marker model is a defined rigid body representing a bone or implant that can be created by the 3D positions of markers known to exist in one patient exam (from sufficiently low crossing-line distance) and used to position the rigid body in other exams for the same patient. The assumption that the rigid body is non-deformable is maintained by the marker model definition.

1.6.5 Longitudinal Migration

Longitudinal migration is movement of an orthopaedic implant over time with respect to the bone in which it is implanted from one postoperative followup time instance to a reference time instance (i.e.- a few days postoperatively).

RSA has shown that continued migration, or MTPM $\geq$ 0.2 mm, of tibial knee components between one year followup and two year followup has 85% positive prediction of continued loosening leading to implant failure.[59] The 0.2 mm of MTPM is considered the detection limit of most RSA systems in assessing TKA.[54, 59] An implant is considered to be stable if MTPM is less than 0.2 mm.[59]

Continuous migration in total ankle replacements may indicate issues with implant loosening and subsequent implant surgical malalignment. Premature failure has been found to be associated with malalignment in the knee replacements.[64] RSA measurement of component migration can thus be used to assess the surgical repeatability and reflects upon surgical technique and implant system efficacy.

1.6.6 Inducible Displacement

Inducible displacement is movement of an orthopaedic implant with respect to the bone in which it is implanted from a *loaded condition* (i.e.- standing) to a reference *unloaded condition* (i.e.- supine) at the same follow-up instance. The motion of the implant as a result of the loading is considered to reflect the quality of the bone-implant interface.[61, 81] This reflects upon the amount of implant osteointegration and/or fibrous ingrowth.

1.7 Purpose

The purpose of this study was to assess the biomechanical stability of the DePuy Mobility™ Total Ankle System. This study will be the first known study of its kind to assess TAA implant micromotion using MBRSA.

1.8 Objectives and Hypotheses

Objective 1: To determine the system precision and to clinically validate that the TAA MBRSA system is capable of detecting clinically significant implant migration or micromotion.

Hypothesis 1: The MBRSA system used will have enough precision in assessing the micromotion of the Mobility™ tibial and talar components to be comparable to other orthopaedic RSA studies.

Approach 1: To address hypothesis 1, the RSA radiographs and data for 20 subjects were be gathered. All exams will be analyzed using Model-based RSA 3.2 software (Medis specials, Leiden, The Netherlands). Output data (x, y, z, rx, ry, rz, MTPM, ME, DIFF, CN) will be processed using a custom MATLAB® 2009a program (The MathWorks, Inc., Natwick, MA). Double exams will be performed to obtain a measure of the system precision.

Objective 2: To determine the longitudinal migration pattern of the Mobility™ tibial and talar components.

Hypothesis 2: The migration data will be comparable to other orthopaedic RSA studies found in the literature showing initial subsidence followed by stabilization.

Approach 2: Follow-up RSA exam data will be gathered for the same 20 subjects from the initial project (see Approach 1). Longitudinal implant migration will be assessed from a few days postoperatively to two year followup for each patient. The migration patterns will be assessed for each subject and the group as a whole.

Objective 3: To determine the inducible displacements of the Mobility™ tibial and talar components.

Hypotheses 3: Displacements will be detectable in patients when comparing their standing (loaded condition) RSA exam to their supine (unloaded condition) RSA exam at set follow-up times.

Approach 3: Additional loaded condition RSA exam data will be gathered on the same 20 subjects (see Approach 2) during their 3 month, 6 month, 1 year and 2 year followup. The inducible translations, rotations and MTPM will be assessed for each subject and the group as a whole.

1.9 Structure of Thesis

This thesis is divided into projects that are each described in a separate chapter. The current chapter, Chapter One, is an introduction to this thesis. Chapter Two describes the standardized bead insertion methodology, a phantom study, and the determination of the TAA MBRSA measurement system precision. Chapter Three presents the two-year longitudinal migration data for the Mobility™ trial. Chapter Four presents the results of the inducible displacement data for the Mobility™. Chapter Five discusses the implications, limitations and conclusions of this thesis. Appendix A provides a sample of the algorithms used to acquire and process the core RSA data. Appendix B contains RSA results that are interesting, but has details that do not need to be directly presented for this thesis. Appendix C provides the marker model and marker matching algorithms and computer code used to overcome minor issues discovered during the RSA analysis of this thesis. Appendix D provides the raw RSA double exam, longitudinal migration and inducible displacement data.

CHAPTER 2 : SYSTEM PRECISION AND CLINICAL VALIDATION

2.1 Introduction

2.1.1 Guidelines for Standardization of Radiostereometry (RSA) of Implants

RSA permits the minimally-invasive and precise determination of an implant's micromotion in three-dimensional space.[51, 52, 54, 55, 58, 60, 63] RSA has been used extensively since its development by Selvik in 1974.[66] Valstar et al (2005),[78] and other researchers[12] have noted that there is a need to establish RSA guidelines early on before the number of RSA studies increase. Such guidelines would improve the interpretability and comparability of the results from all RSA studies.

The accuracy and precision of RSA depends on a large number of factors including radiographic equipment, RSA set-up, number of markers, size of markers, distance between markers and marker configurations.[46, 54, 63, 83] These are all important factors to consider when determining appropriate marker placement as these have an important effect on the quality of the study results.

Double exams are RSA radiograph exams that are taken one after another,[78] where in between the exams the implant component and limb orientations are changed with respect to the radiographs. These are used to assess the measuring error, precision and repeatability of the RSA system by determining the migration of the implants between the two exams that should be theoretically zero. Double exam studies have been

conducted to demonstrate the accuracy of RSA systems in studying implant motion.[57, 61, 78]

The reported accuracy, 95% confidence interval (CI), for marker-based RSA ranges between 0.05 to 0.5 mm for translations and 0.15 to 1.15° for rotations.[30, 31, 79] A study for RSA of TAA using classical marker-based analysis of the Buechel-Pappas™ total ankle prostheses estimates translational accuracy to be 0.13, 0.14, and 0.34 mm for the three directions (x, y, z).[49] Another study on the Scandinavian Total Ankle Replacement® showed 99% confidence interval (CI) of measurements to be a maximum single axis translation of 0.1 mm and rotation of 1.5°.[7] Using MBRSA with a total knee arthroplasty (TKA) prothesis, the precision or standard deviation was 0.22 mm and 0.52° using CAD models,[76] and 0.14 mm and 0.10° using reverse engineered (RE) models.[27] In another MBRSA study, a TKA prosthesis had a maximum standard deviation of 0.04 mm and 0.12°, and slightly worse results were observed for two hip stems.[65] Based on this information an acceptable precision for a MBRSA system assessing TAA would be approximately a maximum standard deviation of translational motion (i.e.- MTE) of 0.15 mm and maximum standard deviation of rotational motion (i.e. - MRE) of 0.5°.

2.1.2 Purpose

The purpose of this project was to determine the system precision and to clinically validate that the TAA MBRSA system is capable of assessing the biomechanical fixation of the implant components. The early development of universal RSA protocols and

standardized reporting of result parameters will allow for improved inter-study and inter-prostheses comparisons in the future as the field of TAA RSA grows. This will prove valuable to clinicians and in the end allow them to select the optimal prosthesis for their patient. The hypothesis is that the MBRSA system used will have sufficient precision to assess the micromotion of the Mobility™ tibial and talar components and be comparable to other orthopaedic RSA studies.

2.2 Methods and Materials

2.2.1 The Phantom Model

A phantom model of the ankle was created using an artificial tibia and talus Sawbones® (Pacific Research Laboratories, Inc., Vashon, WA). The phantom model was used to determine appropriate RSA marker distribution with the prosthesis in place. The prosthesis used in this study was the Mobility™ Total Ankle System (DePuy, Inc., Warsaw, IN).

In this model, after the final tibial and talar cuts were made and prior to final implant insertion six 0.8 mm diameter spherical tantalum markers were inserted into the tibia in a fan-like distribution around the tibial prosthesis in the coronal plane. Similarly, six 0.8 mm diameter tantalum markers were inserted into the talus through the talar component fin hole cuts and just inferior to the talar component thereby decreasing the likelihood that they would be obscured. Of these six, three markers were inserted into each of the lateral and medial talar fin cuts with one marker directed posterior, one anterior, and one

either medial for the medial fin and one lateral for the lateral fin. These marker positions were deemed to be rough guidelines as the placement is imprecise due to the blind and manual nature of marker insertion through the phantom surgical cuts.

Following implant insertion, radiographs were taken using a uniplanar detector system located under a RSA calibration box with the phantom model positioned over the box. A uniplanar RSA calibration box was used that contains 26 fiducial markers for each side and 12 control markers. Radiographs were taken with two radiograph tubes at 20-degree angles from the coronal plane. This radiographic setup is identical to that used for the followup in vivo cases.

The radiographs allowed analysis of the initial marker placement giving due consideration to the guidelines of Valstar et al.[78] These considerations included having greater than three markers, ensuring marker non-collinearity, minimizing marker obstruction by the component, maintaining close marker proximity to the component, a stable setting for the markers, and an adequate distribution (i.e. - low condition number, CN).

Using Model-based RSA 3.2 (Medis specials, Leiden, The Netherlands) the marker placement and distribution was assessed. Assessment was carried out with 3D visualization of the markers and reference to the condition number, Figure 2.1. The results of the phantom study were used to revise the marker placement protocol for the clinical RSA cases.

2.2.2 Findings From the Phantom Study

It was noted that one marker in the talus and two in the tibia had not deployed. This resulted in a satisfactory number of five and four markers in the talus and tibia respectively. The markers in the talus were not obscured or collinear, but were clustered closely together. The markers in the tibia were partially obscured on the lateral view but readily visible on the AP view. They were non-collinear. Both the rigid bodies formed by the markers in the tibia and in the talus were in adequate proximity to the prostheses. The condition numbers were calculated using Model-based RSA 3.2 software (Medis specials, Leiden, The Netherlands). The results were both satisfactory and the CNs were below the ideal point of 50 mm^{-1}. The CNs were 38 and 40 mm^{-1} for the tibia and talus respectively.

2.2.3 Adjustments Due to the Phantom Study

The tibial marker distribution was altered after the phantom study. Specifically, six markers were placed in the tibia in an alternating cross diagonal for three horizontal plane elevations, Figure 2.2. The markers were inserted through the cancellous bone after the implant cuts were made, and as close to the cortical bone as possible to add stability to the markers. In the sagittal plane, the marker distribution was altered so that the each level had two markers, which diagonally placed one anterior-medially and one posterior-laterally for each level, Figure 2.2. The markers of the subsequent level were placed similarly but crossing diagonal to the level above, and this was repeated for the third

level. This alteration in the sagittal plane was to avoid collinear marker placement, and decrease the chance for obscuring of the markers by the tibial component. An additional marker was added after the phantom study into the anterior cortical window bone cutout for the tibial component stem to help determine movement of the tibial window postoperatively, Figure 2.2. This cutout was free from the distal tibia until healing occurred. The marker positions were deemed to be rough guidelines as the placement is imprecise due to the blind and manual nature of marker insertion through the phantom surgical cuts.

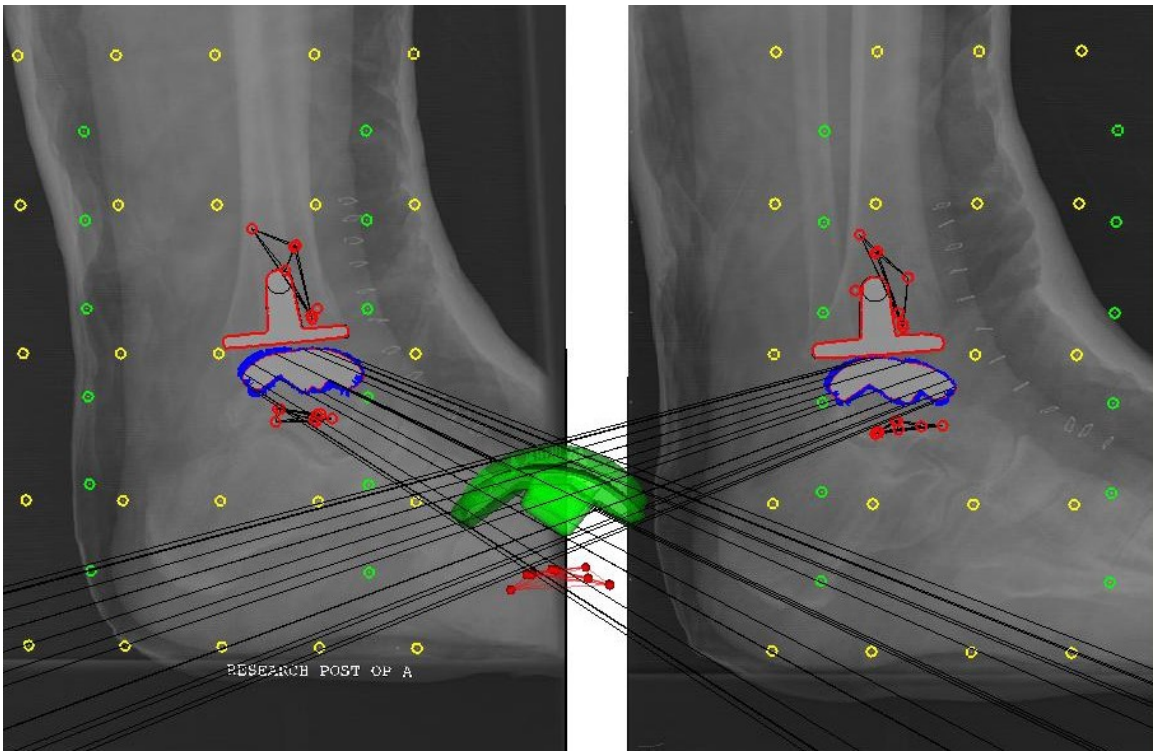

Figure 2.1: Model-based RSA 3.2 Software (Medis Specials, Leiden, The Netherlands) used to visualize marker distribution and marker obscurity, and to determine condition number. Depicted is the model-based location of talar component and talar bone markers. The talar markers are not over-projected and well dispersed.

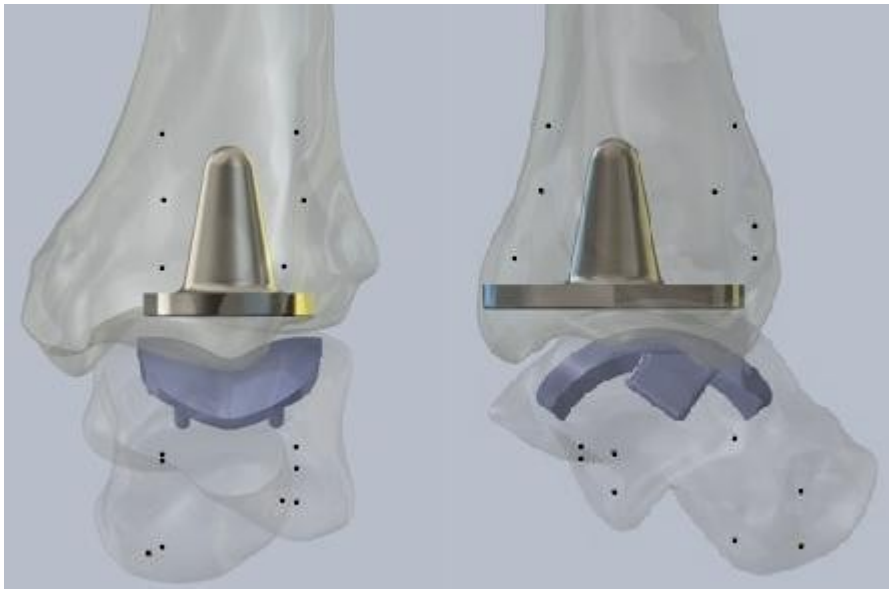

Figure 2.2: Marker insertion locations. 7 markers are implanted into the tibia and 8 markers are implanted into the talus as shown. *Left:* posterior-to-anterior view. *Right:* lateral-to-medial view.

The six initial talar markers were in satisfactory alignment and were not modified. Two additional markers were placed close to the navicular bone in the anterior end of the talus to increase the size of the rigid body formed by the talar markers, and to minimize possible errors caused by the initial close proximity of the talar markers, Figure 2.2.

2.2.4 Double Exam Error Analysis

Twenty patients underwent TAA that implanted the Mobility™. Each subject was identified in numerical order (i.e.- Subject 1 to Subject 20) by his or her time of enrollment into this study. The mean (standard deviation) age was 60.4 (12.2) years old and BMI was 29.1 (2.8) kg/m^2. Half of the subjects were female. The Mobility™

prostheses implanted into these patients ranged from size two to six. One surgeon performed all surgeries. All patients included in this study had given informed consent. Capital Health Research Ethics Board had approved this study.

Double exams were taken within three days postoperatively using the Halifax Stereo Radiography (SR) Suite (Halifax Biomedical Inc., Halifax, Nova Scotia). During the exams the subjects were supine lying to one side on a bed. A uniplanar RSA calibration box was used (26 fiducial markers per side and 12 control markers) with two radiograph tubes that were each oriented at 20° from the vertical. The orientation of the subject with respect to the radiographs was such that the radiographs captured bilateral views of the prostheses.

Precision was determined for the talar and tibial components by examining the migration between the double exams using the standard model-based pose estimation[78] from the Model-based RSA 3.2 software (Medis specials, Leiden, the Netherlands). Supplier generated computer aided design (CAD) models for each of the implant sizes were provided by DePuy, Inc. These models that were used in the manufacture of the prostheses, were converted to meshes by Medis Specials and were imported in the Model-based RSA 3.2 Software. The tibial component double exams were also assessed using the EGS module[29] to determine the migration of the spherical tip as high rotational errors from the tibial component pose estimation were seen due to the symmetry of this component, Figure 2.3. The issue of implant symmetry with MBRSA has been observed with hip stems.[29, 65]

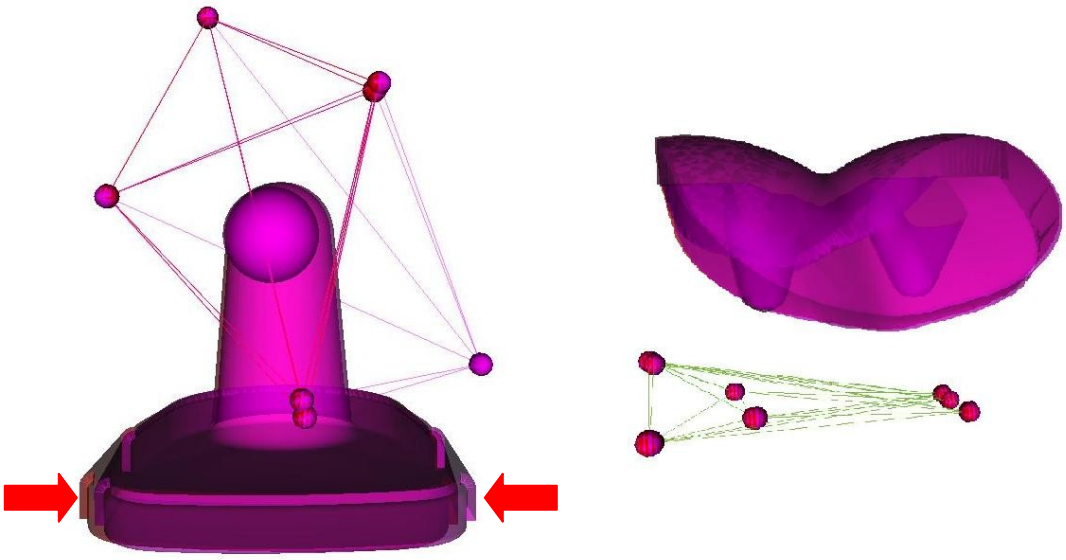

Figure 2.3: Sample double exams results for one subject depicting overlaid implant positions that should be identical. *Right:* The high ghosting (*red arrows*) in the tibial component demonstrated high rotational imprecision of the system along the anterior-to-posterior axis due to the implant's symmetry. Simplifying the implant to its spherical tip, greatly improves the precision. *Left:* The talar component position was precisely repeated in this double exam.

Marker positions with a crossing-line distance (CLD) less than 0.1 mm were preferentially used in cases where the markers are densely packed to reduce the creation of imaginary markers from overlapping back projections within CLD that confounded the studies. This was the case for the marker configurations within the talus and distal tibia. The talar marker models (MMs) were used when needed to overcome issues with a multitude of marker back projection possibilities within the CLD threshold, and also independent marker migration. The tibial MMs were used to overcome issues with marker and implant over projection (i.e. the occluded marker problem[28]), and

independent marker migration as well. The mean error of rigid body fitting (ME) for these components was omitted from the Results as they are inherently zero; the defined MM rigid body does not deform. See Appendix C for the algorithm that generates the marker models.

The implant-based coordinate system was used, such that all positions were oriented with respect to the axes of the respective implants as described by Laende et al (2009).[37] This system of displacement vector projection orientation reduces errors caused by malalignment of the implant with the radiographic detector. The talar and tibial component coordinate systems were centered on the centroid of the implant model and oriented such that the x-axis was posterior to anterior, the y-axis was inferior to superior, and the z-axis was lateral to medial, Figure 2.4. Directional inversions were carried out to correct for anatomical directions for right- and left-sided implants, see Appendix A.

The implant movement was determined between double exams for the three translations (x, y, z), three rotations (Rx, Ry, Rz; where applicable) and maximum total point motion (MTPM) for each subject. Signed values were used for the translations and rotations per Valstar et al's (2005) recommendations for standardized reporting.[78] CN, ME and DIFF were also reported. A custom MATLAB® 2009a program was written to read the Model-based RSA 3.2 double exam output files, compile the data into a small database, process the data, and generate error box plots of the data, see Appendix A for the general algorithm.[37, 65]

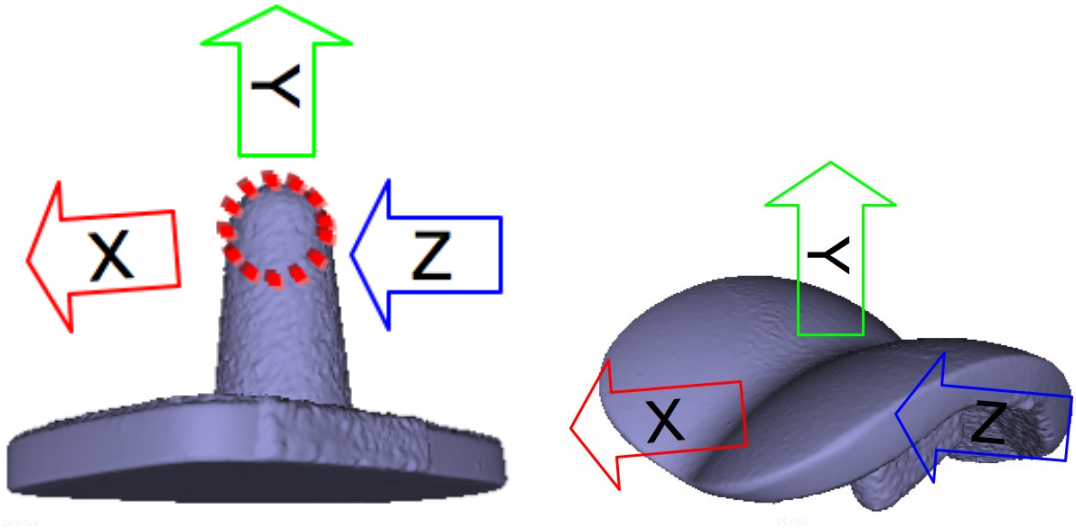

Figure 2.4: The implant coordinate system for the tibial component (*left*) and the talar component (*right*). The tibial component spherical tip is marked by the *red dotted circle*. *Red:* x-direction pointing posterior to anterior. *Green*: y-direction pointing inferior to superior. *Blue*: z-direction pointing lateral to medial.

2.2.6 Statistical Analysis

Descriptive statistics (mean, standard deviation (SD), 95%-confidence interval (95%CI), median, range) were compiled and calculated for the CN, ME, DIFF, x, y, z, R_x, R_y, R_z, and MTPM from the double exams in Microsoft® Excel 2004 for Mac (Microsoft Corporation, Redmond, WA) and MATLAB® 2009a (The MathWorks, Inc., Natwick, MA). The mean/median values indicate systemic error (i.e. measurement drift or bias), while the standard deviation/range represents the system precision. A sample of the algorithms for this code can be found in Appendix A.

An unpaired two-tailed t-test ($\alpha=0.05$) was used to compare and verify differences in ME, DIFF and CN between the tibia and the talar beads. Minitab® 15 software (Minitab Inc., State College, PA) was used to calculate Pearson correlation coefficients and *p*-values between CN, ME, number of matched markers used, and DIFF with respect to MTPM double exam error. These tests were used to look for abnormalities in the parameters.

2.3 Results

2.3.1 Phantom Study Results

The results of the first two cases using the proposed methodology were favorable and comparable. The CNs of the two cases were: case no. 1) tibia = 28 mm^{-1}, talus = 33 mm^{-1}, and case no. 2) tibia = 34 mm^{-1}, talus = 26 mm^{-1}. Two cases were examined using the standard MBRSA protocol.

The second case will be used in the following discussion of the results of marker distribution and standardization of the marker insertion technique. All the markers inserted into the tibia and talus deployed. There were a total of seven markers in the tibia and eight markers in the talus. The markers in the tibia were non-collinear. The marker in the anterior cortical window was not obscured by the prosthesis, as were the remainder of the markers in the tibia. The markers in the talus were well dispersed, not obscured by the component, and with the addition of the last two markers in the talus, the rigid body created was not clustered as in the phantom. As mentioned above, the worst-case CNs

were 34 mm^{-1} and 33 mm^{-1} in the tibia and talus respectively. These were more than adequate.

2.3.2 Double Exam Results

The results of the double exams were compiled into Table 2.1 (CN, ME, DIFF, x, y, z, R_x, R_y, R_z, MTPM), Figure 2.5 (x, y, z), Figure 2.6 (R_x, R_y, R_z), and Figure 2.7 (MTPM) for the talar, tibial components, and tibial component spherical tip. There are no rotational values for the spherical tip as the sphere was rotationally indeterminate during pose estimation. Table 2.1 summarizes the descriptive statistics (mean, SD, 95%CI, median, minimum, maximum) for the double exams. Median and range are used for parameters that are unsigned such as CN, ME, DIFF and MTPM. Figure 2.5, Figure 2.6, and Figure 2.7 use box plots to depict the spread and statistical information of the implants components for the translations, rotations and MTPM respectively. Three of the subjects had incomplete or missed double exams.

In Table 2.1 the SD and 95%CI are redundant measures, but both were shown to make these comparable to the various results formats in the RSA literature. Standardizing the results formats will improve the inter-study comparability as the numbers of TAA RSA studies grow.

The median (range) CN for the tibial bone was 33 mm^{-1} (25-166 mm^{-1}), while the talus bone was 29 mm^{-1} (22-103 mm^{-1}). The difference between them was not significant ($p=0.80$). Except for Subject 1, all of the CNs for all components were below the 50 mm^{-}

[1] threshold deemed optimal at this institution. The marker matches between exams, and number of markers in the MM had a median (range) of 7.5 (3-10) for the talus and 4 (3-6) for the tibia.

Table 2.1: Double exam results for the talar component, tibial component and tibial spherical tip of TAA RSA of the Mobility Total Ankle System (n=17). Grayed region indicates out-of-plane.

	CN [mm^{-1}]	ME [mm]	DIFF [mm]	x [mm]	y [mm]	z [mm]	R_x [°]	R_y [°]	R_z [°]	MTPM [mm]
Talar component										
mean				0.04	0.00	0.01	0.07	0.07	0.07	
stdev				**0.09**	0.04	0.05	0.29	0.36	**0.51**	
95%CI				±0.35	±0.08	±0.10	±0.57	±0.71	±1.00	
median	29	0.07	0.13							0.14
min	22	0.00	0.09							0.01
max	103	0.15	0.19							0.85
Tibial component										
mean				-0.08	0.00	-0.06	-0.03	-0.16	0.22	
stdev				**0.39**	0.10	0.14	0.33	**1.72**	0.81	
95%CI				±0.76	±0.20	±0.27	±0.65	±3.37	±1.59	
median	33	0.04	0.18							0.57
min	25	0.00	0.13							0.06
max	166	0.21	0.22							2.75
Tibial component spherical tip										
mean				-0.01	0.01	0.00				
stdev				**0.07**	0.06	0.03				
95%CI				±0.14	±0.12	±0.06				
median	33	0.04	0.04							0.07
min	25	0.00	0.03							0.01
max	166	0.21	0.06							0.22

Column labels: CN = condition number of the bone markers, ME = mean error of rigid body fitting of the bone markers, DIFF = contour difference of implant, x = posterior to anterior, y = inferior to superior, z = lateral to medial, R_x = lateral to medial tilt (roll), R_y = external to internal rotation (yaw), R_z = posterior to anterior tilt (pitch), and MTPM = maximum total point motion.
Row labels: mean/median = arithmetic average/middle value (system bias), stdev = standard deviation (system error), 95%CI = 95% confidence interval of the sample, min = minimum value, and max = maximum value.

The median (range) DIFF for the tibial component pose estimation was 0.18 mm (0.13-0.22 mm), indicating poor contour matching and issues with model symmetry. Poor contour matching has been attributed to dimensional tolerances of the implants.[76] To

avoid these confounding factors in assessing the system error, EGS pose estimation of the tibial component spherical tip was determined as well.

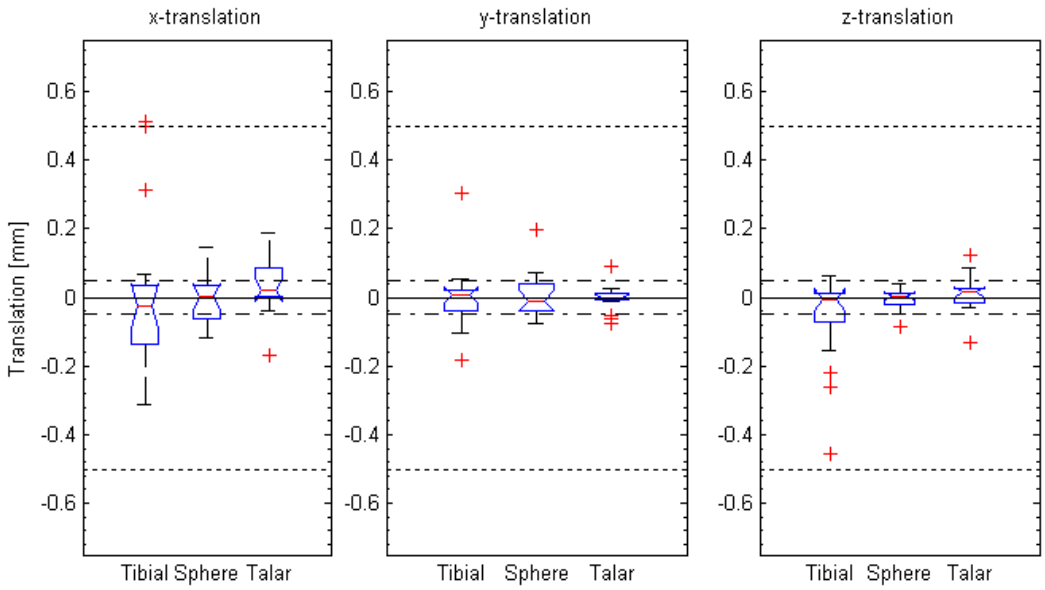

Figure 2.5: Box plots showing translational errors for the tibial component, tibial sphere, and talar component in the x, y, and z directions. Boxes bound 25th to 75th percentiles. The medians are the central *red lines*. Outliers (+) are indicated as outside the whiskers; or 1.5x the inter-quartile range beyond the 25th and 75th percentiles. The dashed and dotted lines show the bounding range of RSA accuracy reported in the literature (0.05-0.5 mm). Overlapping notched regions indicate that there are no significant differences (α = 0.05) between groups.

The mean (standard deviation) DIFF for the talus and tibia bone markers were 0.03 mm (0.02 mm) and 0.03 mm (0.02 mm) respectively. The difference between them was not significant ($p = 0.61$). The low talus and tibia bone marker DIFF demonstrates that the calibration box, and CLD bone marker selections are without issues.

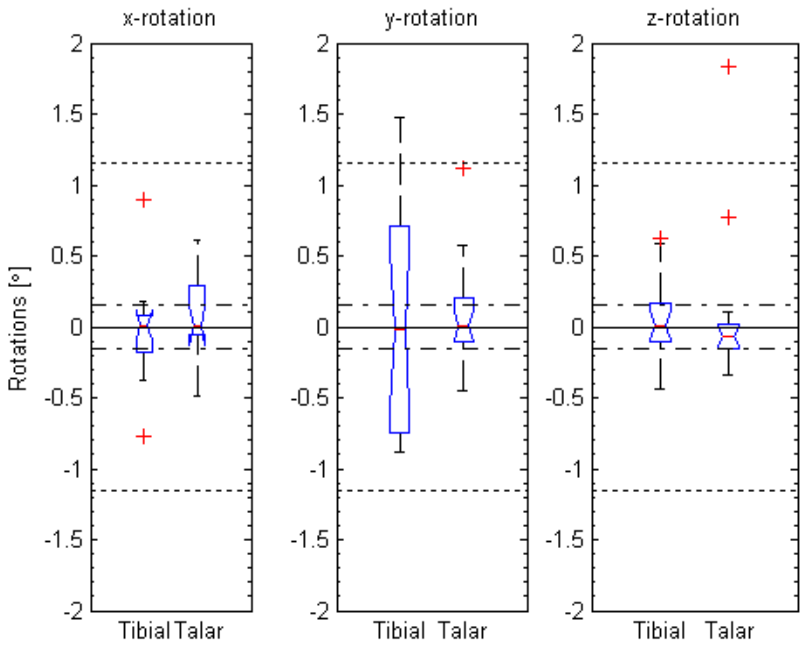

Figure 2.6: Box plots showing rotational errors for the tibial component, and talar component in the x, y, and z directions. Boxes bound 25th to 75th percentiles. The medians are the central *red lines*. Outliers (+) are indicated as outside the whiskers; or 1.5x the inter-quartile range beyond the 25th and 75th percentiles. The dashed and dotted lines show the bounding range of RSA accuracy reported in the literature (0.15-1.15°). Overlapping notched regions indicate that there are no significant differences ($\alpha = 0.05$) between groups.

There was no significant difference ($p = 0.33$) between the ME in the talus of 0.07 mm (0.04 mm) and the tibia of 0.06 mm (0.04 mm). This could suggest that the markers are equally stable in both the talus and the tibia. The markers were sufficiently stable between the double exams to determine precise double exam migration of the implants as ME was below the recommended 0.35 mm in all cases.[78]

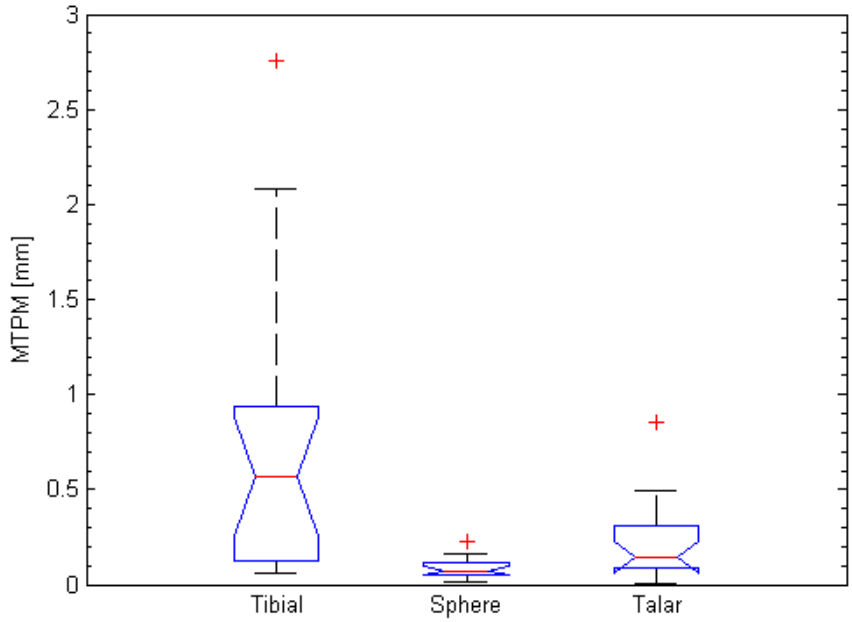

Figure 2.7: Box plots showing double exam errors for the tibial component, tibial sphere, and talar component in terms of maximum total point motion (MTPM). Boxes bound 25th to 75th percentiles. The medians are the central *red lines*. Outliers (+) are indicated as outside the whiskers; or 1.5x the inter-quartile range beyond the 25th and 75th percentiles. Overlapping notched regions indicate that there are no significant differences ($\alpha = 0.05$) between groups.

There was a moderate and significant correlation between CN and the marker matches for the talus ($r = -0.57$, $p = 0.016$), tibia ($r = -0.55$, $p = 0.022$), and both combined ($r = -0.45$, $p = 0.008$). This relationship is intuitive as increasing the number of markers can only reduce the CN.

There was no significant correlation between the MTPM double exam error and number of marker matches for the talar component ($r = -0.47$, $p = 0.059$) or the tibial component spherical tip ($r = -0.11$, $p = 0.68$). There was no correlation between MTPM double

exam error and CN; (*r = 0.39, p = 0.12*) for the talus, (*r = 0.07, p = 0.80*) for the tibia and (*r = 0.27, p = 0.13*) for both combined. Nor was a significant correlation between MTPM double exam error and ME detected; (*r = 0.27, p = 0.38*) for the talus, (*r = 0.19, p = 0.52* for the tibia and (*r = 0.27, p = 0.17*) for both combined. However, there was a high correlation (*r = 0.62, p = 0.000*) between MTPM double exam error and DIFF for all of the talar components, tibial components, and tibial component spherical tips combined.

The detection limit was set to be the range maximum of the double exam for MTPM, Table 2.1 and Figure 2.7. The detection limit was 0.85 mm for the talar component, 2.75 mm for the tibial component and 0.22 mm for the tibial component spherical tip.

2.4 Discussion

2.4.1 Phantom Study

For the phantom study, the slight increase in the CNs for the omitted case was due to the fact that the standardized technique was not precisely followed. With rigid compliance to the marker insertion technique developed in this study, the subsequent two cases had similar CNs resulting from markers placed in reproducible locations. The phantom study provided a stepwise progression in the marker configuration. This allowed for seamless methodological incorporation into the subsequent in vivo study. The marker insertion protocol developed through the phantom study can be used in additional TAA RSA studies.

2.4.2 Double Exams

The double exam results demonstrated that the methodology presented in this study can be used to assess the micromotion of TAA prostheses. The consistently low CNs (all but one were below 50) suggested that there was adequate marker distribution for the tibial and talar bone rigid bodies to act as a reference for their respective implant migrations. The redundancy of markers inserted (greater than three for the minimal rigid body representation), as shown by the median marker matches of 7.5 and 4 for the talus and tibia, allowed for successful evaluation of all the exams despite a few independent marker movements and over projections by the implant. The range in the number of bone markers used for the rigid bodies shows that deployment of markers during insertion was not fully controlled and that the insertion device was not reliable. This had not been an issue with this study due to the marker redundancy, but development on the marker insertion device has since been carried out at this institution.

The translational and rotational precision shown in Table 2.1 is comparable to existing marker-based RSA studies of other TAA implants.[7, 49] The maximum translation error (MTE), expressed as standard deviation, was 0.07 mm for the tibial component spherical tip and 0.09 mm for the talar component. The maximum 95% confidence interval for any direction for both the tibial sphere and the talar component was ±0.18 mm. The maximum rotational error (MRE) was 0.51° for the talar component. The maximum 95% confidence interval was ±1.00°. The MTE and MRE for the tibial component were omitted due to known issues with its symmetry. These maximums were not in the

expected out of plane directions associated with the uniplanar RSA set-up and suggested that the MBRSA pose estimation is a dominant influence.

The loss of rotational precision from this study when compared to other MBRSA studies of knee and hip implants can be attributed to the smaller size of the TAA implants and the CAD model used for the talar component.[27, 65, 76] The correlation ($r = 0.62$, $p = 0.000$) of MTPM and DIFF supports the suggestions from these other studies to use RE models, EGS, and/or low tolerance surface contours when using MBRSA technology. Simplifying the tibial component to its spherical tip greatly improved the results by removing the effects of dimensional tolerancing. In this case, the DIFF was reduced from 0.18 mm (0.13-0.22 mm) for tibial component to 0.04 mm (0.03-0.06 mm) for the tibial component spherical tip.

The unexpected lack of significant correlation of MTPM double exam error with marker matches and CN,[54] is likely due to the lower variation in the number of markers that could be used (also resulting a in lower variation in CN). The lack of correlation between MTPM and ME may be due to the lack of adherence to rigid body assumptions.[54] These results may have also been limited from being significant ($p \leq 0.05$) as a result of the low statistical power of this study. Low statistical power indicates that the sample size is not great enough to determine a statistical difference even if one actually exists in the full population, resulting in a false negative or Type II error. Inclusion of additional subjects may have been able to demonstrate the significance of adequate marker distribution.

The MTPM detection limits were identified as the range maximum. The detection limit values of 0.85 mm for the talar component, 2.75 mm for the tibial component and 0.22 mm for the tibial component spherical tip were used in the analysis of the subsequent studies examining the Mobility™ with the RSA set-up identified in this chapter.

2.5 Conclusions

It has been shown from this study that a reproducible RSA marker insertion technique in both the tibia and talus was established for this TAA prosthesis. The marker configurations used for the talus and tibia in this study can also be used for further studies implanting most other existing TAA prostheses and also AA at this and other institutions. This project has addressed the need to standardize protocols and result formats to allow inter-study comparison for the growing number of RSA studies of TAA. This study also confirms that the MBRSA can precisely and effectively assess the micromotion of TAA components.

2.5.1 Future Considerations

A worthwhile consideration may be to wait until a later longitudinal RSA follow-up such as at one year to do the double exams. This would allow for the bones to heal and remodel, providing an even more stable anchoring for the markers and reduce the double exam ME. It is likely that the double exam error would be reduced.

The follow-up longitudinal migration and inducible displacement studies over two years in these twenty patients will be the first time MBRSA has been used to assess the biomechanical fixation of a TAA prosthesis.

Further areas of study that could be initiated with RSA are measurement of marker motion in the cortical tibial window with respect to the tibial rigid body. This would indicate whether the cortical tibial window is migrating away from the prosthesis or whether it is stable as purported by the designers of the Mobility™ Total Ankle System. The markings on the UHMWPE bearing placed there by the manufacturer are evident on the radiographs and can be utilized by the MBRSA software to determine whether the polyethylene fuses with the component.

CHAPTER 3 : LONGITUDINAL MIGRATION

3.1 Introduction

Long-term implant survival has been strongly related to early implant migration.[32, 59, 68] Pioneering RSA joint replacement studies have shown in the hip by Karrholm et al,[32] and in the knee by Ryd et al,[59] that RSA measurements over a two year period is predictive of aseptic loosening. The established value of RSA in studying knee and hip replacements has made it a viable candidate in assessing the biomechanical stability of TAA.

Longitudinal migration studies have been historically the main mode of assessing orthopaedic implant stability using RSA. [2, 4, 7, 12, 32-34, 49, 51, 52, 59, 70] Longitudinal migration is the time-based micromotion of an implant with respect to the instant beginning immediately after surgery (postoperative).

There are great benefits to using longitudinal RSA studies to evaluate the biomechanical fixation of orthopaedic implants.[33] The first is that some disastrous introductions of new implants and surgical techniques can be potentially prevented by validating them in RSA trials with small sample sizes.[33, 50, 71] Thus the patient exposure to a potentially flawed prosthesis would be limited. The second is that short-term RSA results correlate with and predict long-term clinical results.[33] Furthermore, biomechanical modifications of implants may be identified and implemented allowing for a faster evolution of prosthesis design.

The groundbreaking study by Ryd et al (1995) demonstrated that a maximum total point motion (MTPM) greater than 0.2 mm from one year to two year followup in total knee replacements has been shown to be an 85% positive predictor of continued loosening leading to eventual implant failure.[59] Continuous migration was defined by a MTPM greater than this threshold of 0.2 mm. Implants in this category were likely to continue moving in the bone without becoming properly fixated and eventually migrated to the point of failure. The traditional ten year followup time to evaluate an orthopaedic implant had been reduced to just two years through the use of RSA.

Classical marker-based radiostereometric analysis (RSA) has been used to assess the precise 3D longitudinal migration of the Scandinavian Total Ankle Replacement® (STAR) (W. Link and Co., Hamburg, Germany) tibial and talar implants, and the Buechel-Pappas™ (BP) (Endotec, New Jersey, USA) total ankle prosthesis tibial implant. The results of these studies, indicate that the majority of the implants migrate initially (subside) then stabilize; reported in 6 weeks for the STAR, and 6 months for the BP.[7, 49]

The present study examined the longitudinal migration of the Mobility™ Total Ankle System (DePuy, Indiana, USA) tibial and talar implants using novel model-based RSA (MBRSA) technology over a two-year period. The hypothesis is that the migration data will be comparable to other orthopaedic RSA studies found in the literature showing initial subsidence followed by stabilization.

3.2 Methods and Materials

The same 20 subjects implanted with the Mobility™ that were studied in the System Precision and Clinical Validation chapter (Chapter Two) were assessed in this followup longitudinal migration study.

Uniplanar RSA X-rays were taken at 6 week, 3 month, 6 month, 1 year and 2 year follow-up times using a supine (unloaded condition) position. The RSA radiographic set-up conformed to the procedure described in Chapter Two.

Implant longitudinal migrations were assessed using Model-based RSA 3.2 (Medis specials, Leiden, The Netherlands) with respect to the postoperative reference exam. Implant migration patterns (x, y, z, R_x, R_y, R_z, MTPM) were determined and assessed for each subject using the implant-based coordinate system described in the previous chapter. Migrations were determined using model-based pose estimation.[27, 65] The Elementary Geometric Shapes (EGS) module from the Model-based RSA 3.2 software was used to assess the migration of the tibial component spherical tip.[29] Marker models (MMs) were identified from bone markers and used in cases where there were marker obstructions and/or independent marker migrations.[28] The algorithm for the MM generator used and brought up in the previous chapter is found in Appendix C.

A custom MATLAB® 2009a code (The MathWorks, Inc., Natwick, MA) was used to read migration Model-based RSA 3.2 output files, analyze the migration data, and to generate plots. A sample of the algorithms for this code can be found in Appendix A.

RSA exams were removed where the mean error of rigid body fitting (ME) exceeded 0.2 mm because independent marker migrations appeared to dominate the migration calculations resulting in noisy migration patterns despite being below the suggested 0.35 mm threshold.[78] The same threshold was used by Dunbar et al (2009).[14]

Implant longitudinal migration results were compared with the longitudinal migration marker-based RSA results for the STAR and BP prosthesis.[7, 49] Both of these implants showed a group tendency to subside initially then stabilize.

3.3 Results

3.3.1 Subject Specific Results

The subject-specific longitudinal migration plots for the talar components and tibial component spherical tips are shown in Figure 3.1 and Figure 3.2. The plots for the tibial component were placed in Appendix B in favour of the tibial component spherical tip plots that have a finer detection limit. Some subject-specific migration curves are discontinuous as several patients missed followup appointments. The missed followups included 2 that had no postoperative, 3 that missed their six week, 4 that missed their three month, 2 that missed their six month, 4 that missed their one year, and 5 that missed their two year RSA exams. These omissions can be seen the raw data in Appendix D. Generally for each subject and implant component, the slopes of the migration curves decreased over time.

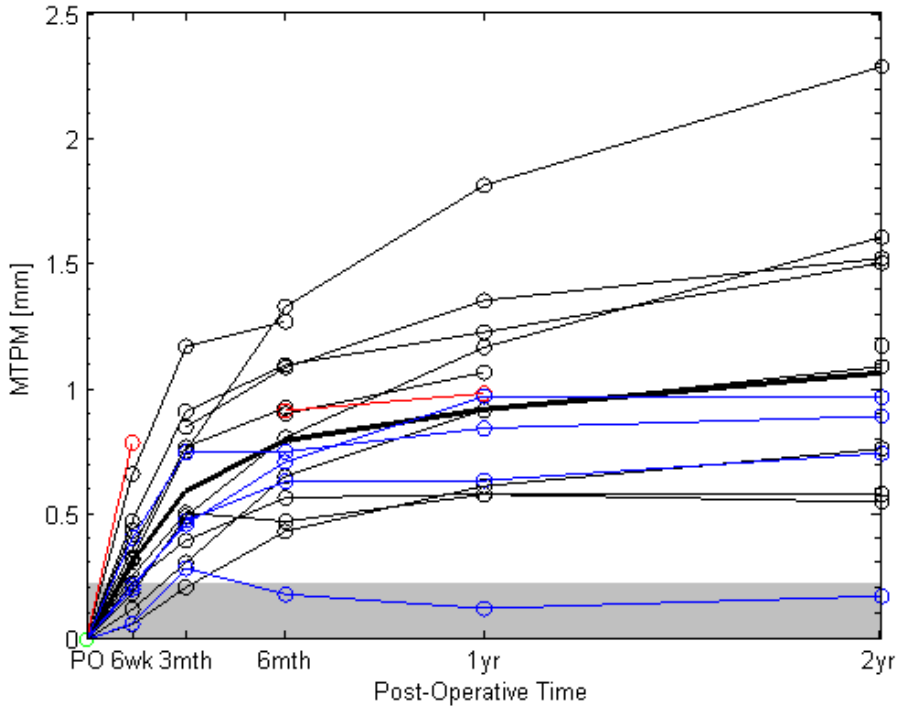

Figure 3.1: Tibial component spherical tip MTPM longitudinal migration. *Thin black:* individual subjects. *Thick black:* group mean. *Red:* subject that underwent surgical revision. *Blue:* subjects with pre- or post-surgical complications. *Shaded region:* shows the detection limit, 0.22 mm, or the minimum motion of any one implant with respect to the postop exam required for definite motion to be detected. The discontinuities and missed data points indicated where the patients missed followup exams or that the exams were unusable.

A surgical revision was carried out on one subject during the follow-up period. Subject 6, had surgical revision after one year to a Hintegra® Total Ankle (Newdeal® SA, Lyon, France) and as a result followup was incomplete. An interesting finding was that the tibial component had a maximum rotation of -7.57° in the R_y-direction at 6 week followup, see Appendix D; this was well beyond the 95%CI of ±3.37°, Table 2.1. This patient is shown in *red* in Figure 3.1 and Figure 3.2.

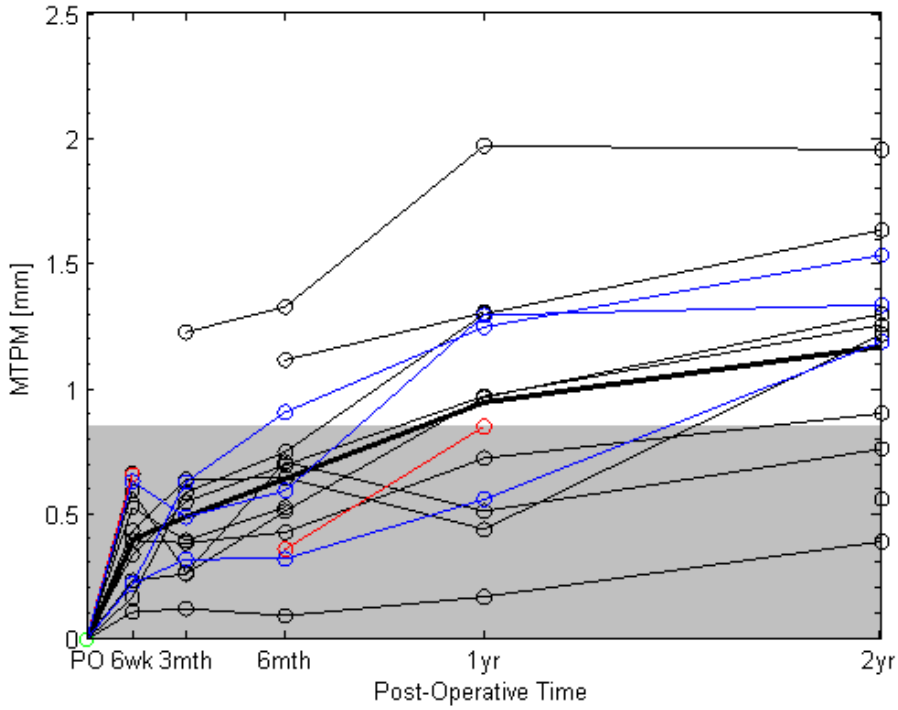

Figure 3.2: Talar component MTPM longitudinal migration. *Light black:* individual subjects. *Thick black:* group mean. *Red:* subject that underwent surgical revision. *Blue:* subjects with pre- or post-surgical complications. *Shaded region:* shows the detection limit, 0.85 mm, or the minimum motion of any one implant with respect to the postop exam required for definite motion to be detected. The discontinuities and missed data points indicated where the patients missed followup exams or that the exams were unusable.

Subjects 11 and 19 were omitted due to missed postoperative exams. Subject 10 was omitted due to substantial independent bone marker migrations (ME > 0.2 mm). Subjects 1, 2, 4, 6, 7, 11 and 14 had pre- or postoperative surgical complications but had complete follow-up. These patients are shown in *blue* in Figure 3.1 and Figure 3.2.

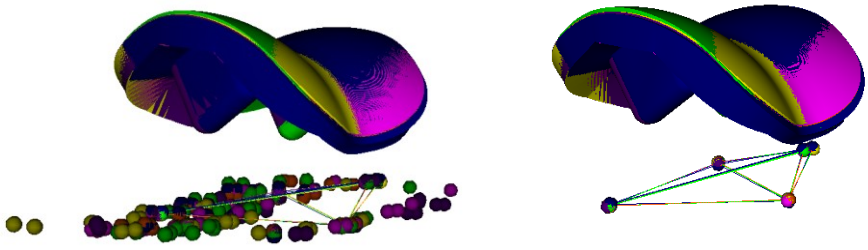

Figure 3.3: Marker matching code reduces marker location possibilities for Subject 2 from a multitude of overlapping back projections. *Left:* 221 possible marker locations from 6 consecutive RSA exams. *Right:* 28 highly repeatable marker locations selected by the marker matching algorithm, see Appendix C. Exam color code: *yellow*: postop, *pink*: 6wks, *blue*: 3mths, *orange*: 6mths, *purple*: 1yr, and *green*: 2yrs.

Marker models (MMs) were used for four of the 17 talus rigid bodies and two of the 17 tibia rigid bodies. In the case of Subject 2, a marker matching code was developed in MATLAB® 2009a to reduce the number of back projection possibilities within crossing-line distance (CLD ≤ 0.5 mm) and to generate a MM, Figure 3.3. This code reduced the possibilities by assuming that the most likely markers locations are those that have moved the least from each successive followup exam. These MM generated was found to be closely similar to the rigid body identified by reducing the CLD threshold to 0.1 mm. The algorithm for the MM generator and marker matching can be found in Appendix C.

3.3.2 Group Results

The talar and tibial implants mean longitudinal migration showed initial subsidence in the y-direction (migration into the bone) followed by stabilization patterns at one year followup. The *thick black lines* on Figure 3.1 and Figure 3.2 show this. It is important to

note that the mean curves contain discontinuous data and should not be considered continuous.

Table 3.1 summarizes the one year and two year followup longitudinal migration results for the Mobility™. The median (range) maximum total point motion (MTPM) seen in Table 3.1 for the implants at 2 year followup were 1.23 mm (0.39-1.95 mm) for the talar implant and 0.96 mm (0.17-2.28 mm) for the spherical tip of the tibia implant. The median and range were used, as MTPM is an unsigned value.

Table 3.1: Longitudinal migration MTPM results at 1 year and 2 years for the talar component, tibial component, and tibial spherical tip of TAA RSA of the Mobility™ Total Ankle System (n=17).

1 Year MTPM [mm]		2 Year MTPM [mm]	
median	range	median	range
Talar component			
0.96	0.17-1.97	1.23	0.39-1.95
Tibial component			
1.80	0.31-3.30	1.98	0.41-5.49
Tibial component spherical tip			
0.94	0.12-1.81	0.96	0.17-2.28

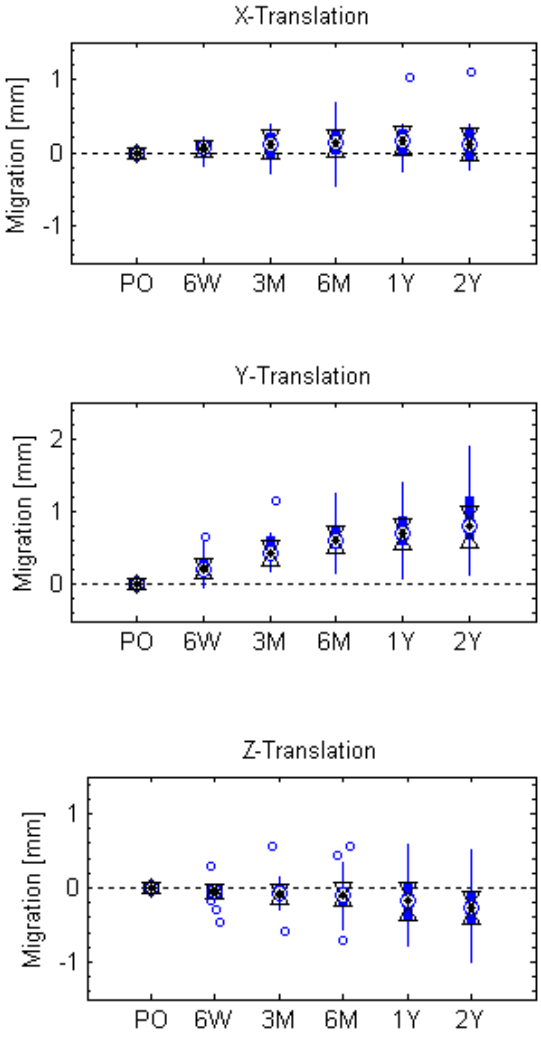

Figure 3.4: XYZ translation box plots for the tibial component spherical tip longitudinal migration. Boxes bound 25th to 75th percentiles. Medians are the centers of the larger circles. Outliers (*circles*) are indicated as outside the whiskers; or 1.5x the inter-quartile range beyond the 25th and 75th percentiles. *Followup times are denoted:* PO = postoperative, 6W = 6 weeks, 3M = 3 months, 6M = 6 months, 1Y = 1 year, and 2Y = 2 years. Overlapping notched regions indicate that there are no significant differences (α = 0.05) between groups.

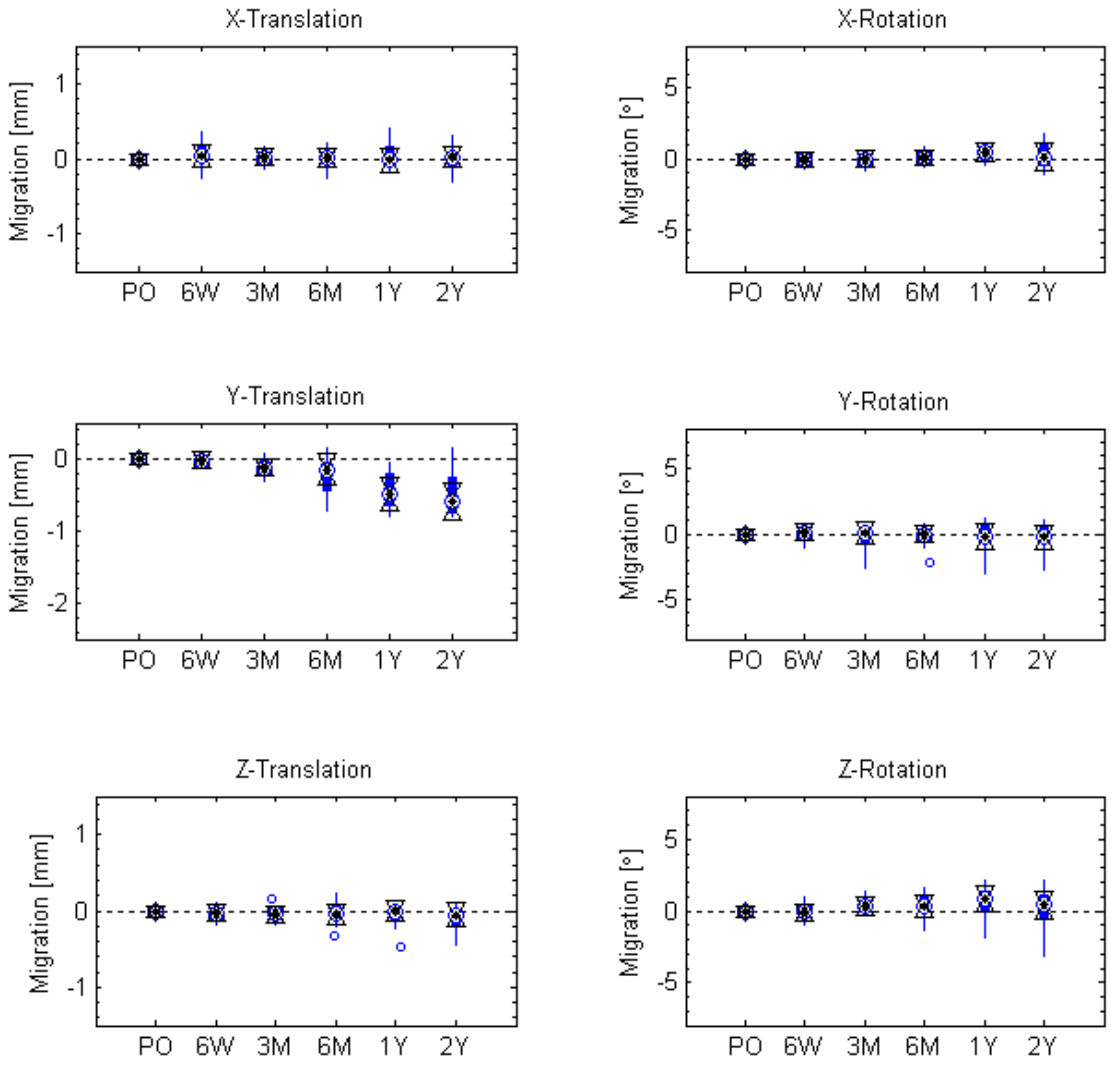

Figure 3.5: XYZ translation (*left*) and rotation (*right*) box plots for the talar component longitudinal migration. Boxes bound 25th to 75th percentiles. Medians are the centers of the larger circles. Outliers (*circles*) are indicated as outside the whiskers; or 1.5x the inter-quartile range beyond the 25th and 75th percentiles. *Followup times are denoted:* PO = postoperative, 6W = 6 weeks, 3M = 3 months, 6M = 6 months, 1Y = 1 year, and 2Y = 2 years. Overlapping notched regions indicate that there are no significant differences ($\alpha = 0.05$) between groups.

Figure 3.4 and Figure 3.5 show the tibial sphere migration and talar component migration respectively in the form of box plots for each of the three directions of motion. The plots

for the tibial component can be found in Appendix B. Subsidence in the y-direction (inferior to superior) is shown to be main direction of movement by these figures. There is high variability in all directions shown by the spread of the box plots.

3.4 Discussion

Thanner et al (1995) has suggested that subsidence may still be the best predictor of painful migration in TAA.[71] The decreasing slope of the subject specific migration curves over time, Figure 3.1 and Figure 3.2, suggests a typical initial subsidence-stabilization behaviour seen in most RSA literature of joint replacement implants.[32, 59] The greatest translational motions over time seen in Figure 3.4 and Figure 3.5 are in the y-direction or inferior to superior direction. This corresponds to the implants subsiding deeper into the bones in the primary direction of loading while walking or standing. Mean and subject-specific subsidence and stabilization patterns in the inferior to superior directions were similar to those seen in previous TAA RSA publications.[7, 49]

One study noted that some complications with TAA are associated with specific TAA implants.[11] The results for the only surgical revision to date, Subject 6, showed that this patient's tibial implant migrated more in the initial 6-week stage than any of the other implants; see Figure 3.1. This suggests that the failure mode of this implant is related to the instability of the tibial component. The symmetry of the conical stem may play a role in its failure as the implant can rotate more freely about the conical axis. This was supported in that the tibial component for Subject 6 had a maximum rotation of R_y = −7.57° at 6 weeks, see Appendix D, where the double exam 95%CI was ±3.37°, Table

2.1. Another nonexclusive possibility is that bone healing and/or osteointegration had not occurred for this subject. It is unfortunate that the MBRSA pose estimation and related rotations are imprecise due to the same symmetry that may be making this component unstable. This could very well be masking the migration of the tibial component in this direction for these patients. To allow for design feedback this migration data will need to be examined further as more revision data becomes available. These results suggest that tibial component stem could be modified to improve stability, such as anti-rotation fins.

Carlsson et al (2005) and Nelissen et al (2006) determined that stabilization of TAA implants had occurred at 6 week followup for the STAR and at 6 month followup for the Buechel-Pappas prosthesis tibial component respectively.[7, 49] Based on the same loose criteria and reduction in migration slope, such that the motion of the implant from 1-2 years is undetectable, in Figure 3.1 and Figure 3.2, stabilization does not appear to occur until 1 year for the Mobility™ for both components for most subjects. The slope of the MTPM migration curves is not detectably different from zero for one to two year motion in all subjects, for both components, except for the tibial spheres of Subjects 9, 12 and 17. This was calculated from the difference between the one and two year MTPM data in Appendix D; only 12 of these subjects have data that allows this calculation due to the ME exclusions.

Detectable MTPM from one to two years, or continuous migration, for TAA may be still predictive of premature failure within 10 years as is seen in TKA.[59] Additional research is required to more completely document the acceptable early migration of different TAA

implant designs and their components. The MPTM threshold of 0.2 mm used in the RSA of total knee arthroplasty may not be suitable for use with total ankle arthroplasty. There are anatomical and physiological differences between the two joints that likely factor into this problem. Further studies are required to establish a threshold for continuous migration such as that identified for arthroplasty of the other lower extremity joints.[34, 59]

The high variability in the subject-specific implant migration shown by the box plots in Figure 3.4 and Figure 3.5 suggests there are also differences in the implant in vivo mechanics. TAA prostheses need to adapt to the broad range of strenuous mechanical conditions due to inter-patient anatomical and activity level variability. This variability may be related to the mean (standard deviation) age of 60.4 (12.2) years old and BMI of 29.1 (2.8) kg/m^2. Subject-specific mechanical conditions may be better captured by appropriate biomechanical studies such as gait analysis,[13, 38, 39, 56] and compared with these longitudinal implant migration results. In this way a correlation may be determined between gait parameters and migration.

3.5 Conclusions

MBRSA has been successfully used for the first-time to assess the biomechanical fixation of a TAA prosthesis. The median (range) MTPM at one year followup was 0.94 mm (0.12-1.81 mm) for the tibial component spherical tip and 0.96 mm (0.17-1.97 mm) for the talar component. At two year followup this was 0.96 mm (0.17-2.28 mm) for the tibial component spherical tip and 1.23 mm (0.39-1.95 mm) for the talar component. The primary direction of migration for both implants was in the y-direction; the implant

subsides directly into the bone in the line of primary loading during standing or walking. For most of the patients the two year longitudinal migration for the Mobility™ demonstrates a typical subsidence-stabilization behaviour seen in many RSA studies of orthopaedic implants.

CHAPTER 4 : INDUCIBLE DISPLACEMENT

4.1 Introduction

Like continuous longitudinal migration of a prosthesis with respect to the bone in which it is embedded, inducible displacement of the prosthesis is regarded as an ominous sign.[61] Inducible displacement is thought to possibly lead to clinical loosening.[61] There was correlation between one year and two year MTPM longitudinal migration and inducible displacement results of a knee arthroplasty tibial monoblock component; up to $r = 0.701$, $p < 0.001$ depending on loading conditions.[81]

Inducible displacement is the instantaneous micromotion of an implant under a *loaded condition* (i.e.- standing) with respect to an *unloaded condition* (i.e.- supine) at the same followup time. This displacement is thought to reflect the quality of the bone-implant interface.[61, 81] There are several RSA studies of total knee arthroplasty (TKA) that examine inducible displacement.[60, 61, 73, 81] There is currently no known published literature on inducible displacement RSA studies for total ankle arthroplasty.

Inducible displacements in TKA components are typically found to be in the range of 0.2 to 1.0 mm.[61, 73, 81] Inducible displacements of less the 0.3 mm in tibial knee components are thought to be due to elasticity of the overlying implant and underlying bone and do not indicate micromotion of the bone-implant interface.[41, 81] Displacements greater than this 0.3 mm plus the measuring system error can be attributed to the behavior of the bone-implant interface. The detection limit for MTPM was 0.85 mm for the talar component and 0.22 mm for the tibial component spherical tip.

The present study examined the inducible displacement of a TAA system's, Mobility™, tibial and talar implants using novel model-based RSA (MBRSA) technology at 3 month, 6 month, 1 year and 2 year followup times. The hypothesis is that displacements will be detectable in patients when comparing their standing (loaded condition) RSA exam to their supine (unloaded condition) RSA exam at the set followup times.

4.2 Methods and Materials

The same 20 subjects implanted with the Mobility™ that were studied in the preceding System Precision and Clinical Validation chapter (Chapter Two) and the simultaneous Longitudinal Migration chapter (Chapter Three) had the inducible displacement of their implants studied.

Uniplanar RSA X-rays taken at 6 week, 3 month, 6 month, 1 year and 2 year follow-up times using a supine (*unloaded condition*) position as a part of the longitudinal migration study. The RSA radiographic set-up conformed to the procedure described in Chapter Two. *Loaded condition* or standing exams were taken at 3 month, 6 month, 1 year and 2 year followup intervals. These RSA exams were taken with the patient standing vertically with their body weight distributed between both legs. The x-ray radiographs and foci were 40° apart and were in the same relative orientation to the subjects as in Chapter Two. The *unloaded condition* and *loaded condition* RSA exams were taken during the same followup appointments. The rest of the RSA radiographic set-up conformed to the procedure described in Chapter Two.

The *loaded condition* or standing exams were compared to the *unloaded condition* or supine exams at the same followup time using Model-based RSA 3.2 (Medis specials, Leiden, The Netherlands). The induced micromotion was determined for the three directions of translation (x, y, z), three directions of rotation (R_x, R_y, R_z) and MTPM for each subject at each time point using the implant-based coordinate system described in the Chapter Two. Implant displacements were determined using model-based pose estimation.[27, 65] The Elementary Geometric Shapes (EGS) module from the Model-based RSA 3.2 software was used to assess the migration of the tibial component spherical tip.[29] Marker models (MMs) were identified from bone rigid bodies and used in cases where there were marker obstructions.[28] The independent marker migrations were less of an issue for this study than in the longitudinal migration study as the markers had very little time to move between exams. The algorithm used for the MM generator is found in Appendix C.

A custom MATLAB® 2009a code (The MathWorks, Inc., Natwick, MA) was used to read inducible displacement Model-based RSA 3.2 output files, analyze the inducible displacement data, and to generate plots. A sample of the algorithms for this code can be found in Appendix A. RSA exams were removed where the mean error of rigid body fitting (ME) exceeded 0.2 mm because independent marker migrations appeared to dominate the displacement calculations despite being below the suggested 0.35 mm threshold.[78] The same threshold was used by Dunbar et al (2009).[14]

4.3 Results

Box plots for the inducible displacement in the three directions of translation (x, y, z) and rotation (R_x, R_y, R_z) for talar components and tibial component spherical tips are shown in Figure 4.2 and Figure 4.4. While their MTPM box plots are shown in Figure 4.3 and Figure 4.5. Some data is discontinuous as several subjects missed followup appointments or did not receive an inducible displacement RSA exam. There were missed inducible displacement results for 3 patients at three months, 2 patients at six months, 3 patients at one year, and 5 patients at two year followup.

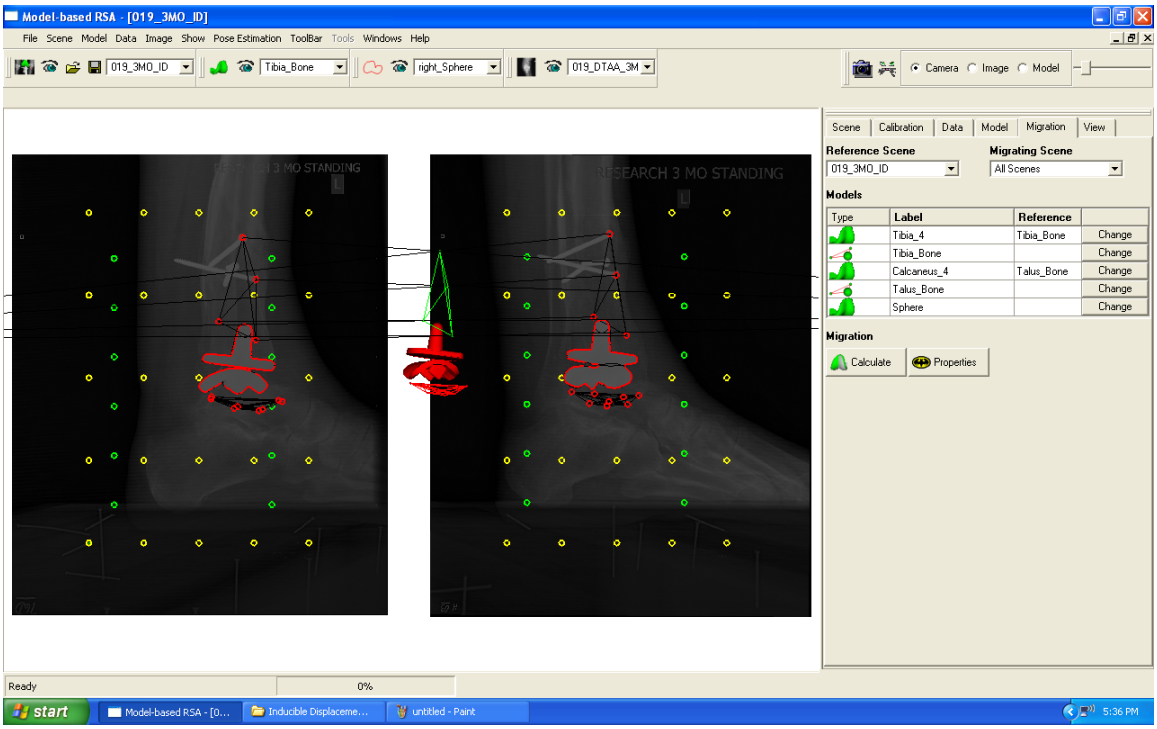

Figure 4.1: Model-based RSA 3.2 (Medis specials, Leiden, The Netherlands) screen shot showing the use of screw heads (upper two red circles in both radiographic views) to compensate for insufficient markers.

Subject 6 had surgical revision after one year and as a result followup was incomplete. Subject 19 required a novel solution for the tibial bony rigid body because insufficient bone markers were visible. In this case, the screw heads from a previous fracture fixation that were not part of the TAA prosthesis were used to act as substitution markers, refer to Figure 4.1. The ME values were less than 0.2 mm and suggested that the screw heads were well fixed.

There is minute evidence of subsidence under the loading condition in the tibial tip in a few implants as indicated by the vertical offset of the box plots in Figure 4.2 (*middle*) in the y-direction. Similarly, there are some implants that are vertical offset in the box plots in Figure 4.2 (*top*) in the x-direction suggesting that some are moving posteriorly under load as indicated by the whiskers.

The tibial component spherical tip demonstrates no measurable inducible displacement in terms of MTPM, greater than 0.22 mm in Figure 4.3 and Table 4.1, at the one year and two year followup times. An indication of this is that the shaded region completely encompasses the full range of the box plots at one year and two year followup in Figure 4.3.

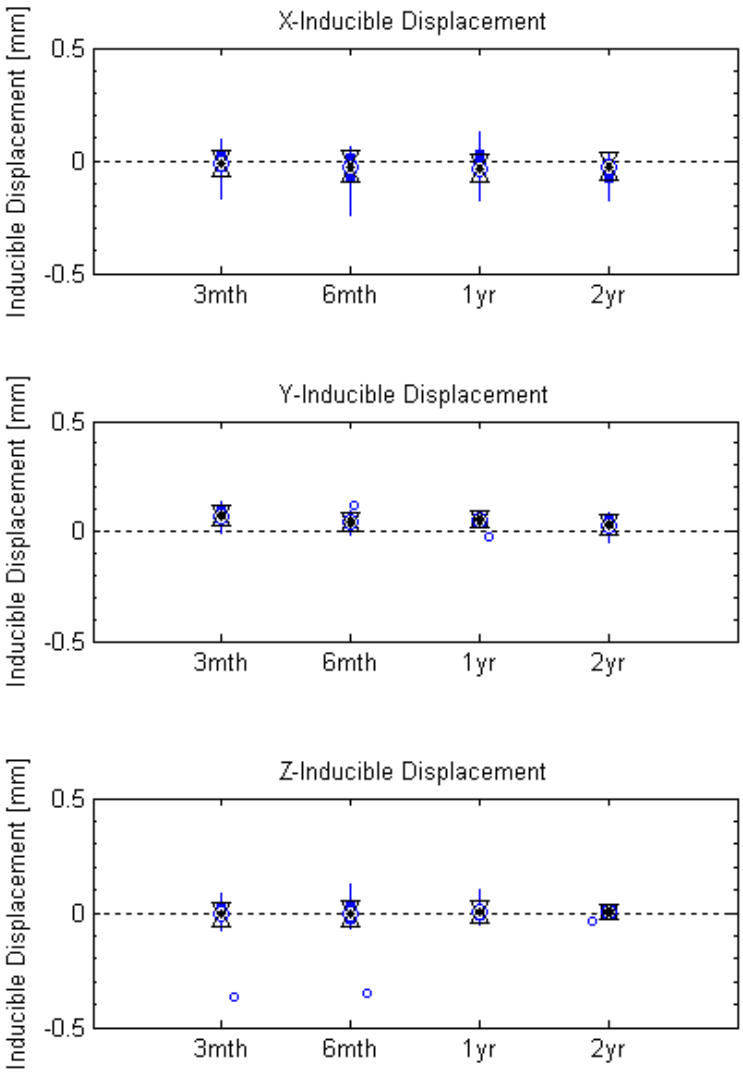

Figure 4.2: XYZ translation box plots for the tibial component spherical tip inducible displacement. Boxes bound 25th to 75th percentiles. Medians are the centers of the larger circles. Outliers (*circles*) are indicated as outside the whiskers; or 1.5x the inter-quartile range beyond the 25th and 75th percentiles. Overlapping notched regions indicate that there are no significant differences ($\alpha = 0.05$) between groups.

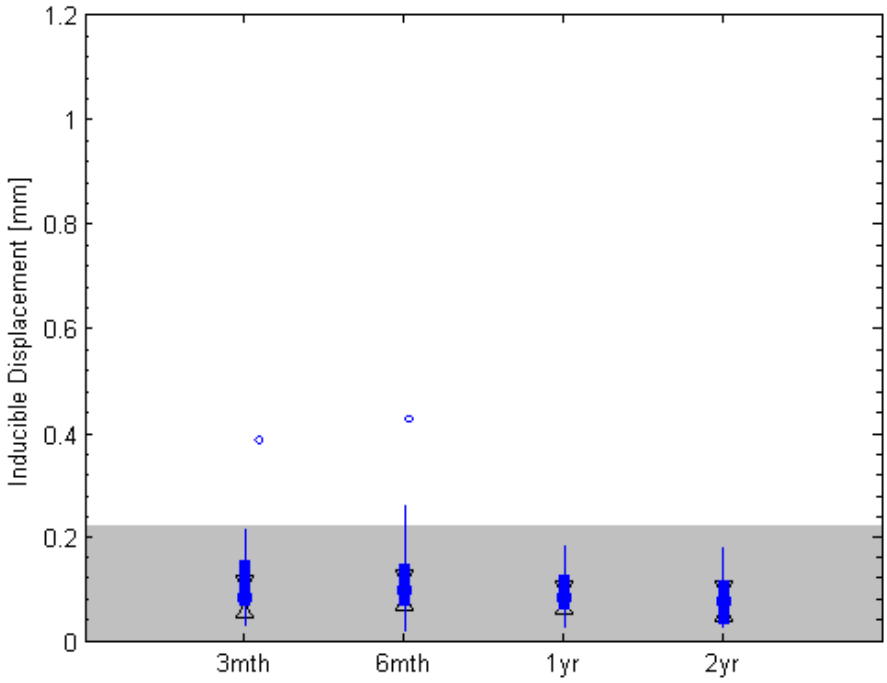

Figure 4.3: MTPM box plots for the tibial component spherical tip inducible displacement. Boxes bound 25th to 75th percentiles. Medians are the centers of the larger circles. Outliers (*circles*) are indicated as outside the whiskers; or 1.5x the inter-quartile range beyond the 25th and 75th percentiles. *Shaded region:* shows the detection limit, 0.22 mm, or the minimum motion of any one implant with respect to the supine exam required for definite motion to be detected. Overlapping notched regions indicate that there are no significant differences ($\alpha = 0.05$) between groups.

The behavior of the talar component under load is very similar to the tibial component sphere. There is slightly more evidence of subsidence (up to 0.15 mm) in the talar component at one and two years as indicated by the vertical offset of the box plots in Figure 4.4 (*middle left*) in the y-direction. There is slight inducible horizontal (xz-plane) motion (up to 0.3 mm) and rotation (up to 3°) in the talar component at one and two years

seen in Figure 4.4. This is the major contributor to MTPM based on the magnitudes. Part of this measured motion may be due to pose estimation errors.

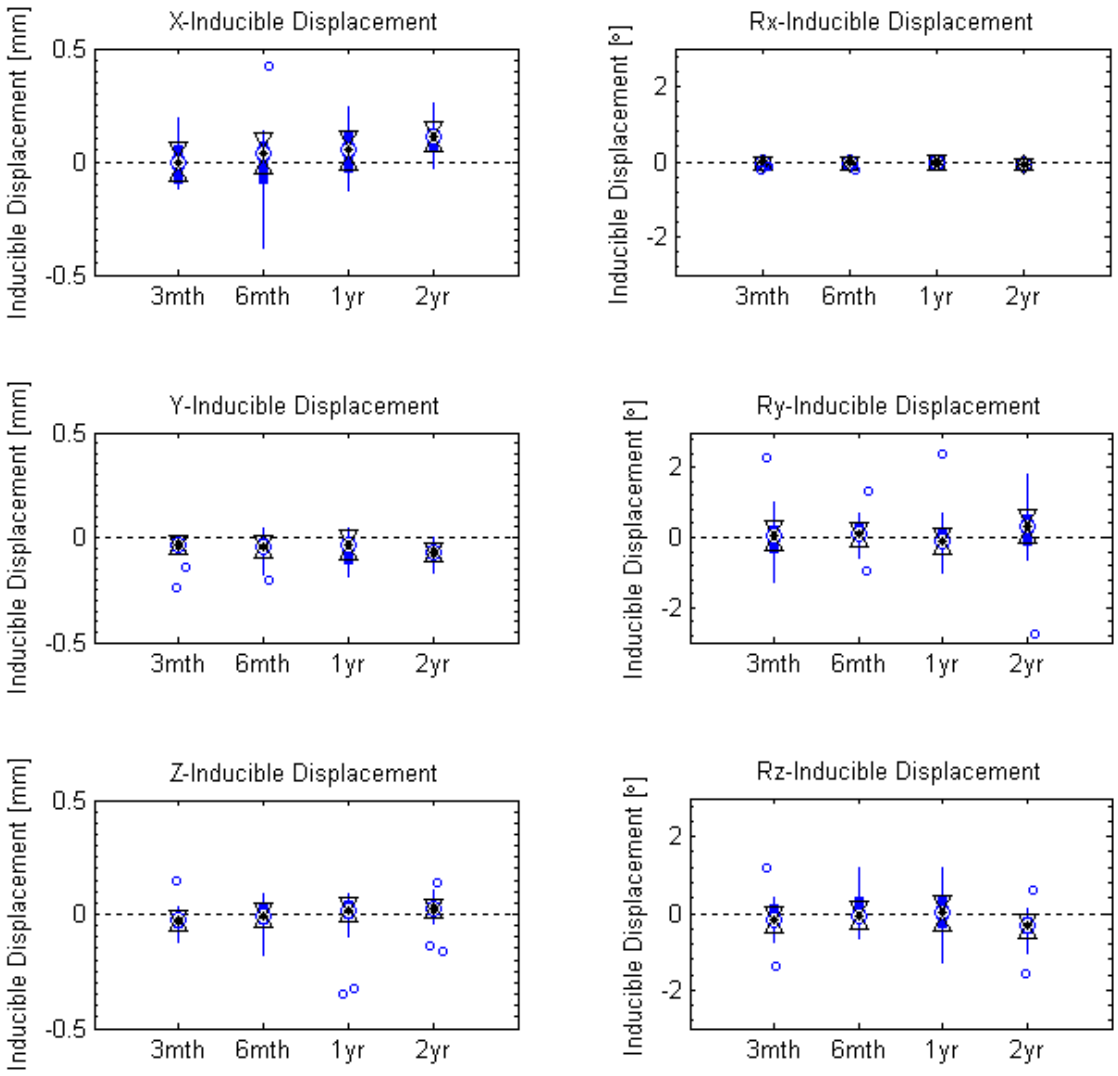

Figure 4.4: XYZ translation and rotation box plots for the talar component inducible displacement. Boxes bound 25th to 75th percentiles. Medians are the centers of the larger circles. Outliers (*circles*) are indicated as outside the whiskers; or 1.5x the inter-quartile range beyond the 25th and 75th percentiles. Overlapping notched regions indicate that there are no significant differences ($\alpha = 0.05$) between groups.

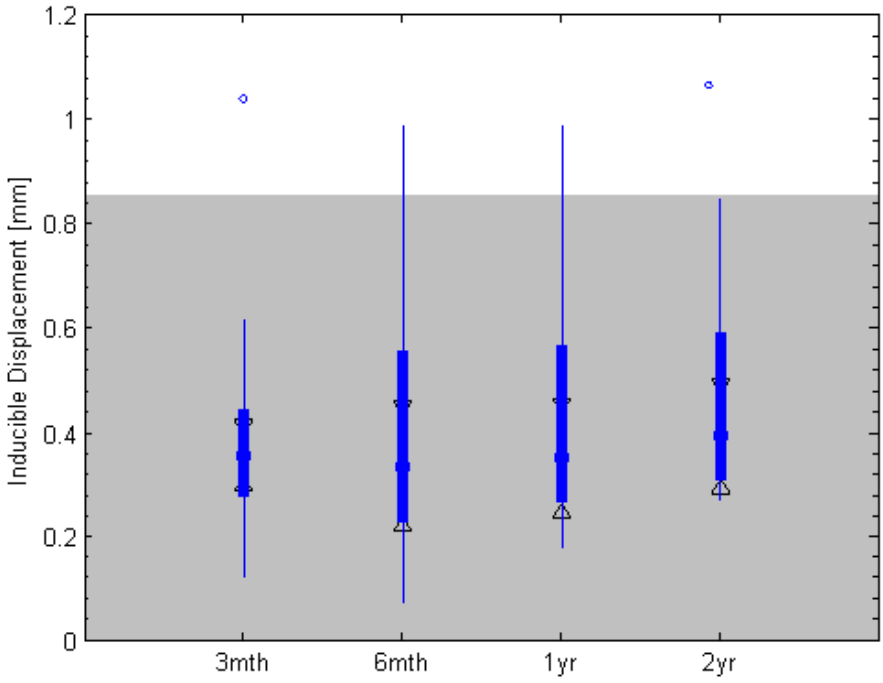

Figure 4.5: MTPM box plots for the talar component inducible displacement. Boxes bound 25th to 75th percentiles. Medians are the centers of the larger circles. Outliers (*circles*) are indicated as outside the whiskers; or 1.5x the inter-quartile range beyond the 25th and 75th percentiles. *Shaded region:* shows the detection limit, 0.85 mm, or the minimum motion of any one implant with respect to the supine exam required for definite motion to be detected. Overlapping notched regions indicate that there are no significant differences ($\alpha = 0.05$) between groups.

The inducible displacement for the MTPM of the talar component, Figure 4.5 and Table 4.1, is slightly more interesting than that of the tibial component spherical tip. At the one year and two year followup times the inducible displacements were almost all below the measurable detection limits (0.85 mm). The highest measured displacement for any one talar component at either of these times was 1.06 mm. Hence, the implant was displaced at least 0.21 mm under loading.

Table 4.1: Inducible displacement MTPM results at 1 year and 2 years for the talar component, and tibial spherical tip of TAA RSA of the Mobility™ Total Ankle System (n=18).

1 Year MTPM [mm]		2 Year MTPM [mm]	
median	range	median	range
Talar component			
0.35	0.18-0.99	0.39	0.27-1.06
Tibial component			
1.36	0.20-4.02	1.22	0.63-3.52
Tibial component spherical tip			
0.09	0.03-0.19	0.08	0.03-0.18

4.4 Discussion

The horizontal plane components, x- and z-axis motion, of the tibial and talar component inducible displacement, Figure 4.2 and Figure 4.4, may be due to a combination of component instability (i.e.- fibrous tissue ingrowth), measurement error (i.e.- out-of-plane and pose estimation), and/or uneven subject-specific loading across the ankle joint.

The inducible displacement results were compared with published literature on total knee arthroplasty (TKA) tibial components,[61, 73, 81] as no literature is known to exist on inducible displacement in TAA implants. This established a range of values that could reasonably be expected in this study. The interpretation of inducible displacement for TKA has been debatable.

The range of two year MTPM inducible displacement for the talar component was 0.27-1.06 mm. This is comparable to that of a total knee arthroplasty tibial component (0.2 to 1.0mm).[61] There is a minute detectable motion in one talar component of at least 0.21

mm that was observed in Figure 4.5 as the detection limit was 0.85 mm. This may just be the elasticity of bones and implants which is thought to account for up to 0.3 mm of inducible displacement in TKA prostheses.[41, 62, 81] Therefore, it is likely that there is no measurable inducible displacement that can be solely attributed to bone-implant interface alone.

The range of one year and two year MTPM inducible displacements for the tibial component spherical tip was 0.03-0.19 mm. There is no detectable motion of the tip because our detection limit is 0.22 mm. This is somewhat comparable to that of knee arthroplasty tibial monoblock component (0.1 to 0.4mm).[81] At this point it is hard to judge whether the tip is rigidly fixated with bone ingrowth or not because the base of the implant may be the more dominant mechanical interface.

There is a low yield in detectable inducible motion seen in Figure 4.3 and Figure 4.5. The signal may be too small if there is high rigidity resulting in little deformation and/or if there is insufficient loading to be detectable. A possible solution to improve load detection may be to increase the loading. The value of additional loading should be evaluated further because this may lead to patient injury. Another would be to alter the direction or type of loading (i.e.- compression, tension or torsion).

The reasons for detecting little or no inducible displacement in terms of MTPM may have been that: 1) the tissues around the Mobility™ were resistant to inducible displacement under these loading conditions, and/or 2) the measurement detection limits were too high

(i.e.- 0.85 mm). MBRSA of the talar component may not be effective in performing measurements of inducible displacement. Patient guarding their treated leg may tend to support most of their weight with their untreated leg and therefore contribute to issues arising from the first reason. It was impossible to determine if this had been occurring with the existing set-up. It is apparent that this is a major drawback of using double leg support as the loaded condition. Control of the loading may have been improved through the use of jigs and/or fixtures that have been used in other studies of inducible displacement.[61, 81]

The stability of the implant-tissue interface has not yet been fully correlated to the complex mechanical relationship with inducible displacement. Additional studies focusing on the ankle joint are required to evaluate this relationship.

4.5 Conclusions

Based on the results of this study the Mobility™ components show no measurable inducible displacement. There was a maximum of 0.21 mm of MTPM inducible displacement in the talar components that can be attributed to tissue deformation that was seen in all of the components studied. This was below the 0.3 mm threshold given for displacement due to the elasticity of the bone surrounding TKA implants under normal body weight.

4.5.1 Future Considerations

For future studies, it may be a worthwhile consideration to examine the value of increasing or isolating the load applied to joint and/or improving the RSA system precision. It may be that MBRSA has limited effectiveness is assessing inducible displacement. Also, further investigation should be carried out on the relationship between longitudinal migration and inducible displacement for TAA in a similar manner as had been done for TKA.[81]

CHAPTER 5 : CONCLUSION

5.1 Summary

Studying TAA implant stability with RSA is a relatively new science application. There are numerous potential benefits from the continuation of these studies that include advancing the understanding the biomechanical relations of TAA implants in vivo, and continuing to develop and improve the survivability of TAA.

In the first project of this thesis the precision of MBRSA system used to assess TAA implant micromotion was determined. The system demonstrated system precision values that were similar in magnitude to other marker-based RSA studies of TAA implants.

The second project of this thesis examined the longitudinal migration of the Mobility™ over two years. The Mobility™ longitudinal migration behavior was the typical pattern of initial subsidence followed by stabilization for most of the patients for both the tibial and talar components. There was no detectable migration observed between the one and two year followup for either of the components in all of the subjects, except for three of the tibial components.

The third project of this thesis examined the inducible displacement of the Mobility™ at 3 month, 6 month, 1 year, and 2 year followup times. At the two year followup, there was no detectable inducible displacement observed for all of the components, except for one talar component with a maximum 0.21 mm of MTPM inducible displacement detected.

These were the first known studies of their kind that use model-based RSA to assess the biomechanical fixation of total ankle arthroplasty prosthesis.

5.2 Implications

5.2.1 Clinical Implications

The feasibility of using the precision metrics of MBRSA to assess the biomechanical stability of TAA prosthesis in widespread clinical studies was demonstrated. Studying the many other TAA implant designs using RSA allows clinicians to assess what implants perform better under certain circumstances. The unnecessary exposure of patients to flawed prosthesis, seen in the past, can be avoided by small well-controlled RSA clinical trials that validate the implants before they become implemented on larger scales.

5.2.2 Technical Implications

Studies assessing the performance of TAA implants would be greatly improved by the multi-centered spread and acquisition of RSA equipment and RSA trained personnel. Inter-implant comparisons would be best carried out by shared collaborations of international and inter-centre RSA databases containing RSA precision, longitudinal migration and inducible displacement data. This would allow significant bolstering of sample sizes that are often small due to the relative rareness of TAA compared to TKA

and THA. Universal standardized RSA procedural guidelines would also be of great benefit to all researchers.

5.3 Limitations

This project was limited by a several general factors. The primary issues were the statistical power, the limited literature on TAA RSA, and the challenges of TAA MBRSA.

The small sample size limited the statistical power of this study. This is a chronic problem with most TAA studies as TAA treatments are not as common as TKA and THA treatments. Despite this common issue, this study had more subjects (n=20) enrolled than either of the two published marker-based RSA studies of TAA (n = 10 and n = 15). The sample size in this study was further decreased as exams had been omitted as the result of missed followup, insufficient bone markers as the result of poor radiographic projection, and bone marker instability.

The limited literature on TAA RSA made it difficult to interpret the results for the longitudinal migration and inducible displacement studies. The limited literature can be attributed to low TAA treatment rates and the fact that TAA is relatively early in its development. Values from TKA RSA studies were used as a reference in several cases to provide an idea of the values that could be expected and to approximate whether the study was progressing in the right direction. The values for continuous migration and the deformation of the bones due to loading associated with TAA need to be assessed

thoroughly to provide a confident and in depth interpretation of the RSA results that is seen with TKA RSA.

There are many challenges presented by using MBRSA to study total ankle arthroplasty. The small size of a TAA and reference bones (talus and distal tibia) poses some challenges with maintaining a high degree of rotational accuracy that is seen in some TKA and THA RSA studies. The ankle prostheses and bone markers are not as well distributed as in TKA and THA studies due to the limited space. There are often issues with bone marker stability and marker-implant over-projection. Increased rotational measurement errors were observed in the classical marker-based RSA studies of the STAR and BP prostheses by Carlsson et al (2005) and Nelissen et al (2006) respectively.[7, 49] These issues are further compounded with MBRSA contour difference errors resulting from shape and size mismatching.

There are other factors to consider as well. With single centered trials it may take a very long time to get enough TAA patient enrollments for even the small sample sizes required for RSA studies. Maintaining staff trained in RSA techniques may also create difficult challenges.

5.4 Future Work

Due to the limited information gleaned from the inducible displacement results of this study it may be a worthwhile endeavor to examine the value and safety implications of increasing or isolating the load applied to joint. Mechanical studies, such as finite

element modeling (FEA) and/or cadaver studies, should be carried out to determine the amount of bone deformation that contributes to this displacement under the set loading conditions.

5.5 Recommendations

Standardizing protocols and result formats early will allow inter-study comparison for the growing number of RSA studies of TAA. This study validates that a reproducible RSA bone marker insertion technique in both the tibia and talus has been established for this TAA prosthesis. The technique described in Chapter Two is transferable to many other TAA RSA studies and hence is recommended for use in new studies.

New MBRSA studies should consider the rotational symmetry of the implant and factor in whether reasonable RSA measurements can be determined by model-based pose estimation. Noting the possible use and substitution of Elementary Geometric Shapes in the pose estimation can substantially increase the precision of the system. Due to CAD model and manufactured implant dimensional differences, implants being assessed by MBRSA may need to be laser scanned to produce a RE RSA model. This is more important when the implant surface tolerances are poorly controlled as in the case of porous or hydroxyapatite (HA) coatings.

Difficulties arising from marker instability can be addressed using the *sum of relative differences* method proposed by Nystrom et al.[53] This method reduces the dramatic computational power needed to determine the most stable rigid body by calculating the

ME for each possible marker combination. This is an alternative method to the marker matching algorithm in Appendix C.

It may be a worthwhile to wait until a later longitudinal RSA follow-up such as at one year to do the double exams. This would allow for the bones to heal and remodel, providing an even more stable anchoring for the markers.

5.6 Concluding Remarks

It has been demonstrated that MBRSA can precisely and effectively assess the micromotion of TAA components. The migration of the Mobility™ showed that it follows the typical initial subsidence followed by stabilization pattern seen in most RSA studies of orthopaedic implants. The migration behavior is comparable to the STAR and BP total ankle prostheses. The inducible displacement of the Mobility™ was for the most part undetectable. Methods at improving the sensitivity of our inducible displacement measures should be examined. This is the first study of its kind internationally for ankle arthroplasty and offers novel insight into the need for prosthetic design change.

Reference List

1. **Ahl, T; Dalen, N; Lundberg, A; Wykman, A:** Biodegradable fixation of ankle fractures. A roentgen stereophotogrammetric study of 32 cases. Acta Orthop Scand **65:** 166-70, 1994.

2. **Alfaro-Adrian, J; Gill, HS; Marks, BE; Murray, DW:** Mid-term migration of a cemented total hip replacement assessed by radiostereometric analysis. Int Orthop **23:** 140-4, 1999.

3. **Anderson, T; Montgomery, F; Carlsson, A:** Uncemented STAR total ankle prostheses. Three to eight-year follow-up of fifty-one consecutive ankles. J Bone Joint Surg Am **85-A:** 1321-9, 2003.

4. **Bottner, F; Su, E; Nestor, B; Azzis, B; Sculco, T; Bostrom, M:** Radiostereometric Analysis: The Hip. HSS Jrnl **1:** 94-99, 2005.

5. **Bragonzoni, L; Russo, A; Girolami, M; Albisinni, U; Visani, A; Mazzotti, N; Marcacci, M:** The distal tibiofibular syndesmosis during passive foot flexion. RSA-based study on intact, ligament injured and screw fixed cadaver specimens. Arch Orthop Trauma Surg **126:** 304-8, 2006.

6. **Buechel, FF, Sr.; Buechel, FF, Jr.; Pappas, MJ:** Twenty-year evaluation of cementless mobile-bearing total ankle replacements. Clin Orthop Relat Res 19-26, 2004.

7. **Carlsson, A; Markusson, P; Sundberg, M:** Radiostereometric analysis of the double-coated STAR total ankle prosthesis: a 3-5 year follow-up of 5 cases with rheumatoid arthritis and 5 cases with osteoarthrosis. SORT **76:** 573, 2005.

8. **Coester, LM; Saltzman, CL; Leupold, J; Pontarelli, W:** Long-term results following ankle arthrodesis for post-traumatic arthritis. J Bone Joint Surg Am **83-A:** 219-28, 2001.

9. **Cracchiolo, A, 3rd; Deorio, JK:** Design features of current total ankle replacements: implants and instrumentation. J Am Acad Orthop Surg **16:** 530-40, 2008.

10. **Daniels, T; Thomas, R:** Etiology and biomechanics of ankle arthritis. Foot Ankle Clin **13:** 341-52, vii, 2008.

11. **Deorio, JK; Easley, ME:** Total ankle arthroplasty. Instr Course Lect **57:** 383-413, 2008.

12. **Derbyshire, B; Prescott, R; Porter, M:** Notes on the use and interpretation of radiostereometric analysis. SORT **80:** 124-130, 2009.

13. **Doets, HC; van Middelkoop, M; Houdijk, H; Nelissen, RG; Veeger, HE:** Gait analysis after successful mobile bearing total ankle replacement. Foot Ankle Int **28:** 313-22, 2007.

14. **Dunbar, MJ; Wilson, DA; Hennigar, AW; Amirault, JD; Gross, M; Reardon, GP:** Fixation of a trabecular metal knee arthroplasty component. A prospective randomized study. J Bone Joint Surg Am **91:** 1578-86, 2009.

15. **Easley, ME; Vertullo, CJ; Urban, WC; Nunley, JA:** Total ankle arthroplasty. J Am Acad Orthop Surg **10:** 157-67, 2002.

16. **Freeman, MA:** Current state of total joint replacement. Br Med J **2:** 1301-4, 1976.

17. **Gebuhr, P; Stentzer, K; Thomsen, F; Levi, N:** Failure of total hip arthroplasty with Boneloc bone cement. Acta Orthopaedica Belgica **66:** 472, 2000.

18. **Gill, LH:** Challenges in total ankle arthroplasty. Foot Ankle Int **25:** 195-207, 2004.

19. **Glazebrook, M:** End-stage ankle arthritis: magnitude of the problem and solutions. Instr Course Lect **59:** 359-65, 2010.

20. **Glazebrook, M; Daniels, T; Younger, A; Foote, CJ; Penner, M; Wing, K; Lau, J; Leighton, R; Dunbar, M:** Comparison of health-related quality of life between patients with end-stage ankle and hip arthrosis. J Bone Joint Surg Am **90:** 499-505, 2008.

21. **Glazebrook, MA; Arsenault, K; Dunbar, M:** Evidence-based classification of complications in total ankle arthroplasty. Foot Ankle Int **30:** 945-9, 2009.

22. **Glazebrook, MA; Holden, D; Mayich, J; Mitchell, M; Boyd, G:** Fibular Sparing Z-Osteotomy Technique for Ankle Arthrodesis. Foot Ankle Int **8:** 34-7, 2009.

23. **Gougoulias, NE; Khanna, A; Maffulli, N:** History and evolution in total ankle arthroplasty. Br Med Bull **89:** 111-51, 2009.

24. **Haddad, SL; Coetzee, JC; Estok, R; Fahrbach, K; Banel, D; Nalysnyk, L:** Intermediate and long-term outcomes of total ankle arthroplasty and ankle arthrodesis. A systematic review of the literature. J Bone Joint Surg Am **89:** 1899-905, 2007.

25. **Horisberger, M; Valderrabano, V; Hintermann, B:** Posttraumatic ankle osteoarthritis after ankle-related fractures. J Orthop Trauma **23:** 60-7, 2009.

26. **Hurschler, C; Seehaus, F; Emmerich, J; Kaptein, BL; Windhagen, H:** Comparison of the model-based and marker-based roentgen stereophotogrammetry methods in a typical clinical setting. J Arthroplasty **24:** 594-606, 2009.

27. **Kaptein, B; Valstar, E; Stoel, B; Rozing, P; Reiber, J:** A new model-based RSA method validated using CAD models and models from reversed engineering. Journal of Biomechanics **36:** 873-882, 2003.

28. **Kaptein, B; Valstar, E; Stoel, B; Rozing, P; Reiber, J:** A new type of model-based Roentgen stereophotogrammetric analysis for solving the occluded marker problem. Journal of Biomechanics **38:** 2330-2334, 2005.

29. **Kaptein, BL; Valstar, ER; Spoor, CW; Stoel, BC; Rozing, PM:** Model-based RSA of a femoral hip stem using surface and geometrical shape models. Clin Orthop Relat Res **448:** 92-7, 2006.

30. **Kaptein, BL; Valstar, ER; Stoel, BC; Rozing, PM; Reiber, JH:** Evaluation of three pose estimation algorithms for model-based roentgen stereophotogrammetric analysis. Proc Inst Mech Eng H **218:** 231-8, 2004.

31. **Karrholm, J:** Roentgen stereophotogrammetry. Review of orthopedic applications. Acta Orthop Scand **60:** 491-503, 1989.

32. **Karrholm, J; Borssen, B; Lowenhielm, G; Snorrason, F:** Does early micromotion of femoral stem prostheses matter? 4-7-year stereoradiographic follow-up of 84 cemented prostheses. J Bone Joint Surg Br **76:** 912-7, 1994.

33. **Karrholm, J; Gill, RH; Valstar, ER:** The history and future of radiostereometric analysis. Clin Orthop Relat Res **448:** 10-21, 2006.

34. **Karrholm, J; Malchau, H; Snorrason, F; Herberts, P:** Micromotion of femoral stems in total hip arthroplasty. A randomized study of cemented, hydroxyapatite-coated, and porous-coated stems with roentgen stereophotogrammetric analysis. J Bone Joint Surg Am **76:** 1692-705, 1994.

35. **Kiss, J; Murray, DW; Turner-Smith, AR; Bulstrode, CJ:** Roentgen stereophotogrammetric analysis for assessing migration of total hip replacement femoral components. Proc Inst Mech Eng [H] **209:** 169-75, 1995.

36. **Kitaoka, HB; Patzer, GL:** Clinical results of the Mayo total ankle arthroplasty. J Bone Joint Surg Am **78:** 1658-64, 1996.

37. **Laende, EK; Deluzio, KJ; Hennigar, AW; Dunbar, MJ:** Implementation and validation of an implant-based coordinate system for RSA migration calculation. J Biomech **42:** 2387-93, 2009.

38. **Leardini, A; Benedetti, M; Berti, L; Bettinelli, D; Nativo, R; Giannini, S:** Rear-foot, mid-foot and fore-foot motion during the stance phase of gait. Gait & Posture **25:** 453-462, 2007.

39. **Leardini, A; Benedetti, M; Catani, F; Simoncini, L; Giannini, S:** An anatomically based protocol for the description of foot segment kinematics during gait. Clinical Biomechanics **14:** 528-536, 1999.

40. **Lewis, G:** Biomechanics of and research challenges in uncemented total ankle replacement. Clin Orthop Relat Res 89-97, 2004.

41. **Little, RB; Wevers, HW; Siu, D; Cooke, TD:** A three-dimensional finite element analysis of the upper tibia. J Biomech Eng **108:** 111-9, 1986.

42. **Lofvenberg, R; Karrholm, J:** The influence of an ankle orthosis on the talar and calcaneal motions in chronic lateral instability of the ankle: A stereophotogrammetric analysis. The American Journal of Sports Medicine **21:** 224-230, 1993.

43. **Lofvenberg, R; Karrholm, J; Ahlgren, O:** Ligament reconstruction for ankle instability. A 5-year prospective RSA follow-up of 30 cases. Acta Orthop Scand **65:** 401-7, 1994.

44. **Lofvenberg, R; Karrholm, J; Selvik, G; Hansson, LI; Ahlgren, O:** Chronic lateral instability of the ankle. Roentgen stereophotogrammetry of talar position. Acta Orthop Scand **60:** 34-9, 1989.

45. **Madanat, R; Moritz, N; Larsson, S; Aro, HT:** RSA applications in monitoring of fracture healing in clinical trials. Scand J Surg **95:** 119-27, 2006.

46. **Makinen, TJ; Mattila, KT; Maattanen, H; Aro, HT:** Comparison of digital and conventional radiostereometric image analysis in an ankle phantom model. Scand J Surg **94:** 233-8, 2005.

47. **Malchau, H; Herberts, P; Eisler, T; Garellick, G; Soderman, P:** The Swedish Total Hip Replacement Register. J Bone Joint Surg Am **84-A Suppl 2:** 2-20, 2002.

48. **Myerson, M; Won, H:** Primary and Revision Total Ankle Replacement Using Custom-Designed Prostheses. Foot and Ankle Clinics of North America **13:** 521-538, 2008.

49. **Nelissen, RGHH; Doets, HC; Valstar, ER:** Early migration of the tibial component of the Buechel-Pappas Total Ankle Prosthesis. Clinical Orthopaedics and Related Research **448:** 246-151, 2006.

50. **Nilsson, KG; Dalen, T:** Inferior performance of Boneloc bone cement in total knee arthroplasty: a prospective randomized study comparing Boneloc with Palacos using radiostereometry (RSA) in 19 patients. Acta Orthop Scand **69:** 479-83, 1998.

51. **Nilsson, KG; Karrholm, J; Carlsson, L; Dalen, T:** Hydroxyapatite coating versus cemented fixation of the tibial component in total knee arthroplasty: prospective randomized comparison of hydroxyapatite-coated and cemented tibial components with 5-year follow-up using radiostereometry. J Arthroplasty **14:** 9-20, 1999.

52. **Nilsson, KG; Karrholm, J; Ekelund, L; Magnusson, P:** Evaluation of micromotion in cemented vs uncemented knee arthroplasty in osteoarthrosis and rheumatoid arthritis. Randomized study using roentgen stereophotogrammetric analysis. J Arthroplasty **6:** 265-78, 1991.

53. **Nystrom, L; Soderkvist, I; Wedin, PA:** A note on some identification problems arising in roentgen stereo photogrammetric analysis. J Biomech **27:** 1291-4, 1994.

54. **Onsten, I; Berzins, A; Shott, S; Sumner, DR:** Accuracy and precision of radiostereometric analysis in the measurement of THR femoral component translations: human and canine in vitro models. J Orthop Res **19:** 1162-7, 2001.

55. **Onsten, I; Nordqvist, A; Carlsson, AS; Besjakov, J; Shott, S:** Hydroxyapatite augmentation of the porous coating improves fixation of tibial components. A randomised RSA study in 116 patients. J Bone Joint Surg Br **80:** 417-25, 1998.

56. **Piriou, P; Culpan, P; Mullins, M; Cardon, JN; Pozzi, D; Judet, T:** Ankle replacement versus arthrodesis: a comparative gait analysis study. Foot Ankle Int **29:** 3-9, 2008.

57. **Ranstam, J; Ryd, L; Onsten, I:** Accurate accuracy assessment: review of basic principles. Acta Orthop Scand **71:** 106-8, 2000.

58. **Ryd, L:** Migration of hydroxyapatite coated femoral prostheses. Journal of Bone & Joint Surgery, British Volume **1993:** 681-7, 1993.

59. **Ryd, L; Albrektsson, BE; Carlsson, L; Dansgard, F; Herberts, P; Lindstrand, A; Regner, L; Toksvig-Larsen, S:** Roentgen stereophotogrammetric analysis as a predictor of mechanical loosening of knee prostheses. J Bone Joint Surg Br **77:** 377-83, 1995.

60. **Ryd, L; Lindstrand, A; Rosenquist, R; Selvik, G:** Micromotion of conventionally cemented all-polyethylene tibial components in total knee replacements. A roentgen stereophotogrammetric analysis of migration and inducible displacement. Arch Orthop Trauma Surg **106:** 82-8, 1987.

61. **Ryd, L; Lindstrand, A; Rosenquist, R; Selvik, G:** Tibial component fixation in knee arthroplasty. Clin Orthop Relat Res 141-9, 1986.

62. **Ryd, L; Toksvig-Larsen, S:** Early postoperative fixation of tibial components: an in vivo roentgen stereophotogrammetric analysis. J Orthop Res **11:** 142-8, 1993.

63. **Ryd, L; Yuan, X; Lofgren, H:** Methods for determining the accuracy of radiostereometric analysis (RSA). Acta Orthop Scand **71:** 403-8, 2000.

64. **Saltzman, CL; Amendola, A; Anderson, R; Coetzee, JC; Gall, RJ; Haddad, SL; Herbst, S; Lian, G; Sanders, RW; Scioli, M; Younger, AS:** Surgeon training and complications in total ankle arthroplasty. Foot Ankle Int **24:** 514-8, 2003.

65. **Seehaus, F; Emmerich, J; Kaptein, BL; Windhagen, H; Hurschler, C:** Experimental analysis of Model-Based Roentgen Stereophotogrammetric Analysis (MBRSA) on four typical prosthesis components. J Biomech Eng **131:** 041004, 2009.

66. **Selvik, G:** Roentgen stereophotogrammetry. A method for the study of the kinematics of the skeletal system. Acta Orthop Scand Suppl **232:** 1-51, 1989.

67. **Shepherd, DE; Seedhom, BB:** Thickness of human articular cartilage in joints of the lower limb. Ann Rheum Dis **58:** 27-34, 1999.

68. **Soballe, K; Toksvig-Larsen, S; Gelineck, J; Fruensgaard, S; Hansen, ES; Ryd, L; Lucht, U; Bunger, C:** Migration of hydroxyapatite coated femoral prostheses. A Roentgen Stereophotogrammetric study. J Bone Joint Surg Br **75:** 681-7, 1993.

69. **Soderkvist, I; Wedin, PA:** Determining the movements of the skeleton using well-configured markers. J Biomech **26:** 1473-7, 1993.

70. **Stefansdottir, A; Franzen, H; Johnsson, R; Ornstein, E; Sundberg, M:** Movement pattern of the Exeter femoral stem: a radiostereometric analysis of 22 primary hip arthroplasties followed for 5 years. Acta orthopaedica Scandinavica **75:** 408-414, 2004.

71. **Thanner, J; Freij-Larsson, C; Karrholm, J; Malchau, H; Wesslen, B:** Evaluation of Boneloc. Chemical and mechanical properties, and a randomized clinical study of 30 total hip arthroplasties. Acta Orthop Scand **66:** 207-14, 1995.

72. **Thomas, R; Daniels, TR; Parker, K:** Gait analysis and functional outcomes following ankle arthrodesis for isolated ankle arthritis. J Bone Joint Surg Am **88:** 526-35, 2006.

73. **Uvehammer, J; Karrholm, J:** Inducible displacements of cemented tibial components during weight-bearing and knee extension observations during dynamic radiostereometry related to joint positions and 2 years history of migration in 16 TKR. J Orthop Res **19:** 1168-77, 2001.

74. **Valderrabano, V; Horisberger, M; Russell, I; Dougall, H; Hintermann, B:** Etiology of ankle osteoarthritis. Clin Orthop Relat Res **467:** 1800-6, 2009.

75. **Valderrabano, V; Nigg, BM; von Tscharner, V; Stefanyshyn, DJ; Goepfert, B; Hintermann, B:** Gait analysis in ankle osteoarthritis and total ankle replacement. Clin Biomech (Bristol, Avon) **22:** 894-904, 2007.

76. **Valstar, E; de Jong, F; Vrooman, H; Rozing, P; Reiber, J:** Model-based Roentgen stereophotogrammetry of orthopaedic implants. Journal of Biomechanics **34:** 715-722, 2001.

77. **Valstar, E; Nelissen, R; Reiber, J; Rozing, P:** The use of Roentgen stereophotogrammetry to study micromotion of orthopaedic implants. ISPRS Journal of Photogrammetry and Remote Sensing **56:** 376-389, 2002.

78. **Valstar, ER; Gill, R; Ryd, L; Flivik, G; Borlin, N; Karrholm, J:** Guidelines for standardization of radiostereometry (RSA) of implants. Acta Orthop **76:** 563-72, 2005.

79. **Valstar, ER; Vrooman, HA; Toksvig-Larsen, S; Ryd, L; Nelissen, RG:** Digital automated RSA compared to manually operated RSA. J Biomech **33:** 1593-9, 2000.

80. **van den Heuvel, A; Van Bouwel, S; Dereymaeker, G:** Total ankle replacement. Design evolution and results. Acta Orthop. Belg. **76:** 150-161, 2010.

81. **Wilson, DA; Astephen, JL; Hennigar, AW; Dunbar, MJ:** Inducible Displacement of a Trabecular Metal Tibial Monoblock Component. J Arthroplasty 2009.

82. **Wu, W; Su, F; Cheng, Y; Huang, P; Chou, Y; Chou, C:** Gait analysis after ankle arthrodesis. Gait & Posture **11:** 54-61, 2000.

83. **Yuan, X; Ryd, L:** Accuracy analysis for RSA: a computer simulation study on 3D marker reconstruction. Journal of Biomechanics **33:** 493-498, 2000.

84. **Zatsiorsky, VM** (1998). *Kinematics of Human Motion.* Windsor ON: Human Kinetics.

APPENDIX A: Double Exam Error, Migration and Inducible Displacement Analysis Description Algorithms and Sample Code

General:

Open MBRSA 3.2 Exam Files

Read migration or inducible displacement files into one array

Search array for fields that identify implant type.

Read line by line, and identify and record parameters into array.

Parameters recorded for each comparison (i.e. with respect to reference postop or supine RSA exam) are:

[Exam number, x, y, z, rx, ry, rz, markers used, ME, CN, MTPM]

Correct for sides by multiplying matrices such that:

x = posterior to anterior motion

y = inferior to superior motion

z = medial to lateral motion

rx = medial/lateral tilt

ry = internal/external rotation

rz = posterior/anterior tilt

for example:

patientimplantsides=[0 0 1 1 1 1 0 0 0 0 0 1 1 1 0 0 1 1 0 0];

Rsideaxiscorr= [-1 1 -1 -1 -1 1]; Lsideaxiscorr= [1 1 -1 -1 1 -1];

Double Exams:

Replace all empty values with NaN,

Calculate & record: nanmean, nanstd, nanmedian, nanmin and nanmax

Use MatLab Boxplot function for x, y, z, rx, ry, rz, MTPM parameters

Longitudinal Migration:

Replace all empty values with NaN,

There is one large file with double exams, 6 WK, 3 MO, 6 MO, 1 YR and 2 YR files that need to be read for each patient

Group and plot parameters based on followup time

Inducible Displacement:

Replace all empty values with NaN,

There are separate 3 MO, 6 MO, 1 YR and 2 YR files that need to be read for each patient

Group and plot parameters based on followup time

APPENDIX B: Figures for the Tibial Component Longitudinal Migration

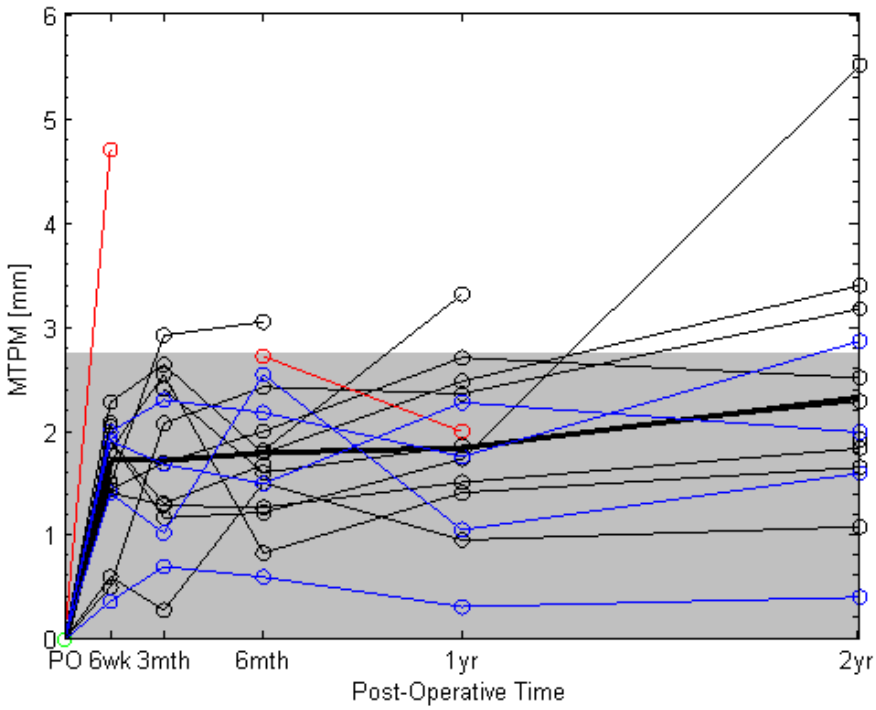

Tibial component MTPM longitudinal migration. *Thin black:* individual subjects. *Thick black:* group mean. *Red:* subject that underwent surgical revision. *Blue:* subjects with pre- or post-surgical complications. *Shaded region:* shows the detection limit, 2.75 mm, or the minimum motion of any one implant with respect to the postop exam required for definite motion to be detected.

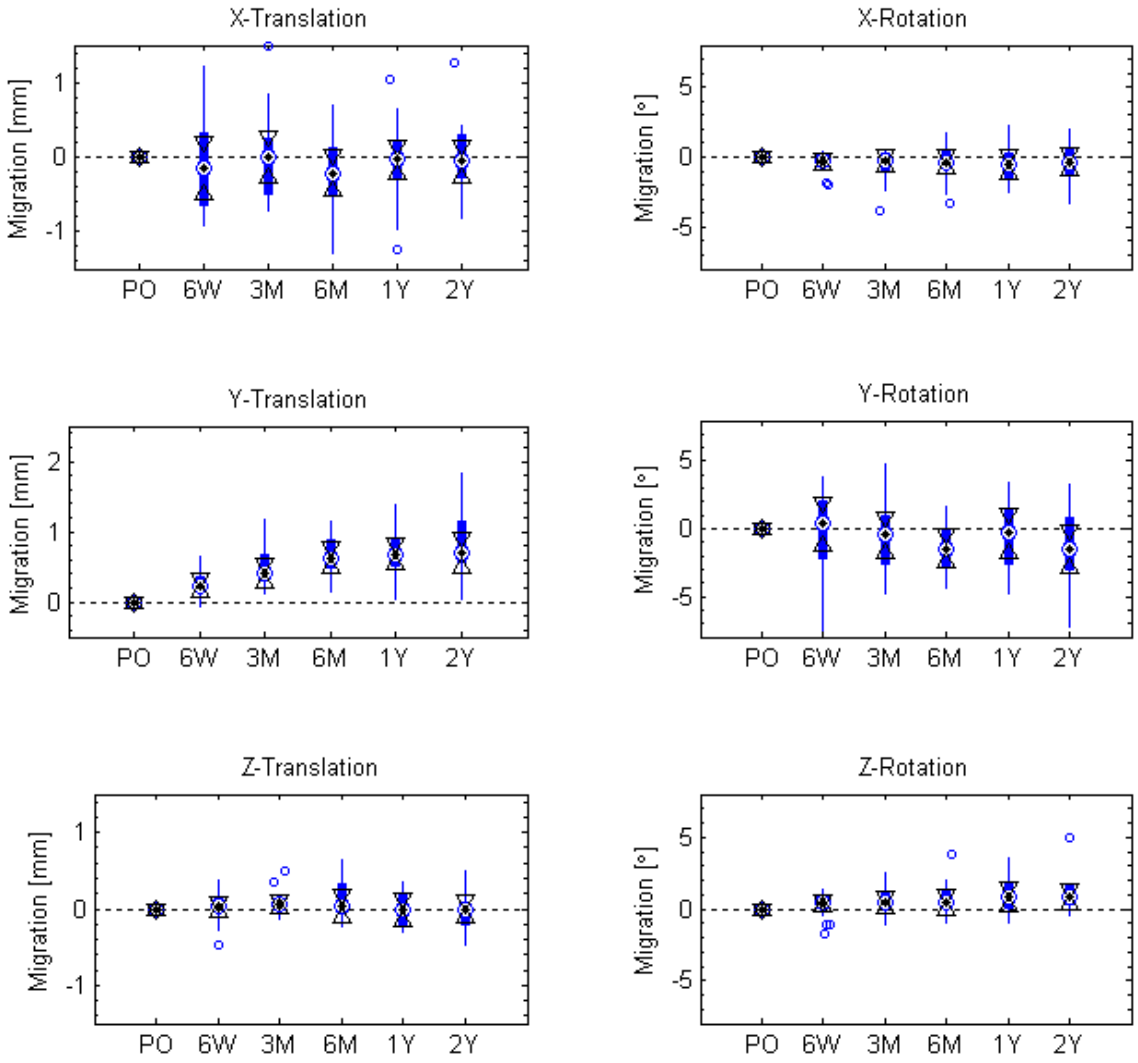

XYZ translation (*left*) and rotation (*right*) box plots for the tibial component longitudinal migration. Boxes bound 25th to 75th percentiles. Medians are the centers of the larger circles. Outliers (*circles*) are indicated as outside the whiskers; or 1.5x the inter-quartile range beyond the 25th and 75th percentiles. *Followup times are denoted:* PO = postoperative, 6W = 6 weeks, 3M = 3 months, 6M = 6 months, 1Y = 1 year, and 2Y = 2 years. Overlapping notched regions indicate that there are no significant differences (α = 0.05) between groups.

APPENDIX C: Marker Matching - Marker Model and Marker Matching Description of Algorithms and Sample Code

Marker model generator algorithm:

export or copy MBRSA points to a text file

read m-points x,y,z coordinates into and m by 3 array

calculate centroid (i.e. mean of x, y, z)

subtract centroid values from each point to create marker model points

save as a text file

import into MBRSA as a marker model

Marker matching algorithm:

Determine the scenes to be compared, for example:

scenes = ['POA';'POB';'6WK';'3MT';'6MT';'1YR';'2YR']

Export the possible marker locations based on crossing line distance <= 0.5 mm for each RSA exam.

Convert all points to their respective local coordinate system based on the implant coordinate system. This done by transformation matrix; see LocalPositions.m Matlab Code below.

Compare marker locations by distance formulae across exams for all possible marker locations and sort by distance.

Determine optimal marker selection by neural-network like node finding,

for example:

base likelihood of marker existing on near zero distance between two adjacent exams

if bead exists and postop and continuously exists in all exams in same spot then increase likelihood of keeping this marker position existing

if marker disappears in any exams then decrease likelihood of marker position marker existing

sort marker positions (with respect to the implant) by overall likelihood of marker existing

turn markers on or off based in MBRSA software on a high likelihood of marker existing

```
LocalPositions.m %MatLab Code Last revision: 18September2009 @1735
function [local] = LocalPositions(BeadLocations,ImplantLocation)
% returns transformation matrix, T with given inputs
n = size(BeadLocations,1)
local = zeros(n,3); ptglobal = zeros(1,3); ptlocal = zeros(1,3)
rx = ImplantLocation(2,1)*pi()/180
ry = ImplantLocation(2,2)*pi()/180
rz = ImplantLocation(2,3)*pi()/180
Rx = [1 0 0; 0 cos(rx) -sin(rx); 0 sin(rx) cos(rx)]
Ry = [cos(ry)  0 sin(ry); 0 1 0; -sin(ry) 0 cos(ry)]
Rz = [cos(rz) -sin(rz) 0; sin(rz) cos(rz) 0; 0 0 1]
R = Rz*Rx*Ry % may need to use Zyx, Xyz
```

```
Tlcs = [1 0 0 0; ImplantLocation(1,1) R(1,1) R(1,2) R(1,3); ImplantLocation(1,2) R(2,1)
        R(2,2) R(2,3); ImplantLocation(1,3) R(3,1) R(3,2) R(3,3)]
for pts = 1:n
        ptglobal = BeadLocations(pts,:); ptlocal = inv(Tlcs)*[1 ptglobal(1) ptglobal(2)
        ptglobal(3)]';local(pts,:)= [ptlocal(2) ptlocal(3) ptlocal(4)]
end
```

APPENDIX D: Raw RSA Double Exam, Longitudinal Migration and Inducible Displacement Data

Migration Exams: 2 = double, 10 = 6 wk, 20 = 3 mth, 30 = 6 mth, 40 = 1 yr, 50 = 2yr

Inducible Exams: 25 = 3 mth, 35 = 6 mth, 45 = 1 yr, 55 = 2yr

TIBIAL COMPONENT MIGRATION DATA

subject	RSA exam	x	y	z	rx	ry	rz	markers	ME	minrel CN	abs CN	MTPM
1	2	0.50	-0.18	0.00	0.90	0.55	-0.44	3	0.05	1.42	166	0.77
1	10	0.81	0.10	0.05	-0.51	-3.05	0.16	4	0.10	1.42	42	1.90
1	20	1.48	0.27	0.09	-1.20	-0.11	0.13	4	0.15	1.42	42	1.68
1	30	-0.33	0.49	0.08	-1.56	-3.09	-0.41	5	0.18	1.42	38	1.49
1	40	1.03	0.44	-0.22	-2.00	3.62	-0.07	5	0.16	1.42	38	2.27
1	50	1.51	0.35	0.08	-2.38	1.22	0.48	4	0.15	1.42	42	1.98
2	2	-0.08	0.02	-0.26	-0.17	1.48	-0.23	6	0.04	1.42	28	0.71
2	10	0.20	0.23	0.10	-0.23	3.15	0.41	6	0.12	1.42	28	1.40
2	20	0.25	0.40	0.36	0.22	1.40	0.18	6	0.19	1.42	28	1.02
2	30	-0.62	0.44	0.67	0.33	-4.10	0.23	6	0.19	1.42	28	2.54
2	40	0.24	0.49	0.37	0.24	1.65	0.82	6	0.17	1.42	28	1.05
2	50	0.19	0.57	0.51	0.44	-2.88	0.64	5	0.12	1.42	29	1.59
3	2	0.31	-0.03	-0.02	0.05	-0.51	0.16	4	0.03	1.59	34	0.48
3	10	0.56	0.18	0.18	-0.63	3.55	0.53	3	0.04	1.59	49	1.81
3	20	0.86	0.37	0.00	-1.00	4.91	0.16	3	0.06	1.59	49	2.54
3	30	0.21	0.38	0.17	-0.51	1.41	0.09	4	0.11	1.59	34	0.83
3	40	0.67	0.32	0.23	-0.93	1.99	0.52	3	0.06	1.59	49	1.41
3	50	0.44	0.46	-0.01	-1.04	3.45	0.24	4	0.15	1.59	34	1.65
4	2	-0.02	0.02	0.01	0.01	0.09	-0.09	3	0.01	1.45	42	0.06
4	20	-0.67	0.71	0.04	0.62	-2.77	2.32	3	0.09	1.45	42	2.40
4	30	0.17	0.93	0.00	-0.18	-2.58	1.47	3	0.12	1.45	42	1.60
4	40	-0.01	1.32	-0.10	-0.04	1.31	1.78	3	0.09	1.45	42	1.85
4	50	-0.15	1.52	-0.32	-0.35	-3.13	1.69	3	0.07	1.45	42	2.28
5	2	-0.09	0.03	-0.02	-0.38	-0.89	0.58	3	0.21	1.42	33	0.57
5	10	-0.85	0.11	0.09	0.23	-1.58	-1.03	3	0.12	1.42	33	1.41
5	20	0.05	0.26	0.08	0.40	2.65	-0.36	3	0.15	1.42	33	1.29
5	30	0.22	0.43	0.38	1.82	-1.33	0.26	3	0.09	1.42	33	1.26
5	40	0.22	0.64	0.31	1.67	1.01	0.79	3	0.18	1.42	33	1.51
5	50	0.23	0.81	0.40	2.15	-0.97	0.95	3	0.06	1.42	33	1.83
6	2	-0.93	0.05	-0.22	0.08	-3.26	-0.16	4	0.06	1.47	33	2.08
6	10	-2.28	0.62	-0.16	-1.85	-7.57	-1.70	4	0.05	1.47	33	4.69
6	30	-1.30	0.71	0.04	-1.10	-4.36	-0.88	4	0.12	1.47	33	2.71
6	40	-1.24	0.76	0.08	-1.89	-2.34	-0.91	4	0.06	1.47	33	1.99
7	2	0.02	0.00	0.01	0.03	0.26	-0.01	5	0.02	1.34	30	0.12
7	10	-0.15	0.09	0.19	0.00	0.37	-0.42	3	0.16	1.34	43	0.37
7	20	0.03	0.21	-0.14	0.57	0.94	0.43	3	0.10	1.34	43	0.70
7	30	-0.13	0.14	0.28	0.27	-0.46	0.53	3	0.09	1.34	39	0.60
7	40	-0.18	0.04	0.10	0.47	-0.08	-0.03	4	0.18	1.34	30	0.31
7	50	-0.06	0.04	0.12	0.59	-0.49	0.25	5	0.13	1.34	30	0.41
8	2	-0.03	0.01	-0.05	0.09	0.27	0.21	4	0.12	1.31	33	0.18
8	10	0.16	0.27	-0.01	-0.36	0.82	0.44	4	0.12	1.31	33	0.50
8	20	-0.36	0.42	0.07	-0.42	-3.85	0.50	4	0.08	1.31	33	2.07
8	30	-0.53	0.49	-0.10	-0.29	-3.85	1.85	4	0.10	1.31	33	2.42
8	40	-0.42	0.52	0.17	-0.19	-3.83	1.40	4	0.17	1.31	33	2.35
8	50	-0.83	0.59	0.02	-0.21	-4.94	1.80	4	0.19	1.31	33	3.17
9	10	-0.91	0.17	-0.24	-0.15	-2.07	0.46	4	0.07	1.23	41	1.90
9	20	-0.04	0.42	0.06	-0.10	-1.54	1.30	4	0.07	1.23	41	1.17
9	30	-0.11	0.74	-0.22	-0.42	0.48	1.14	3	0.04	1.23	45	1.22
9	40	-0.09	0.71	-0.23	-1.35	-2.85	1.49	4	0.04	1.23	41	1.73
9	50	-2.16	1.42	-0.41	-1.54	-7.31	1.05	4	0.06	1.23	41	5.49
10	2	-0.14	-0.09	0.02	-0.22	1.27	0.12	NaN	NaN	1.40	29	0.64
10	10	0.66	0.22	0.01	-0.07	3.91	1.04	NaN	NaN	1.40	29	2.04
12	2	0.01	0.00	0.00	0.00	-0.18	-0.01	5	0.00	1.51	34	0.08
12	10	-0.41	0.43	0.39	-0.84	1.82	-1.09	5	0.04	1.51	34	1.44
12	20	0.08	0.67	0.07	-2.34	0.91	-1.04	4	0.05	1.51	41	1.69

12	30	0.07	0.82	0.02	-2.64	1.74	-1.01	5	0.10	1.51	34	1.99
12	40	-0.06	0.89	0.18	-2.48	-4.82	-1.03	3	0.05	1.51	52	2.70
12	50	0.18	1.06	-0.01	-3.31	-1.53	-0.47	3	0.01	1.51	52	2.50
13	2	-0.31	0.30	0.06	-0.17	-0.72	0.62	NaN	NaN	1.19	34	0.82
13	10	-0.78	0.33	0.01	-0.07	-1.49	0.41	NaN	NaN	1.19	34	1.51
13	30	-0.29	0.93	0.05	1.40	0.69	1.25	NaN	NaN	1.19	34	1.81
13	40	-0.96	1.12	-0.17	2.35	-1.59	2.80	NaN	NaN	1.19	34	3.30
14	2	-0.05	0.01	0.03	0.01	-0.09	0.01	5	0.02	1.22	29	0.11
14	10	1.23	-0.06	0.12	-0.41	-1.89	0.75	5	0.05	1.22	29	1.99
14	20	0.58	0.32	0.49	-0.46	-3.73	1.19	3	0.09	1.22	42	2.29
14	30	0.73	0.51	0.39	-0.75	-2.85	0.70	5	0.13	1.22	29	2.17
14	40	0.54	0.77	-0.26	-1.58	-0.50	1.84	4	0.13	1.22	35	1.75
14	50	1.27	0.68	0.03	-1.24	-3.29	1.93	4	0.13	1.22	35	2.86
15	2	0.00	-0.06	-0.01	0.15	-0.02	0.01	3	0.04	1.48	37	0.12
15	10	-0.63	0.35	-0.47	-0.28	2.93	0.08	3	0.21	1.48	37	1.90
15	20	-0.64	0.61	-0.14	0.02	-1.02	0.65	3	0.22	1.48	37	1.30
15	30	-1.03	0.77	-0.07	0.63	-0.69	0.32	3	0.21	1.48	37	1.67
15	50	-0.09	1.06	-0.48	1.42	1.90	-0.16	3	0.09	1.48	37	1.92
16	2	-0.98	0.04	0.04	0.04	-4.45	0.16	5	0.07	1.28	28	2.75
16	10	-0.47	0.29	-0.02	0.52	-3.38	1.24	4	0.13	1.28	33	2.08
17	2	0.07	-0.01	-0.02	0.18	-0.80	-0.27	6	0.15	1.48	26	0.40
17	10	-0.60	0.35	0.14	-0.60	-4.44	0.44	5	0.15	1.48	30	2.27
17	20	-0.71	0.66	0.21	-0.87	-4.78	0.80	4	0.15	1.48	36	2.63
17	30	-0.09	1.08	-0.14	-0.71	-2.41	2.09	4	0.20	1.48	32	1.78
17	40	0.00	1.41	-0.17	-0.83	-2.80	3.66	3	0.26	1.48	45	2.47
17	50	-0.57	1.85	-0.18	-1.22	-2.48	5.03	3	0.30	1.48	45	3.39
18	2	-0.13	0.01	-0.15	-0.28	3.02	-0.08	4	0.09	1.40	35	1.30
18	10	-0.06	-0.03	0.03	-0.12	1.32	0.23	5	0.16	1.40	35	0.60
18	20	-0.06	0.11	-0.07	0.19	-0.20	-0.28	5	0.22	1.40	35	0.28
18	30	-0.57	0.54	-0.09	0.96	-1.60	-0.26	5	0.14	1.40	35	1.50
18	40	-0.29	0.60	-0.29	0.22	0.03	0.63	4	0.10	1.40	35	0.95
18	50	-0.19	0.70	-0.13	0.34	0.62	0.88	5	0.11	1.40	35	1.08
20	2	0.51	-0.10	-0.46	-0.77	1.21	3.19	3	0.03	1.39	40	1.66
20	10	0.25	0.67	-0.28	-2.00	0.41	1.52	3	0.27	1.39	40	1.49
20	20	-0.52	1.20	0.13	-3.79	-0.72	2.69	3	0.82	1.39	40	2.91
20	30	-0.48	1.17	0.57	-3.29	-1.00	3.84	3	0.87	1.39	40	3.04

TIBIAL COMPONENT SPHERICAL TIP MIGRATION DATA

subject	RSA exam	x	y	z	rx	ry	rz	markers	ME	minrel CN	abs CN	MTPM
1	2	0.04	0.07	-0.09	0.90	0.55	-0.44	3	0.05	5.73	166	0.12
1	10	0.09	0.17	-0.06	-0.51	-3.05	0.16	4	0.10	5.73	42	0.20
1	20	0.17	0.42	-0.13	-1.20	-0.11	0.13	4	0.15	5.73	42	0.47
1	30	0.11	0.56	-0.27	-1.56	-3.09	-0.41	5	0.18	5.73	38	0.63
1	40	0.14	0.53	-0.32	-2.00	3.62	-0.07	5	0.16	5.73	38	0.63
1	50	0.12	0.65	-0.34	-2.37	1.22	0.48	4	0.15	5.73	42	0.74
2	2	-0.05	-0.02	0.01	-0.17	1.48	-0.23	6	0.04	6.13	28	0.05
2	10	0.16	0.21	0.30	-0.21	5.80	0.33	6	0.12	6.13	28	0.40
2	20	0.25	0.42	0.56	0.23	3.98	0.07	6	0.19	6.13	28	0.75
2	30	0.25	0.42	0.57	0.33	-1.45	0.12	6	0.19	6.13	28	0.75
2	40	0.28	0.49	0.62	0.27	3.96	0.72	6	0.17	6.13	28	0.84
2	50	0.33	0.62	0.55	0.45	-0.23	0.52	5	0.12	6.13	29	0.89
3	2	-0.11	-0.02	0.02	0.05	-0.51	0.16	4	0.03	6.24	34	0.12
3	10	0.06	0.24	-0.07	-0.63	3.55	0.53	3	0.04	6.24	49	0.25
3	20	-0.10	0.47	-0.17	-1.00	4.91	0.16	3	0.06	6.24	49	0.50
3	30	0.02	0.46	-0.10	-0.51	1.41	0.09	4	0.11	6.24	34	0.47
3	40	-0.07	0.55	-0.14	-0.93	1.99	0.52	3	0.06	6.24	49	0.58
3	50	0.06	0.47	-0.27	-1.04	3.45	0.24	4	0.15	6.24	34	0.55
4	2	-0.06	0.00	0.03	0.01	0.09	-0.09	3	0.01	6.04	42	0.06
4	20	0.40	0.73	0.17	0.62	-2.77	2.32	3	0.09	6.04	42	0.85
4	30	0.45	0.98	-0.16	-0.18	-2.58	1.47	3	0.12	6.04	42	1.08
4	40	0.19	1.32	-0.22	-0.04	1.31	1.78	3	0.09	6.04	42	1.35
4	50	0.14	1.48	-0.28	-3.24	-3.02	0.41	3	0.07	6.04	42	1.52
5	2	0.03	0.07	-0.04	-0.38	-0.89	0.58	3	0.21	6.31	33	0.08

5	10	-0.08	0.06	0.06	0.23	-1.58	-1.03	3	0.12	6.31	33	0.12
5	20	-0.14	0.24	0.13	0.40	2.65	-0.36	3	0.15	6.31	33	0.31
5	30	0.18	0.50	0.37	1.82	-1.33	0.26	3	0.09	6.31	33	0.65
5	40	0.41	0.65	0.50	1.73	1.02	0.80	3	0.18	6.31	33	0.91
5	50	0.40	0.88	0.49	2.15	-0.97	0.95	3	0.06	6.31	33	1.09
6	2	0.05	0.02	0.00	0.08	-3.26	-0.16	4	0.06	6.01	33	0.05
6	10	-0.17	0.61	-0.46	-1.85	-7.57	-1.70	4	0.05	6.01	33	0.78
6	30	-0.30	0.66	-0.55	-1.10	-4.36	-0.88	4	0.12	6.01	33	0.91
6	40	-0.24	0.74	-0.60	-1.89	-2.34	-0.91	4	0.06	6.01	33	0.98
7	2	-0.06	-0.04	0.04	0.03	0.26	-0.01	5	0.02	5.80	30	0.08
7	10	0.04	0.05	0.00	0.00	0.37	-0.42	3	0.16	5.80	43	0.06
7	20	-0.03	0.23	-0.17	0.57	0.94	0.43	3	0.10	5.80	43	0.28
7	30	-0.07	0.17	0.00	0.27	-0.46	0.52	3	0.09	5.80	39	0.18
7	40	-0.04	0.08	-0.08	0.47	-0.08	-0.03	4	0.18	5.80	30	0.12
7	50	-0.09	0.13	-0.07	0.59	-0.49	0.25	5	0.13	5.80	30	0.17
8	2	-0.06	-0.04	-0.01	0.09	0.27	0.21	4	0.12	5.82	33	0.07
8	10	0.05	0.21	-0.06	-0.36	0.82	0.44	4	0.12	5.82	33	0.23
8	20	0.12	0.37	-0.04	-0.42	-3.85	0.50	4	0.08	5.82	33	0.39
8	30	0.26	0.50	0.02	-0.29	-3.85	1.85	4	0.10	5.82	33	0.56
8	40	0.25	0.52	0.07	-0.19	-3.83	1.40	4	0.17	5.82	33	0.58
8	50	0.08	0.57	-0.03	-0.21	-4.94	1.80	4	0.19	5.82	33	0.58
9	10	0.09	0.16	-0.02	-0.15	-2.01	0.46	4	0.07	5.90	41	0.19
9	20	0.20	0.44	-0.09	-0.10	-1.48	1.29	4	0.07	5.90	41	0.49
9	30	0.29	0.71	-0.23	-0.42	0.51	1.14	3	0.04	5.90	45	0.80
9	40	0.05	0.98	-0.63	-1.34	-2.79	1.49	4	0.04	5.90	41	1.16
9	50	-0.23	1.39	-0.77	-1.54	-7.26	1.05	4	0.06	5.90	41	1.60
10	2	-0.12	-0.08	0.00	-0.22	1.27	0.12	NaN	NaN	6.00	29	0.14
10	10	-0.03	0.32	-0.05	0.38	3.92	-0.58	NaN	NaN	6.00	29	0.33
12	2	0.00	0.01	0.00	0.00	-0.18	-0.01	5	0.00	6.28	34	0.01
12	10	-0.10	0.36	-0.29	-0.84	1.82	-1.09	5	0.04	6.28	34	0.47
12	20	-0.17	0.66	-0.60	-2.34	0.91	-1.04	4	0.05	6.28	41	0.91
12	30	-0.26	0.80	-0.70	-2.64	1.74	-1.01	5	0.10	6.28	34	1.09
12	40	-0.26	0.90	-0.79	-2.48	-4.82	-1.03	3	0.05	6.28	52	1.22
12	50	-0.12	1.11	-1.00	-3.31	-1.53	-0.47	3	0.01	6.28	52	1.50
13	2	0.11	0.20	-0.02	-0.17	-0.72	0.62	NaN	NaN	5.77	34	0.22
13	10	0.09	0.18	-0.02	-0.07	-1.49	0.41	NaN	NaN	5.77	34	0.20
13	30	0.15	0.77	0.43	1.40	0.69	1.25	NaN	NaN	5.77	34	0.90
13	40	0.35	0.93	0.38	2.35	-1.59	2.80	NaN	NaN	5.77	34	1.06
14	2	0.02	0.04	0.00	0.01	-0.09	0.01	5	0.02	5.76	29	0.05
14	10	0.13	0.16	-0.06	-0.41	-1.89	0.75	5	0.05	5.76	29	0.22
14	20	0.25	0.38	0.03	-0.46	-3.73	1.19	3	0.09	5.76	42	0.46
14	30	0.41	0.56	-0.13	-0.75	-2.85	0.71	5	0.13	5.76	29	0.71
14	40	0.30	0.82	-0.42	-1.24	-3.28	1.93	4	0.13	5.76	35	0.97
14	50	0.33	0.80	-0.43	-1.24	-3.29	1.93	4	0.13	5.76	35	0.96
15	2	0.00	-0.03	0.00	0.13	-0.02	-0.09	3	0.04	6.17	37	0.03
15	10	0.04	0.35	-0.07	-0.30	2.94	-0.02	3	0.21	6.17	37	0.36
15	20	-0.28	0.71	-0.08	0.00	-1.02	0.55	3	0.22	6.17	37	0.77
15	30	-0.45	0.81	-0.03	0.61	-0.69	0.22	3	0.21	6.17	37	0.92
15	50	-0.20	1.15	-0.10	1.39	1.90	-0.26	3	0.09	6.17	37	1.17
16	2	-0.07	0.04	0.03	0.04	-4.45	0.16	5	0.07	5.75	28	0.09
16	10	0.22	0.36	0.08	0.52	-3.38	1.24	4	0.13	5.75	33	0.43
17	2	0.15	-0.05	-0.05	0.17	-0.80	-0.27	6	0.15	6.00	26	0.16
17	10	0.09	0.26	-0.16	-0.60	-4.44	0.44	5	0.15	6.00	30	0.32
17	20	0.40	0.57	-0.28	-0.87	-4.78	0.80	4	0.15	6.00	36	0.75
17	30	0.71	1.08	-0.29	-0.71	-2.41	2.09	4	0.20	6.00	32	1.33
17	40	1.02	1.43	-0.44	-0.83	-2.80	3.66	3	0.26	6.00	45	1.81
17	50	1.09	1.91	-0.62	-1.22	-2.48	5.03	3	0.30	6.00	45	2.28
18	2	0.03	-0.05	-0.02	-0.28	3.02	-0.08	4	0.09	5.95	35	0.06
18	10	0.03	-0.05	-0.01	-0.12	1.32	0.23	5	0.16	5.95	35	0.06
18	20	0.11	0.18	0.00	0.19	-0.20	-0.28	5	0.22	5.95	35	0.21
18	30	0.08	0.42	-0.07	0.96	-1.60	-0.26	5	0.14	5.95	35	0.43
18	40	0.05	0.60	-0.12	0.22	0.03	0.63	4	0.10	5.95	35	0.61
18	50	0.20	0.73	-0.06	0.34	0.62	0.89	5	0.11	5.95	35	0.76
20	2	-0.07	-0.01	0.01	-0.77	1.21	3.19	3	0.03	5.70	40	0.07

20	10	-0.07	0.65	-0.01	-2.00	0.41	1.52	3	0.27	5.70	40	0.66
20	20	-0.08	1.16	-0.11	-3.74	-1.72	2.69	3	0.82	5.70	40	1.17
20	30	-0.03	1.27	-0.01	-2.96	-0.98	2.90	3	0.87	5.70	40	1.27

TALAR COMPONENT MIGRATION DATA

subject	RSA exam	x	y	z	rx	ry	rz	markers	ME	min rel CN	abs CN	MTPM
1	2	0.19	0.09	0.02	0.61	0.58	-0.30	5	0.08	1.93	103	0.49
1	10	-0.07	0.04	-0.05	0.26	-0.25	0.27	7	0.10	1.93	72	0.22
1	20	0.02	-0.27	-0.17	-0.86	-0.94	-0.21	7	0.06	1.93	72	0.63
1	30	0.01	-0.47	-0.21	-0.39	-0.86	-1.40	7	0.08	1.93	72	0.91
1	40	0.22	-0.70	-0.24	-0.50	-0.94	-1.88	6	0.03	1.93	93	1.24
1	50	0.05	-0.76	-0.23	-1.09	-0.52	-2.22	6	0.09	1.93	72	1.53
2	2	0.16	-0.05	-0.13	-0.39	0.34	-0.20	NaN	NaN	1.85	40	0.39
2	10	-0.01	-0.08	-0.10	-0.29	-0.24	-0.10	NaN	NaN	1.85	40	0.22
2	20	0.03	-0.12	0.01	0.37	0.34	-0.38	NaN	NaN	1.85	40	0.32
2	30	0.07	-0.12	-0.05	0.16	0.48	-0.40	NaN	NaN	1.85	40	0.32
2	40	0.17	-0.17	-0.04	0.32	0.75	-0.92	NaN	NaN	1.85	40	0.56
2	50	-0.13	-0.21	0.02	0.94	-0.08	-3.14	NaN	NaN	1.85	40	1.19
3	2	0.01	0.01	0.03	0.07	-0.26	-0.13	8	0.15	2.14	26	0.12
3	10	0.19	-0.10	-0.10	0.07	-1.10	0.03	7	0.11	2.14	27	0.59
3	20	0.11	-0.13	-0.04	0.21	0.18	-0.31	6	0.11	2.14	27	0.27
3	30	-0.27	-0.10	0.27	0.99	0.03	-1.10	6	0.12	2.14	29	0.71
3	40	-0.06	-0.23	0.06	0.41	-0.71	-0.62	6	0.07	2.14	27	0.51
3	50	-0.08	-0.29	0.11	0.58	-0.91	-1.27	6	0.07	2.14	27	0.76
4	2	0.00	0.00	-0.02	-0.05	0.14	0.10	8	0.07	1.90	28	0.07
4	20	-0.13	-0.12	-0.05	-0.24	-2.57	1.48	7	0.08	1.90	29	1.22
4	30	0.01	-0.46	-0.08	-0.59	-2.22	1.68	7	0.12	1.90	29	1.32
4	40	0.44	-0.80	0.10	1.13	-2.95	1.33	7	0.09	1.90	29	1.97
4	50	0.29	-0.76	0.04	1.91	-2.73	0.83	7	0.08	1.90	29	1.95
5	2	-0.02	0.01	0.02	0.01	-0.03	-0.07	4	0.02	1.81	38	0.04
5	10	-0.26	0.05	-0.07	-0.38	0.21	-0.15	4	0.07	1.81	38	0.39
5	20	-0.02	-0.12	0.07	-0.08	0.76	0.16	4	0.04	1.81	38	0.38
5	30	-0.20	-0.14	0.07	0.12	0.06	0.74	3	0.07	1.81	38	0.43
5	40	-0.12	-0.38	-0.10	-0.33	1.28	-0.13	4	0.05	1.81	38	0.72
5	50	-0.32	-0.56	-0.45	-0.49	0.23	-0.02	4	0.07	1.81	38	0.90
6	2	0.17	-0.08	0.09	0.41	-0.08	-0.09	8	0.09	2.00	26	0.30
6	10	0.37	-0.10	0.03	-0.12	0.52	-1.00	8	0.13	2.00	26	0.66
6	30	-0.23	-0.06	-0.05	0.37	0.21	-0.03	6	0.08	2.00	34	0.36
6	40	-0.02	-0.49	0.03	0.43	1.05	0.86	8	0.08	2.00	26	0.85
7	2	0.00	0.01	-0.01	-0.05	0.02	0.01	10	0.04	1.74	22	0.03
8	2	0.02	-0.01	0.04	0.00	0.20	-0.10	8	0.10	1.67	27	0.12
8	10	-0.01	-0.11	0.02	0.52	0.02	-0.24	8	0.12	1.67	27	0.34
8	20	0.02	-0.30	-0.07	0.49	0.40	-0.18	8	0.16	1.67	27	0.55
8	30	0.06	-0.49	-0.33	-0.25	0.29	0.27	7	0.11	1.67	28	0.69
8	40	0.18	-0.57	-0.46	0.42	1.01	0.93	7	0.07	1.67	28	0.97
8	50	0.01	-0.61	-0.39	0.93	0.38	1.34	7	0.16	1.67	28	1.25
9	10	0.04	0.01	0.06	0.21	0.12	-0.16	5	0.09	1.57	39	0.17
9	20	-0.02	-0.16	0.15	0.71	-0.75	0.48	5	0.11	1.57	39	0.59
9	30	0.13	-0.35	0.11	0.85	-0.30	0.09	5	0.11	1.57	39	0.75
9	40	-0.16	-0.57	0.00	0.96	-0.77	1.64	5	0.10	1.57	39	1.30
9	50	0.07	-0.77	0.01	1.77	-0.97	0.50	4	0.13	1.57	42	1.63
10	2	0.10	0.00	0.02	0.04	-0.09	-0.09	8	0.07	1.82	28	0.14
12	2	0.00	0.00	0.00	0.00	0.01	-0.01	8	0.00	2.00	38	0.01
12	10	0.08	0.02	0.01	-0.07	-0.05	-0.03	8	0.05	2.00	38	0.11
12	20	0.04	0.00	-0.04	-0.22	0.08	-0.10	8	0.10	2.00	38	0.12
12	30	0.00	-0.02	0.05	0.04	-0.08	-0.15	7	0.08	2.00	39	0.09
12	40	-0.15	-0.02	0.03	-0.10	0.05	0.03	7	0.05	2.00	39	0.17
12	50	-0.14	0.03	-0.06	-0.56	-0.46	0.35	8	0.06	2.00	38	0.39
13	2	0.01	-0.06	0.12	0.46	1.11	1.83	4	0.13	1.50	34	0.85
13	10	-0.02	-0.05	0.13	0.43	0.96	0.98	4	0.03	1.50	34	0.66
13	30	0.22	-0.72	0.10	0.27	-0.47	0.97	4	0.11	1.50	34	1.11
13	40	0.05	-0.67	0.05	0.95	-0.22	1.29	4	0.06	1.50	34	1.30
14	2	0.04	0.00	0.02	-0.01	-0.12	0.01	7	0.06	1.54	23	0.09

14	10	0.19	-0.03	-0.19	-0.72	0.40	1.06	7	0.17	1.54	22	0.63
14	20	-0.14	-0.06	-0.02	-0.30	0.68	0.58	7	0.09	1.54	25	0.49
14	30	-0.05	-0.33	-0.04	-0.17	0.95	0.39	7	0.13	1.54	25	0.59
14	40	-0.08	-0.74	0.01	0.54	0.74	1.34	6	0.14	1.54	27	1.29
14	50	0.02	-0.80	-0.01	0.43	0.74	1.55	5	0.16	1.54	27	1.33
15	2	-0.04	0.03	0.02	0.20	0.22	-0.34	3	0.02	1.86	36	0.17
15	10	0.14	0.03	0.00	0.32	0.91	-0.52	3	0.03	1.86	36	0.53
15	20	0.15	0.11	-0.11	0.00	0.34	0.51	3	0.03	1.86	36	0.39
15	30	0.02	0.17	-0.16	-0.41	0.00	1.01	3	0.05	1.86	36	0.53
15	50	0.02	0.19	-0.20	-0.74	0.69	-0.01	3	0.09	1.86	36	0.56
16	2	0.08	0.02	-0.03	-0.21	-0.46	0.01	7	0.05	1.62	29	0.28
16	10	-0.05	0.02	-0.02	-0.24	-0.89	0.38	7	0.17	1.62	29	0.43
16	20	0.19	-0.03	-0.06	0.13	-1.00	0.82	6	0.14	1.62	31	0.64
16	30	0.20	-0.03	-0.05	0.14	-1.02	0.83	6	0.14	1.62	31	0.64
16	40	0.12	-0.04	-0.12	-0.22	-0.69	0.36	7	0.08	1.62	29	0.44
16	50	0.32	-0.54	-0.04	-0.98	1.23	0.46	7	0.14	1.62	29	1.22
17	2	0.07	0.00	0.00	0.31	0.00	0.03	9	0.06	1.98	30	0.12
17	10	0.04	-0.02	-0.08	-0.27	0.27	-0.27	7	0.19	1.98	39	0.23
17	20	0.09	0.01	-0.14	-0.27	-0.11	0.45	8	0.16	1.98	31	0.26
17	30	0.10	-0.15	-0.04	-0.16	-0.24	1.20	6	0.14	1.98	40	0.51
17	40	-0.04	-0.28	-0.20	-0.13	-0.96	2.30	6	0.14	1.98	40	0.96
17	50	0.08	-0.64	-0.25	-0.21	-0.65	2.24	6	0.12	1.98	40	1.30
18	2	0.05	0.00	-0.03	-0.49	-0.32	-0.24	6	0.11	1.80	29	0.26
20	2	-0.17	0.01	-0.03	0.29	-0.04	0.77	5	0.04	1.93	49	0.32

TIBIAL COMPONENT INDUCIBLE DISPLACEMENT DATA

subject	RSA exam	x	y	z	rx	ry	rz	markers	ME	minrel CN	abs CN	MTPM
1	25	0.10	0.09	0.06	-0.63	1.30	0.06	4	0.19	1.50	41	0.63
1	35	0.44	0.07	-0.09	0.13	2.16	-0.19	4	0.11	1.49	41	1.24
1	45	-0.23	0.07	0.34	1.02	-5.70	-0.11	4	0.05	1.42	42	2.35
1	55	-0.72	0.28	0.25	-0.11	-0.90	-0.05	4	0.06	1.51	41	1.11
2	25	-0.11	0.01	0.01	0.32	-8.68	0.70	6	0.07	1.39	28	3.50
2	35	-0.58	-0.13	-0.14	0.51	-8.25	3.04	6	0.08	1.41	28	4.18
2	45	0.43	0.14	-0.09	0.09	1.64	-1.15	6	0.12	1.37	29	1.21
2	55	-0.71	0.09	0.13	-0.07	0.81	-0.38	5	0.03	1.48	29	1.00
3	25	-0.04	0.09	-0.06	-0.02	-3.76	-0.43	3	0.22	1.55	48	1.37
3	45	-0.59	0.16	-0.24	-0.04	-0.89	-0.32	3	0.06	1.49	49	0.94
3	55	0.37	0.01	-0.17	0.04	-2.27	-0.10	4	0.08	1.60	34	1.21
4	25	-0.61	-0.24	0.27	0.46	-1.29	-1.92	5	0.03	1.41	31	1.34
4	45	-0.78	-0.18	0.24	-0.80	-6.23	3.53	5	0.02	1.47	31	3.69
4	55	-0.02	0.02	0.29	-0.18	8.53	0.86	4	0.03	1.50	38	3.39
5	25	-0.75	0.18	-0.14	-0.04	-4.23	-1.68	3	0.09	1.39	33	2.41
5	35	-2.07	0.24	-0.11	-0.15	-7.73	-0.82	4	0.10	1.31	32	5.09
5	45	-0.81	0.11	-0.23	-0.26	-0.46	-1.62	3	0.07	1.37	33	1.36
5	55	-0.85	0.20	-0.34	-0.68	0.11	-0.70	3	0.13	1.30	34	1.22
6	35	0.04	0.20	-0.05	0.38	-2.19	2.09	4	0.10	1.48	33	1.20
6	45	0.81	0.11	-0.25	-0.11	4.39	-0.69	4	0.09	1.50	33	2.47
7	25	-0.95	0.15	-0.42	0.30	4.23	-0.62	3	0.06	1.40	47	2.56
7	35	0.21	0.02	-0.02	0.13	0.70	0.05	4	0.04	1.47	29	0.47
7	45	0.00	0.09	-0.07	-0.04	0.28	0.22	3	0.03	1.45	50	0.20
7	55	-0.77	0.19	-0.35	-0.41	-3.69	-0.55	3	0.07	1.44	50	2.20
8	25	-0.25	-0.03	0.23	0.13	-0.02	-0.43	4	0.08	1.36	34	0.47
8	35	0.94	0.07	0.10	0.22	5.05	-0.97	4	0.16	1.35	34	3.10
8	45	-0.81	0.04	-0.02	-0.11	-1.34	0.20	4	0.13	1.34	33	1.36
8	55	-0.56	0.00	0.16	-0.15	0.49	-0.83	4	0.07	1.36	33	0.83
9	25	-0.81	0.02	-0.33	-0.23	-3.00	-0.60	5	0.03	1.28	39	2.15
9	35	0.00	0.07	0.12	-0.04	-1.60	0.05	4	0.06	1.20	39	0.80
9	45	-1.00	0.32	-0.24	-0.22	0.94	-0.30	5	0.07	1.29	38	1.46
9	55	0.07	0.06	0.19	-0.29	3.08	-0.75	4	0.06	1.32	45	1.66
10	25	-0.89	0.09	0.28	0.59	-2.49	0.72	5	0.12	1.40	36	1.98
10	35	-1.07	0.11	-0.06	-0.21	-2.21	-0.39	5	0.10	1.37	34	1.83
10	45	-1.87	0.25	0.32	0.13	-6.10	-1.29	6	0.11	1.38	30	4.02
10	55	0.11	0.14	0.10	-0.26	0.82	-1.85	4	0.12	1.46	41	0.86

11	25	-0.47	0.11	0.12	0.00	1.56	-2.11	4	0.08	1.36	43	1.17
11	35	-0.94	-0.06	0.01	-0.14	0.20	-1.41	4	0.08	1.33	42	1.38
11	45	-0.67	-0.01	-0.05	-0.73	-0.46	0.40	4	0.03	1.27	39	0.96
11	55	-0.17	0.06	0.08	-0.19	2.67	-1.82	4	0.06	1.38	43	1.31
12	35	0.02	0.07	-0.06	-0.16	0.29	-0.35	5	0.04	1.48	34	0.20
12	45	-0.68	0.13	-0.33	-0.49	2.51	-0.25	3	0.05	1.36	45	1.67
12	55	-0.98	0.24	0.39	0.40	-1.09	-0.56	3	0.04	1.43	47	1.43
13	35	-0.09	-0.04	0.07	0.04	-1.33	0.90	4	0.11	1.29	28	0.84
13	45	-0.08	0.01	0.24	-0.19	0.44	-0.70	3	0.05	1.18	37	0.45
14	25	0.62	-0.09	-0.29	0.09	2.70	0.11	3	0.05	1.25	43	1.89
14	35	-0.09	0.00	-0.50	0.15	2.12	-0.54	5	0.15	1.27	30	1.30
14	45	0.07	-0.02	0.36	-0.18	0.00	-0.13	4	0.07	1.27	36	0.41
14	55	0.18	0.14	-0.21	0.03	6.87	-1.50	4	0.05	1.26	36	3.52
15	25	0.30	0.13	-0.02	-0.44	2.62	0.10	4	0.15	1.46	39	1.27
15	35	-0.17	0.03	-0.02	0.05	0.39	0.31	4	0.13	1.44	39	0.37
15	55	-0.07	0.03	-0.07	0.15	1.44	-0.02	4	0.18	1.43	38	0.63
16	25	-0.02	0.20	-0.22	-0.44	1.01	-0.11	4	0.04	1.31	35	0.60
16	35	-0.82	0.24	-0.12	-0.45	-0.26	-0.12	4	0.04	1.31	35	0.94
16	45	0.49	-0.08	-0.44	-0.27	-0.70	0.35	4	0.07	1.29	32	0.87
16	55	-0.88	0.10	0.59	-0.26	-0.71	0.02	3	0.05	1.29	59	1.38
17	25	-0.07	0.09	0.02	-0.15	-2.31	-0.10	4	0.06	1.51	37	0.89
17	35	-1.43	0.19	0.28	0.34	-8.41	-0.58	5	0.07	1.49	30	4.29
17	45	-1.23	0.25	0.05	0.35	-4.76	0.19	4	0.05	1.48	37	2.88
18	25	-0.69	0.30	-0.24	-0.34	-0.26	-1.17	4	0.08	1.40	36	1.15
18	35	-0.84	0.06	-0.04	-1.17	-2.57	-1.50	4	0.16	1.38	35	1.75
18	45	-0.16	0.09	-0.10	-0.24	-1.62	0.44	5	0.05	1.44	30	0.85
18	55	-0.72	0.24	-0.29	-0.29	-0.30	-1.30	4	0.04	1.39	36	1.21
19	25	-0.60	0.11	-0.02	0.06	-1.37	-2.28	4	0.13	1.34	21	1.34
19	35	-0.89	0.18	-0.48	-0.50	-2.49	-1.62	3	0.08	1.38	33	1.85
20	25	0.23	0.03	0.50	0.09	-0.12	0.22	3	0.01	1.40	41	0.61
20	35	0.75	0.24	-0.41	-0.01	-2.06	-1.62	3	0.08	1.41	40	1.81

TIBIAL COMPONENT SPHERICAL TIP INDUCIBLE DISPLACEMENT DATA

subject	RSA exam	x	y	z	rx	ry	rz	markers	ME	minrel CN	abs CN	MTPM
1	25	0.06	0.13	-0.04	-0.63	1.30	0.06	4	0.19	6.00	41	0.15
1	35	0.07	0.01	0.06	0.13	2.16	-0.19	4	0.11	5.99	41	0.09
1	45	-0.08	0.09	0.11	1.02	-5.70	-0.11	4	0.05	5.70	42	0.16
1	55	0.03	0.08	-0.02	-0.11	-0.90	-0.05	4	0.06	6.01	41	0.09
2	25	0.10	0.07	0.07	0.32	-8.61	0.70	6	0.07	5.84	28	0.14
2	35	0.07	0.06	0.04	0.51	-8.25	3.04	6	0.08	5.92	28	0.10
2	45	0.05	0.05	-0.02	0.08	1.98	-1.15	6	0.12	5.81	29	0.07
2	55	-0.02	0.03	0.00	-0.07	0.81	-0.38	5	0.03	6.16	29	0.03
3	25	-0.02	0.05	-0.03	0.05	6.14	-0.44	3	0.22	6.23	48	0.06
3	45	0.14	0.03	-0.04	-0.04	-0.89	-0.32	3	0.06	6.02	49	0.15
3	55	0.04	0.06	-0.01	0.04	-2.27	-0.10	4	0.08	6.43	34	0.07
4	25	-0.02	0.02	0.02	0.46	-1.29	-1.92	5	0.03	5.94	31	0.03
4	45	0.02	0.02	0.00	-0.80	-6.23	3.53	5	0.02	6.10	31	0.03
4	55	0.00	0.08	0.02	2.54	8.39	2.00	4	0.03	6.25	38	0.08
5	25	0.06	0.05	-0.02	-0.04	-4.23	-1.68	3	0.09	6.18	33	0.08
5	35	-0.24	0.09	-0.07	-0.15	-7.73	-0.82	4	0.10	5.91	32	0.26
5	45	-0.17	0.04	-0.05	-0.32	-0.47	-1.63	3	0.07	6.08	33	0.19
5	55	-0.06	0.07	0.00	-0.68	0.11	-0.70	3	0.13	5.81	34	0.09
6	35	-0.05	0.05	-0.06	0.38	-2.19	2.09	4	0.10	6.04	33	0.09
6	45	-0.05	0.04	0.02	-0.11	4.39	-0.69	4	0.09	6.03	33	0.07
7	25	-0.01	0.06	-0.04	0.31	4.23	-0.63	3	0.06	5.95	47	0.07
7	35	-0.01	0.02	0.01	0.13	0.71	0.05	4	0.04	6.13	29	0.03
7	45	-0.02	0.05	0.03	-0.04	-0.35	0.22	3	0.03	6.03	50	0.06
7	55	0.03	0.00	0.01	-0.41	-3.69	-0.55	3	0.07	6.02	50	0.03
8	25	-0.06	0.04	0.04	0.13	-0.02	-0.43	4	0.08	6.00	34	0.08
8	35	-0.02	-0.01	0.00	0.22	5.05	-0.97	4	0.16	6.03	34	0.02
8	45	-0.04	0.04	-0.01	-0.11	-1.34	0.20	4	0.13	5.98	33	0.06
8	55	0.01	0.03	0.00	-0.16	0.49	-0.83	4	0.07	6.05	33	0.03
9	25	0.01	0.07	-0.01	0.10	-2.99	1.39	5	0.03	6.08	39	0.08

9	35	0.01	0.05	0.01	-0.04	-1.58	0.05	4	0.06	5.78	39	0.06
9	45	-0.06	0.07	0.01	-0.22	0.94	-0.30	5	0.07	6.11	38	0.09
9	55	-0.14	0.09	0.01	-0.29	3.08	-0.75	4	0.06	6.18	45	0.17
10	25	0.03	0.12	0.07	0.59	-2.49	0.72	5	0.12	5.92	36	0.15
10	35	-0.08	0.12	0.09	-0.21	-2.21	-0.39	5	0.10	5.84	34	0.17
10	45	0.08	0.07	0.03	0.13	-6.10	-1.29	6	0.11	5.91	30	0.11
10	55	-0.12	-0.02	0.03	-0.26	0.82	-1.85	4	0.12	6.09	41	0.13
11	25	-0.17	0.11	-0.07	0.00	1.56	-2.11	4	0.08	6.02	43	0.22
11	35	-0.09	0.04	-0.03	-0.14	0.20	-1.41	4	0.08	5.85	42	0.11
11	45	-0.06	0.10	-0.05	-0.73	-0.46	0.40	4	0.03	5.73	39	0.12
11	55	-0.03	0.03	-0.03	-0.19	2.67	-1.82	4	0.06	6.09	43	0.05
12	35	-0.03	0.10	-0.03	-0.16	0.29	-0.35	5	0.04	6.16	34	0.11
12	45	-0.04	0.04	0.04	-0.49	2.51	-0.25	3	0.05	5.78	45	0.07
12	55	-0.01	0.03	0.02	0.40	-1.09	-0.56	3	0.04	6.07	47	0.03
13	35	0.01	0.02	0.10	0.04	-1.33	0.90	4	0.11	5.99	28	0.10
13	45	0.04	0.07	0.00	-0.19	0.44	-0.70	3	0.05	5.65	37	0.09
14	25	-0.01	0.15	0.09	0.09	2.70	0.11	3	0.05	5.88	43	0.17
14	35	-0.14	0.06	0.03	0.16	2.12	-0.54	5	0.15	5.96	30	0.15
14	45	-0.10	0.08	-0.04	-0.43	2.79	-0.19	4	0.07	5.96	36	0.13
14	55	-0.12	0.09	0.01	0.03	6.87	-1.50	4	0.05	5.95	36	0.15
15	25	-0.16	0.12	-0.01	-0.44	2.62	0.10	4	0.15	6.09	39	0.20
15	35	-0.11	0.02	-0.01	-7.09	-1.49	0.95	4	0.13	6.08	39	0.11
15	55	-0.18	0.03	-0.04	0.15	1.44	-0.02	4	0.18	5.99	38	0.18
16	25	0.04	-0.01	-0.04	-0.44	1.01	-0.10	4	0.04	5.85	35	0.06
16	35	0.06	-0.02	-0.06	-0.45	-0.26	-0.12	4	0.04	5.85	35	0.09
16	45	0.01	0.05	-0.04	-0.27	-0.70	0.35	4	0.07	5.80	32	0.07
16	55	-0.06	0.03	0.01	-0.26	-0.71	0.02	3	0.05	5.78	59	0.07
17	25	-0.13	0.07	0.00	-0.15	-2.31	-0.10	4	0.06	6.02	37	0.15
17	35	-0.04	0.04	0.14	0.34	-8.41	-0.58	5	0.07	5.98	30	0.15
17	45	0.08	0.08	0.03	0.35	-4.76	0.19	4	0.05	5.96	37	0.12
18	25	-0.05	0.05	0.05	-0.34	-0.26	-1.17	4	0.08	5.94	36	0.09
18	35	0.04	0.02	-0.05	-1.17	-2.57	-1.50	4	0.16	5.90	35	0.07
18	45	-0.04	-0.03	0.00	-0.24	-1.62	0.44	5	0.05	6.12	30	0.05
18	55	-0.05	-0.05	0.04	-0.29	-0.30	-1.30	4	0.04	5.92	36	0.08
19	25	0.03	0.11	-0.37	0.06	-1.37	-2.28	4	0.13	5.89	21	0.39
19	35	-0.24	0.03	-0.35	-0.49	-2.49	-1.63	3	0.08	5.92	33	0.43
20	25	-0.01	0.06	0.00	0.09	0.88	0.22	3	0.01	5.70	41	0.06
20	35	0.03	0.07	-0.01	-0.01	-2.06	-1.62	3	0.08	5.73	40	0.07

TALAR COMPONENT INDUCIBLE DISPLACEMENT DATA

subject	RSA exam	x	y	z	rx	ry	rz	markers	ME	min rel CN	abs CN	MTPM
1	25	0.00	-0.07	-0.05	0.25	-0.55	-0.30	5	0.05	2.05	86	0.26
1	35	0.07	-0.06	-0.04	-0.02	-0.33	0.39	7	0.09	1.99	77	0.24
1	45	-0.05	-0.05	0.01	-0.05	-0.11	1.10	5	0.03	1.95	123	0.33
1	55	0.03	-0.09	0.01	-0.18	-0.66	-0.33	6	0.10	1.96	76	0.29
2	25	-0.04	0.02	-0.02	0.12	0.05	-0.28	NaN	NaN	1.79	42	0.12
2	35	0.12	0.05	0.00	0.03	-0.24	-0.22	NaN	NaN	1.79	42	0.23
2	45	-0.13	0.01	0.09	0.25	-0.05	-0.52	NaN	NaN	1.84	43	0.27
2	55	0.11	-0.10	0.03	0.32	1.86	-1.02	NaN	NaN	1.86	36	0.85
3	25	-0.11	-0.05	-0.07	0.22	-0.74	-0.29	6	0.21	2.04	26	0.38
3	45	0.06	-0.08	-0.10	-0.27	-0.02	-0.44	8	0.22	2.01	24	0.27
3	55	0.16	-0.04	-0.01	0.00	0.64	-0.10	6	0.08	2.14	27	0.38
4	25	0.07	0.00	-0.07	-0.38	2.26	-1.37	6	0.08	1.82	28	1.04
4	45	-0.10	-0.01	-0.07	-0.02	-0.55	0.43	7	0.05	1.87	28	0.35
4	55	-0.03	-0.08	0.03	0.20	-2.74	0.60	7	0.06	1.93	29	1.06
5	25	-0.02	-0.03	0.02	0.35	-0.46	0.46	6	0.10	1.77	34	0.29
5	35	0.08	-0.04	-0.02	-0.27	0.12	0.44	6	0.10	1.66	33	0.26
5	45	0.05	0.01	0.00	0.05	-0.33	0.46	5	0.09	1.76	37	0.21
5	55	0.14	-0.09	0.05	0.04	0.32	-0.14	8	0.07	1.66	30	0.29
6	35	-0.15	0.01	0.09	1.19	-0.08	3.05	6	0.14	1.94	34	0.99
6	45	-0.05	-0.03	0.02	0.27	-1.03	0.01	7	0.09	2.04	26	0.40
7	25	-0.12	0.01	-0.03	0.07	-1.25	0.39	9	0.06	1.75	23	0.59

7	35	-0.39	-0.20	-0.13	-0.09	-0.13	-0.51	9	0.08	1.76	23	0.58
7	45	0.05	-0.18	0.02	0.58	2.39	-1.04	9	0.12	1.80	27	0.98
7	55	0.04	-0.12	0.14	0.07	0.64	-1.55	9	0.04	1.76	23	0.55
8	25	0.09	-0.01	-0.08	-0.20	0.43	0.29	8	0.09	1.67	27	0.29
8	35	0.01	-0.07	0.08	0.37	1.33	-0.04	7	0.19	1.61	27	0.59
8	45	0.04	0.05	0.10	0.41	0.40	0.06	7	0.14	1.61	26	0.30
8	55	0.09	0.00	0.12	0.57	1.21	-0.50	7	0.16	1.62	27	0.69
9	25	0.06	-0.03	0.00	-0.08	0.30	0.15	6	0.05	1.61	34	0.20
9	35	0.05	0.02	-0.01	-0.18	0.30	-0.27	8	0.07	1.54	31	0.21
9	45	0.12	-0.15	0.03	-0.04	-0.26	-1.29	7	0.17	1.61	33	0.56
9	55	0.00	-0.07	-0.01	-0.08	0.53	-0.45	7	0.13	1.61	31	0.32
10	25	-0.12	-0.14	-0.02	-0.53	0.04	0.16	6	0.15	1.83	38	0.36
10	35	-0.10	-0.05	0.04	0.06	0.04	-0.26	5	0.11	1.77	30	0.19
10	45	0.15	-0.08	0.05	0.22	0.27	-0.43	5	0.11	1.80	41	0.28
10	55	0.15	-0.06	0.03	-0.05	0.54	-0.51	8	0.05	1.88	28	0.39
11	25	0.20	-0.03	0.04	0.28	0.17	-0.26	7	0.09	1.62	26	0.30
11	35	0.15	-0.01	0.09	0.60	-0.04	-0.08	8	0.09	1.61	24	0.30
11	45	-0.07	-0.01	0.07	0.36	0.32	1.24	8	0.04	1.64	26	0.45
11	55	0.14	-0.06	0.10	0.46	0.32	-0.09	6	0.05	1.58	26	0.30
12	35	-0.09	0.00	0.02	-0.01	0.06	-0.05	7	0.05	1.90	39	0.11
12	45	0.07	-0.03	0.00	0.13	-0.35	0.06	6	0.09	1.83	42	0.21
12	55	0.26	0.01	0.02	0.20	0.56	-0.32	8	0.07	1.88	36	0.49
13	35	-0.11	-0.05	-0.05	-0.29	-0.96	-0.06	8	0.09	1.58	25	0.54
13	45	0.16	-0.18	-0.35	-1.93	-1.02	-0.42	5	0.06	1.49	32	0.99
14	25	0.06	-0.02	-0.13	-0.59	0.08	1.21	8	0.10	1.58	22	0.55
14	35	-0.19	-0.11	-0.07	-0.15	0.47	1.21	8	0.08	1.58	22	0.55
14	45	0.12	-0.02	-0.32	-1.11	-0.26	0.31	7	0.12	1.57	23	0.59
14	55	0.09	-0.05	-0.04	0.10	-0.34	0.18	5	0.10	1.57	23	0.27
15	25	-0.09	-0.06	-0.01	-0.46	-0.27	-0.16	6	0.05	1.79	30	0.30
15	35	0.02	-0.01	-0.01	-0.01	0.13	-0.05	7	0.02	1.78	28	0.07
15	55	0.04	-0.05	0.02	0.20	-0.65	-0.29	6	0.13	1.80	31	0.33
16	25	-0.10	-0.02	-0.05	-0.56	0.32	-0.60	7	0.08	1.68	30	0.36
16	35	-0.10	-0.02	-0.05	-0.54	0.37	-0.60	7	0.08	1.68	30	0.37
16	45	-0.08	-0.02	0.07	-0.07	-0.10	-0.21	8	0.11	1.73	30	0.18
16	55	0.12	-0.11	-0.16	-0.57	0.11	-0.55	5	0.13	1.70	41	0.48
17	25	0.07	-0.07	-0.06	-0.32	-0.33	0.07	7	0.12	1.95	38	0.21
17	35	0.05	-0.09	0.05	-0.31	0.76	0.15	5	0.05	1.97	51	0.38
17	45	0.17	-0.16	0.05	-0.35	-0.24	0.64	6	0.02	1.98	41	0.40
18	25	0.07	-0.24	-0.07	-0.06	1.05	-0.53	6	0.12	1.78	28	0.62
18	35	0.43	-0.18	-0.18	-0.56	0.39	-0.66	7	0.06	1.76	26	0.78
18	45	0.25	-0.13	-0.02	-0.24	0.77	-0.35	7	0.05	1.81	27	0.59
18	55	0.19	-0.16	-0.14	-0.73	0.05	-0.77	7	0.08	1.77	26	0.60
19	25	0.01	-0.06	0.15	0.64	0.13	-0.74	7	0.09	1.74	25	0.41
19	35	0.05	-0.04	0.02	0.47	-0.59	0.83	6	0.07	1.79	29	0.42
20	25	-0.11	-0.04	0.00	-0.09	-0.81	-0.09	6	0.13	1.91	47	0.38
20	35	0.12	-0.05	0.02	-0.11	0.32	-0.29	6	0.05	1.93	48	0.27